2016-04-12

Activation of mTORC1 Improves Cone Cell Metabolism and Extends Vision in Retinitis Pigmentosa Mice: A Dissertation

Aditya Venkatesh
University of Massachusetts Medical School

ACTIVATION OF mTORC1 IMPROVES CONE CELL METABOLISM AND EXTENDS VISION IN RETINITIS PIGMENTOSA MICE

A Dissertation Presented

By

ADITYA VENKATESH

Submitted to the Faculty of the
University of Massachusetts
Graduate School of Biomedical Sciences, Worcester

in partial fulfillment of the requirements for the degree of

DOCTOR OF PHILOSOPHY

April 12, 2016

Interdisciplinary Graduate Program

ACTIVATION OF mTORC1 IMPROVES CONE CELL METABOLISM AND EXTENDS VISION IN RETINITIS PIGMENTOSA MICE

A Dissertation Presented
By
ADITYA VENKATESH

This work was undertaken in the Graduate School of Biomedical Sciences
Interdisciplinary Graduate Program

The signature of the Thesis Advisor signifies validation of Dissertation content

_____
Claudio Punzo, Thesis Advisor

The signatures of the Dissertation Defense Committee signify completion and approval as to style and content of the Dissertation

_____
Barbara A. Osborne, Ph.D., Member of Committee

_____
Francis Chan, Ph.D., Member of Committee

_____
Hemant Khanna, Ph.D., Member of Committee

_____
Daryl Bosco, Ph.D., Member of Committee

The signature of the Chair of the Committee signifies that the written dissertation meets the requirements of the Dissertation Committee

_____
Eric Baehrecke, Ph.D., Chair of Committee

The signature of the Dean of the Graduate School of Biomedical Sciences signifies that the student has met all graduation requirements of the school.

_____
Anthony Carruthers, Ph.D.,
Dean of the Graduate School of Biomedical Sciences
Interdisciplinary Graduate Program
April 12, 2016

To my family

Acknowledgements

This body of work could not have been possible without the contribution of various people. I owe everything to my family, especially my **grandparents**. They have been my first mentors, guiding lights and made me the person who I am today. It was my grandmother's dream that I pursue a doctoral degree, and I am so thrilled that she is here to live this moment. My **parents** have made endless sacrifices and provided relentless support to ensure that I could follow my aspirations. Despite being miles away from me in India, their moral support got me through all those difficult days (and nights) in the lab. I am indeed blessed to have them attend my thesis defense and witness my work over the last six years, which is more theirs than mine. My younger brother **Anirudh**, who I share almost everything with; I thank you for keeping me sane through graduate school. You have been my best friend, confidante and actually, an older brother to me.

I joined the lab of **Claudio Punzo** after rotating through five labs in two universities. Thank you for accepting me as your first PhD student and giving me the opportunity to work on a project that has given me a new appreciation for the complexities of studying a disease entirely in vivo. Thank you for also giving me the freedom to drive the project forward in directions that fascinated me the most. Thank you for always having your door open and allowing us to walk into your office at any time, and making last minute corrections on my proposals/abstracts over the weekend. Thank you for also putting up with me through all my frustrating moments.

I am also thankful to have an excellent TRAC Committee comprising of **Eric Baehrecke**, **Francis Chan**, **Hemant Khanna** and **Daryl Bosco**. Your insightful suggestions have greatly helped shape this work. I am blessed to have Eric Baehrecke as my TRAC Chair; he has been my 'Godfather' and his encouragement and support through the years have motivated me to excel in my work. Additionally, I will always be indebted to him for the career opportunities he has facilitated for me. I am also thankful to Francis Chan, Daryl Bosco and Hemant Khanna for being enthusiastic and supportive mentors. I am grateful to have **Barbara Osborne** as the external examiner for my defense exam. I started my scientific journey in the US in her laboratory and she has always been an inspiration and support through the years.

I could not have survived six years of graduate school if not for my amazing co-workers. Thank you **Marina Zieger**, **Lolita Petit** and **Shan Ma** for dealing with me through these years! You guys are some of the best people I have ever met and I feel privileged to have really gotten to know you. Lolita, your edits on the first draft of my manuscript have taught me how to write scientifically. Marina, thank you for your emotional support and all those delicious meals. Shan, thank you for teaching me the value of organization.

I would also like to thank Assistant Dean **Ken Knight**, without who I would not have been a graduate student at UMass. I am thankful to my rotation advisors **Sharon Cantor**, **Fen-Biao Gao**, and **Heidi Tissenbaum** for giving me the opportunity to grow as a scientist. I would also like to thank **Satinder Rawat** and **Anita Ballesteros** at the Office

of Technology Management for the opportunity to learn about the commercial value of science and for their guidance with regard to my career. I am especially grateful to Satinder for giving me the confidence to venture into areas outside of academic science and I will always value his support and mentoring. I would also like to thank **Mary Ellen Lane**, Associate Dean, for patiently working with me through the graduation process.

I am deeply indebted to my aunt, uncle and cousins **Neel** and **Sanjay**. They are my family here in the US and I truly value their emotional support. I would also like to thank **Ken-Edwin Aryee**, **Sean Houlihan**, **Emmanuel Bikorimana** and **Richeek Pradhan** for being amazing roommates over these years. A big shout out to my friends; **Arvind Venkatesan**, **Jia Li**, **Kelly Limoncelli**, **Sourav Roy Choudhury, Lakshmi Kumaraguruparan**, **Shobhana Gopalakrishnan, Abla Tannous**, and **Priya Devarajan**. I am also thankful to the members of my gym CrossFit CenterMass for helping me unwind every evening.

I am thankful to **Margaret Humphries** for being a mother to all of us here at the Gene Therapy Center. I will miss your love, care and all those delicious brownies! Thank you to the administrative staff, especially **Denise Maclachlan** and **Chloe Hinrichs**, for all your help with scheduling my seminars. The Gene Therapy Center has been truly an amazing department to work in.

Finally, I would like to thank **God** for all his blessings.

Abstract

Retinitis Pigmentosa (RP) is an inherited photoreceptor degenerative disease that leads to blindness and affects about 1 in 4000 people worldwide. The disease is predominantly caused by mutations in genes expressed exclusively in the night active rod photoreceptors; however, blindness results from the secondary loss of the day active cone photoreceptors, the mechanism of which remains elusive. Here, we show that the mammalian target of rapamycin complex 1 (mTORC1) is required to delay the progression of cone death during disease and that constitutive activation of mTORC1 is sufficient to maintain cone function and promote cone survival in RP. Activation of mTORC1 increased expression of genes that promote glucose uptake, retention and utilization, leading to increased NADPH levels; a key metabolite for cones. This protective effect was conserved in two mouse models of RP, indicating that the secondary loss of cones can be delayed by an approach that is independent of the primary mutation in rods. However, since mTORC1 is a negative regulator of autophagy, its constitutive activation led to an unwarranted secondary effect of shortage of amino acids due to incomplete digestion of autophagic cargo, which reduces the efficiency of cone survival over time. Moderate activation of mTORC1, which promotes expression of glycolytic genes, as well as maintains autophagy, provided more sustained cone survival. Together, our work addresses a long-standing question of non-autonomous cone death in RP and presents a novel, mutation-independent approach to extend vision in a disease that remains incurable.

Table of Contents

List of Figures

List Of Abbreviations

(in alphabetical order)

4EBP1: eukaryotic initiation factor 4E binding protein 1

AFLY: autophagy linked FYVE protein

AIF: apoptosis inducing factor

AMP: adenosine monophosphate

AMPK: AMP kinase

ATG: autophagy-related gene

ATP: adenosine triphosphate

Bcl-2: B cell lymphoma-2

CASP: caspase

cKO: cone-specific knockout

CNTF: ciliary-derived neurotrophic factor

eEF: eukaryotic elongation factor

eIF: eukaryotic initiation factor

ERG: electroretinogram/electroretinography

FOXO: forkhead box

G6PD: Glucose-6-phosphate dehydrogenase

GAP: GTPase activating protein

GC: ganglion cell

GCL: ganglion cell layer

GDP: Guanosine diphosphate

GLUT1: Glucose transporter-1

GTP: Guanosine triphosphate

HDAC: histone deacetylase

HIF-1α: Hypoxia inducible factor-1α

HKII: Hexokinase II

INL: inner nuclear layer

IRS: insulin receptor substrate

IS: inner segment

LC3: microtubule-associated protein 1 light chain 3

ME1: Malic enzyme-1

MERTK: mer tyrosine kinase proto-oncogene

mTOR: Mammalian target of rapamycin

mTORC1: Mammalian target of rapamycin complex 1

mTORC1: Mammalian target of rapamycin complex 2

NADPH: Nicotinamide adenine dinucleotide phosphate

NRL: neural retina-specific leucine zipper protein

NXNL1: nucleoredoxin-like 1

OCT optical coherence tomography

ONL: outer nuclear layer

OS: outer segment

PDE6A: phosphodiesterase 6α

PDE6B: phosphodiesterase 6β

PDK1: 3-phosphoinositide dependent protein kinase

PI3K: phosphatidylinositol-3-kinase

PIP2: phosphatidylinositol diphosphate

PIP3: phosphatidylinositol triphosphate

PKC: protein kinase C

PKM2: pyruvate kinase M2

PPP: pentose phosphate pathway

PR: photoreceptor

PRAS40: proline-rich AKT substrate 40kDa

PRPF: pre mRNA processing factor

rAAV: recombinant adeno-associated virus

RAG: recombination activating gene

RAPTOR: Regulatory associated protein of TOR

rd1: retinal degeneration-1

rd10: retinal degeneration-10

RdCVF: Rod-derived cone viability factor

Rheb: Ras homolog enriched in brain

RHO: rhodopsin

RICTOR: Rapamycin insensitive companion of TOR

ROS: reactive oxygen species

RP: Retinitis Pigmentosa

RPE: retinal pigment epithelium

S6K: S6 kinase

Ser: Serine

SGK: serum and glucocorticoid-regulated kinase

SREBP: sterol regulatory element binding protein

TFEB: transcription factor EB

Thr: Threonine

TSC: tuberous sclerosis complex

ULK: unc-like kinase

WD repeat: tryptophan(W)-aspartic acid(D) repeat

XIAP: X-linked inhibitor of apoptosis

Preface

Chapter II is entirely a first-author manuscript that is currently published in the *Journal of Clinical Investigation*.

Venkatesh A., Ma S., Le Y. Z., Hall M. N., Ruegg M. A., Punzo C. (2015). Activated mTORC1 promotes long-term cone survival in retinitis pigmentosa mice. *J of Clinc. Inves.:* 125 (4): 1446-1458.

Chapter III is also a first-author manuscript that is currently under review in *Cell Death and Disease*. In both manuscripts, figures were renumbered to include supplementary data into the body of the thesis. Parts of Chapter IV and Chapter V are also integrated into the two manuscripts.

Shan Ma performed the electroretinography (ERG) experiments in both Chapters II and III. Besides, she also characterized the cone survival kinetics upon loss of *Pten* and *Tsc1* in the *rd1* and wild type backgrounds and is a co-author on both manuscripts. All other experiments in the thesis were performed by me. Michael N. Hall, Markus A. Rüegg and Yun Z. Le who are co-authors on the manuscript derived from Chapter II provided the $Raptor^{c/c}$, $Rictor^{c/c}$ and M-opsin Cre mice

Claudio Punzo supervised all the research conducted and is the corresponding author on the manuscripts derived from Chapters II and III.

CHAPTER I

Introduction

The neural retina and photoreceptors:

The retina is a neuro-epithelial tissue that is situated at the back of the eye and initiates the process of vision[1]. Three nuclear layers characterize the tissue, each comprising of groups of highly specialized neurons (Figure 1.1 A and B)[2-4]. The photoreceptors (PRs) constitute about 75% of all retinal cells and are specialized to capture photons of light in an elaborate structure referred to as the outer segment (OS) (See Figure 1.1 C). The OS is densely packed with lipids and proteins known as opsins, which are 7 transmembrane G-protein coupled receptors that covalently bind the light-sensitive chromophore (retinal), which mediates the absorption of light[5-7]. In addition to the OS, PRs also have an inner segment (IS), which constitutes the cytoplasm of the cell and is rich in mitochondria[8]. The cell bodies of the PRs are located in the outer nuclear layer (ONL).

There are two types of PRs that contribute to vision, rods and cones. In the human and mouse retina, the distribution of rods and cones is such that rods make up about 95-97% of the total PRs, while cones account for the remaining 3-5%[2,9]. The rod PRs can be activated by a single photon of light, however they become unresponsive upon constant light exposure and hence mediate only dim light or night vision[10].

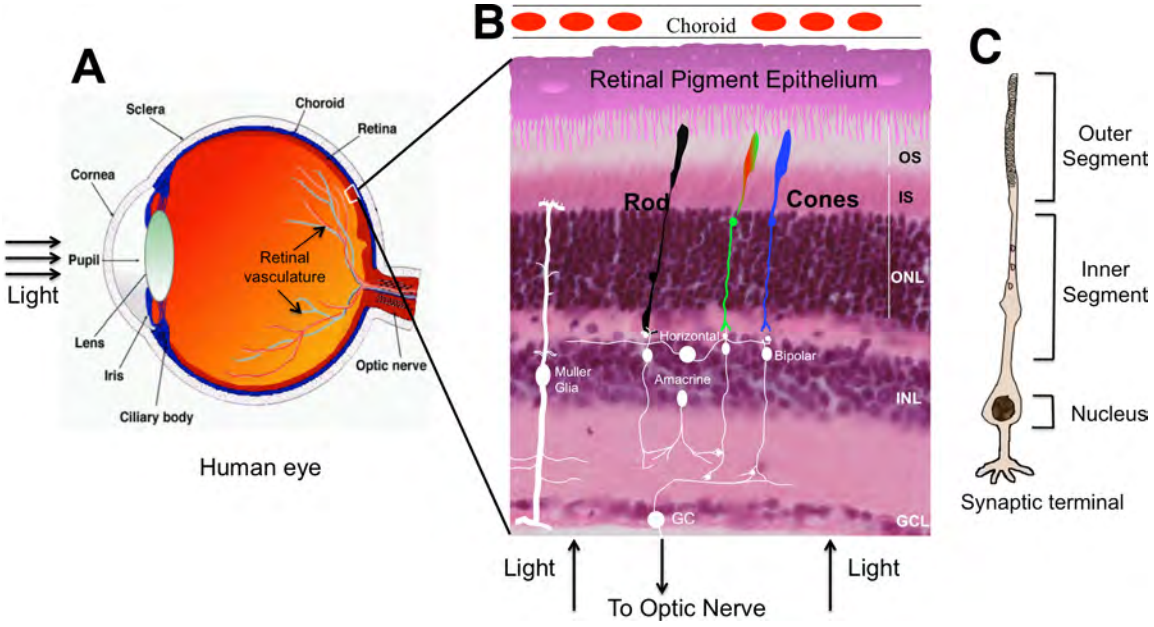

Figure 1.1: Human eye and retinal cell types: Schematic of the human eye (**A**) and haematoxylin and eosin staining of a mouse retinal cross section (**B**) showing the various retinal neurons and the retinal pigment epithelium above. The photoreceptor (PR) cells that initiate the process of vision are of two types, rods and cones. A schematic of a PR cell is illustrated in (**C**). PRs possess an elaborate structure comprising of an outer segment (OS), inner segment (IS) and their nuclei are located in the outer nuclear layer (ONL). (INL: inner nuclear layer, GC: ganglion cell, GCL: ganglion cell layer)

The cone PRs on the other hand, are about 100 times less sensitive to light when compared to rods however, unlike rods they have faster response kinetics and hence can function upon constant light exposure[7]. Therefore, cones mediate daylight vision. In humans, there are three types of cones that are distinguished by the presence of specific opsin proteins that promote the absorption of light of short (blue), medium (green) and long (red) wavelengths, which allows for highly specialized color vision[7,11]. Each cone expresses only one of the 3 opsins (blue, green or red). On the contrary, rods possess only

one opsin known as rhodopsin, which absorbs light in the medium wavelength range. Humans possess a cone-rich region in the center of the retina known as the macula, which confers high-acuity central vision[11]. In contrast, mice have no macula and only two cone opsins that recognize either short or medium wavelengths of light[12,13]. Cones located in the ventral region of the retina in mice however, express both opsins.

Upon absorption of a photon by a PR cell, there is a cascade of biochemical events that converts the captured light into an electrochemical signal. This process is known as phototransduction[14,15]. The signal from PRs is then passed on to bipolar cells, which are located in the inner nuclear layer (INL) and from there, to neurons in the ganglion cell layer (GCL). The axons from the GCL converge to form the optic nerve, which outputs to the visual centers in the brain[15]. In addition to bipolar cells, the INL has horizontal and amacrine cells, which serve to modulate the visual response[3]. The retina also has a glial cell type known as the Müller glia, which traverse the entire tissue and form the blood retinal barrier[16]. The neurons in the INL and GCL receive nutrients and oxygen from the retinal vasculature (Figure 1.1 A). However, the PRs are primarily located in an avascular area, and the nourishment for these cells is derived from the retinal pigment epithelium (RPE), which in turn obtains nutrients from the choroidal vasculature above[17,18]. RPE cells possess microvilli, which are in close association with PR OSs to mediate the transfer of nutrients and oxygen. The RPE also plays a critical role in the regeneration of the chromophore that is required for the visual cycle. Once a photon hits the chromophore, there is a cis to trans isomerization that occurs, which needs to be reversed

to allow for the absorption of a new photon. This involves the shuttling of the chromphore to the RPE, where the isomerization is reversed and then transported back to the PR OSs[19]. Moreover, PRs are known to shed about 10% of their OS every day, which is phagocytized by RPE cells[20,21]. Therefore, RPE cells are critical for the normal functioning of PRs and we will describe these in more detail in subsequent sections of the thesis. Finally, RPE cells are packed densely with pigment granules known as melanosomes, except in albinos, where there is no pigmentation. Melanosomes help in the absorption of scattered light, thereby improving the efficiency of the optical system and reducing photo-oxidative stress[22].

Since PRs constitute about 75% of all retinal cells[2,3] and are required to initial the visual response, diseases that cause blindness often arise from loss of PRs and these may be caused due to genetic defects (inherited) or a combination of genetic and environmental risk factors (acquired). We will focus of inherited PR diseases, which can be broadly classified as cone, cone-rod or rod-cone dystrophies[23]. In the case of cone dystrophy, the disease-causing mutations are expressed in cone-specific genes, while in cone-rod dystrophy; the diseased genes may be expressed in both PR cell types. In either condition, cones are preferentially affected, leading to loss of daylight and color vision. However in some cases of cone-rod dystrophy, both rods and cone may degenerate simultaneously. In case of rod-cone dystrophy, mutations are in genes that are expressed exclusively in rods or in both PR cell types, but preferentially affect rods. Interestingly, in humans and mice, loss of rods is always followed by the degeneration of cones, but loss of cones has a

negligible effect on rods[24-27]. Therefore, even if the mutation only affects the night-active rod PRs, cones degenerate as well leading to the secondary loss of daylight vision. This is particularly interesting because other neurons such as bipolar cells or horizontal cells which form synapses with rods are not affected until the end stages of blindness[28], which raises the question as to why cones are preferentially affected upon loss of rods. Besides being a fundamental question in retinal biology, it is also critical to understand the mechanism of this secondary cone death as it plays a critical role in the retinal degenerative disease Retinitis Pigmentosa, which is the focus of this thesis.

Retinitis Pigmentosa:

Retinitis Pigmentosa (RP) is a group of inherited retinal diseases that lead to blindness due to the loss of rod and cone PRs. The disease has a prevalence of about 1 in 4000 people worldwide and affects more than 1 million individuals[29]. In about 50-60% of cases, the disease is inherited as an autosomal recessive trait, while it is autosomal dominant in 30-40% and X-linked in about 10% of cases[29]. The term ‘Retinitis’ is a misnomer since the term ‘-itis’ is generally used to denote inflammation. While the initial perception was that RP was an inflammatory disorder, it is now clear that this is not the case and there are clear genetic factors that cause it[30]. ‘Pigmentosa’ on the other hand, was used to denote the appearance of pigmentation due to RPE cells that migrate into the neural retina following loss of the PRs[30,31]. This can be observed by fundus photographs of the eye and is also illustrated in Figure 1.2 B.

Thus far, over 60 genes have been identified that when mutated cause RP (RetNet: https://sph.uth.edu/retnet/). While most of these are PR-specific genes, there are exceptions to this. For example, *MERTK* (mer tyrosine kinase proto-oncogene) is a gene that is expressed in RPE cells and is involved in phagocytosis of the PR outer segments. Mutations in this gene cause autosomal-recessive RP due to accumulation of debris in the sub-retinal space, which is the area between the PRs and the RPE[32]. Additionally, dominant mutations in genes such as *PRPF8* and *PRPF3* (pre-mRNA processing factor) are ubiquitously expressed[33,34], however they preferentially affect PRs, the reason for which still remains enigmatic[29]. Moreover, there are instances where patients with RP develop other complications, in which case it is classified as a syndrome. The most common syndrome is Usher's syndrome where visual dysfunction is accompanied by hearing impairment. Another example of syndromic RP is Bardet-Biedl syndrome, where RP is associated with other complications such as obesity, renal disease and other developmental delays[35].

Most RP patients harbor mutations in rod-specific genes due to which RP is synonymous with rod-cone dystrophy[29] (RetNet: https://sph.uth.edu/retnet/). Among these, mutations in the *RHODOPSIN (RHO)* gene alone account for about 25% of the cases of autosomal-dominant RP[29,30]. The disease has a variable onset, with some patients developing vision loss in childhood, while most patients do not experience any apparent symptoms until mid-adulthood[36]. Patients first experience night blindness from the loss of rod PRs, followed by a condition known as tunnel vision, where peripheral vision is lost due to

degeneration of cone PRs in the peripheral areas of the retina. The central region of the retina, which has the cone-rich macula, is always the last to deteriorate in cases of rod-cone dystrophy[30].

In majority of RP cases, patients are unaware of the initial night blindness because in today's modern world with electricity, there is almost no requirement for night vision. However, by the time this stage is reached, there is already severe reduction in cone function, even prior to loss of cone PRs. In fact, a measurement of visual function using electroretinography (ERG) shows that patients as early as 6 years of age already show a decline in visual function, although they do not show any apparent symptoms of RP until adulthood[36]. The ERG measures the electric response that is produced to a light stimulus and is recorded by placing electrodes on the surface of the eye[29]. The ERG allows for early detection of the disease, evaluation of disease progression and its response to treatment[36-38]. Figure 1.2 (A) illustrates examples of ERG recordings from mice with and without RP. The mouse model of RP illustrated here is the retinal degeneration-1 (*rd1)* model[39] and a rapid decline in light-adapted ERG recordings is observed as early as postnatal day (P) 21 in this model, a time point when cone death has just initiated[13,40]. We will describe this model in further detail during subsequent sections of the thesis. Additionally, there are other techniques that may be used to measure the extent of PR degeneration. Optical coherence tomography (OCT) measures the thickness of the ONL and allows for evaluation of retinal morphology in vivo[41]. Fundus photography, performed with an ophthalmoscope allows the physician to obtain images of the back of

the eye, in order to detect pigment granule deposition which are indicative of late stages of RP[31]. Figure 1.2 (B) shows fundus photographs from wild type and *rd1*-mutant mice to illustrate the pigmentation that is observed in RP. Attenuated blood vessels and optic disk pallor are also observed at this stage[30,36]. Finally, due to its genetic inheritance, the family history of the patient also plays an important role in the diagnosis[42].

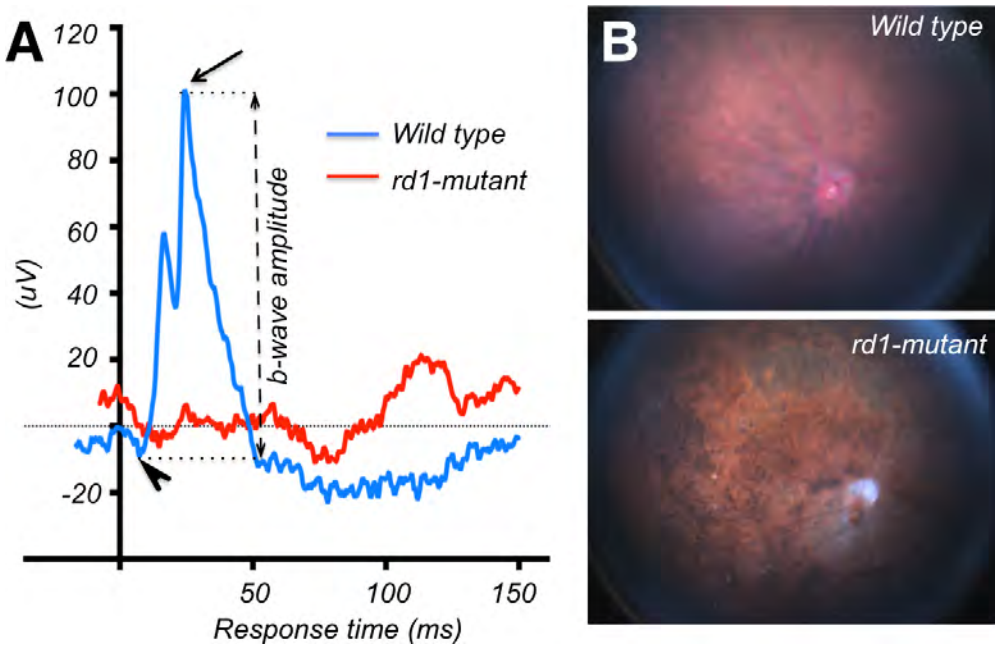

Figure 1.2: Pathological features of RP in mice. (**A**) Representative photopic (light-adapted) ERG recordings from wild type and *rd1* mice. The Y-axis represents the current that is produced in the retina following a light stimulus and is plotted against time after which the stimulus was applied (X-axis). In response to a light stimulus, the PRs hyperpolarize resulting in a negative deflection (arrowheads) known as the a-wave. This is followed by depolarization of the post-synaptic bipolar cells, producing a positive deflection (arrow) known as the b-wave[43,44]. The amplitude of the b-wave is measured from the trough of the a-wave to the peak of the b-wave[45] and is commonly used as a readout of retinal function. ERG responses from *rd1* mice are very low as early as post-natal day 21 (P21). (**B**) Representative funduscopy images from wild type (above) and *rd1* mice (below) at 2 months of age, where retinal pigmentation deposits becomes visible.

Despite the advances made in the identification of genes responsible for RP, there is currently no effective treatment for the condition apart from limited success obtained with vitamin and dietary supplementation[29]. The aldehyde form of Vitamin A is retinal, which forms the visual chromophore, critical for PR function[46]. Clinical trials where patients with RP were administered high doses of Vitamin A (15,000 IU per day) showed modest improvement in visual function as measured by ERG recordings and visual acuity tests[38,47]. Apart from Vitamin A, studies were conducted with docosahexaenoic acid (DHA), an omega-3-fatty acid that forms an important component of the PR membranes[48]. Although DHA supplementation did not show any significant improvement in RP patients[49,50], another study found that RP patients had significantly lower concentrations of DHA in their red blood cells when compared to healthy controls[51]. Recently, a clinical trial reported that X-linked RP patients with DHA supplementation showed modest improvement in visual field tests[52]. However, none of these trials were tested for durations beyond 4-6 years and hence the long-term effects of Vitamin A or DHA supplementation are unknown. Also, continuous intake of high doses of vitamins may not be beneficial to the overall health of individuals[53-55]. More recently, gene replacement strategies using viral vectors have entered clinical trials. The most successful example of gene replacement in humans so far is for Leber's congenital amaurosis-2, a special case of early onset RP caused by recessive mutations in *RPE65* (retinal pigment epithelium-specific 65kDa protein), a gene that is required for proper functioning of the RPE[56]. Proof of concept studies for the therapy in dogs yielded extremely promising results with restoration and preservation of visual function for up to 11 years following

gene delivery[57-62]. While treated patients displayed improvements in visual function, these effects did not persist long-term for all patients and they continued to exhibit PR loss[63,64]. One could speculate several reasons for the limited success in humans such as inefficient vector transduction and/or late stage of intervention when there is already significant PR loss. Therefore, more detailed understanding of the pathology and progression of the disease are critical to develop stage-specific therapies to delay loss of vision. Over the last few decades, several efforts are being made in this direction and these can be broadly classified into three categories, which are related to the stages of progression of the disease, as depicted in Figure 1.3.

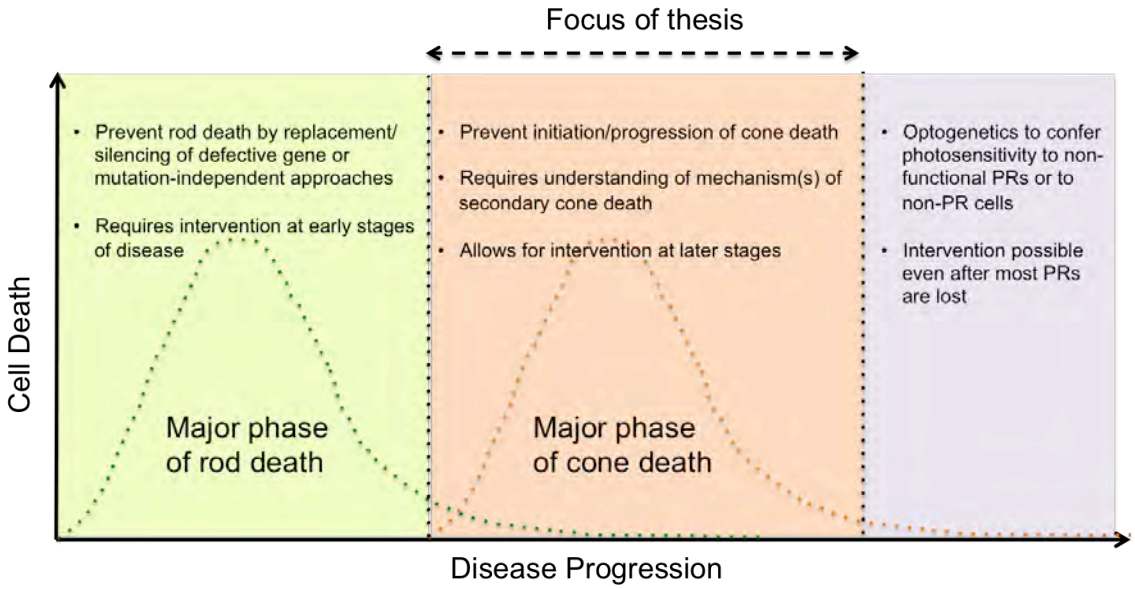

Figure 1.3: Stages of therapeutic intervention for RP. This thesis is focused on understanding the mechanism of secondary cone death, which follows the initial loss of rod PRs. (Figure modeled from Punzo et al, 2012[65])

Stages of therapeutic intervention for RP:

1. Inhibition of rod or early PR death
2. Inhibition of secondary cone death
3. Restoration of visual sensitivity by optogenetics

We will elaborate on each of these approaches, with special emphasis on the second approach, since that forms the basis of this thesis.

1. Inhibition of rod death:

The first approach is to prevent or delay rod death, since rods are the PRs that are affected first in most cases and preventing rod death would also inhibit secondary loss of cones. The most straightforward strategy is to replace the diseased gene with a normal allele in cases of recessive RP[66-68]. For dominant RP, this would involve using approaches like RNA interference (RNAi) or ribozyme to silence the dominant allele[69-71]. While these strategies have been successfully employed in animal models, translating this to humans would depend on establishing clinical studies for every gene. About 60 disease-causing genes have been identified to cause RP and yet, these represent only about 60% of the patient population[29]. Therefore, mutation-independent approaches that allow different patient groups to be treated with a similar strategy represent a more feasible and practical alternative to this approach. This however depends on a deeper understanding of the disease mechanism in order to identify targets for therapeutic intervention that can be applied to a broad spectrum of disease mutations.

Mutation-independent approaches to delay PR death:

Many disease-causing genes in RP are part of the rod phototransduction pathway or encode structural components of the rod outer segments. Recessive mutations in these genes therefore affect normal PR physiology. One example is cGMP phosphodiesterase, an enzyme that forms a critical component of the visual cascade, the absence of which leads to the accumulation of cGMP and elevated levels of calcium, leading to PR cell death[40,72,73]. Loss of this enzyme can be caused due to recessive mutations in *PDE6A* or *PDE6B* genes[29,72,74]. The *rd1* mouse model of RP that was discussed briefly previously also harbors a loss of function mutation in the *Pde6b* gene. In cases of dominant RP, many patients are affected by mutations in *RHODOPSIN*. PR death in such cases is due to misfolding and/or aggregation of mutant RHODOPSIN or from a defect in the structure of the outer segments[29,75-77]. While the primary cause of degeneration in these cases is different, studying the downstream effects of the cellular response may lead to the identification of targets that can be employed to delay PR loss. In this regard, understanding the mechanism of execution of cell death has been an attractive avenue of research. Under various stress conditions, apoptosis, which is a form of programmed cell death, is known to be the main mechanism of rod cell death[13,78]. Apoptosis is executed by cell death proteases called caspases, which recognize specific sequences in their target proteins and cause their cleavage[79]. The X-lined inhibitor of apoptosis (XIAP) is a protein that can bind to caspases and inhibit their function[80]. In this regard, over-expression of XIAP using recombinant adeno-associated viral (rAAV) vectors has been shown to protect PRs both structurally as well as functionally in dominant models of RP, caused by

the P23H or S334ter mutations in the *Rhodopsin* gene[81]. Further, in the *rd10* mouse model of RP, which is also caused by a loss of function mutation in the *Pde6b* gene[82], XIAP was able to improve the efficiency of gene-replacement with the *Pde6b* gene[83]. Moreover, rAAV mediated over-expression of XIAP in rod precursor cells has also been shown to extend their survival when transplanted into a degenerating mouse model of RP[84]. Cell transplantation based therapies using PR precursor cells are an active area of research to replace PRs in a mutation-independent manner and encouraging results have been obtained by these approaches in animal models[85-87]. However, the long-term survival of the newly transplanted donors in a degenerating environment may be a hurdle and supplementation with XIAP or other mechanisms to extend their survival may improve their efficiency.

Another approach to delay PR death is through the administration of neuroprotective factors such as brain derived neuroprotective factor[88], glial cell-line derived neuroprotective factor[89] and the ciliary derived neuroprotective factor (CNTF)[90-92], all of which confer neuroprotection in animal models of RP. Among these, CNTF has been extensively studied and shown to be effective in various animal models of RP, although its mechanism of action is not understood yet. A recent study showed that gene therapy with *Cntf* conferred long-term protection to both rod and cone PRs in a mouse model of RP[93]. The positive data from these experiments have encouraged clinical trials for late and early stage RP where capsules are implanted into the eye to release CNTF (NCT00447980 and NCT00447993, from clinicaltrials.gov). The data from animal

models as well as results of the clinical trials may further encourage the development of gene therapy strategies using *CNTF*.

Another approach to delay PR death has been through the use of the histone deacetylase *Hdac4*, the expression of which has been shown to delay both rod and cone death and restore function in the *rd1* mouse model of RP[94,95]. However, the ability of *Hdac4* to extend PR survival in other models remains to be tested.

A recent and rather creative approach to delay PR death leverages a specific developmental difference between rods and cones. The neural retina-specific leucine zipper protein (*NRL*) is expressed in PR progenitor cells that are fated to become rods[96]. In the *rd1* mouse model, removing *Nrl* from adult rods caused them to become more cone-like, making them less vulnerable to the primary mutation, thereby improving PR survival as well as function[97]. This approach can principally be applied in a mutation-independent manner to any rod-specific mutation.

Collectively, these studies show that it is possible to target common nodes in the rod degeneration process and that mutation-independent approaches a more attractive strategy for therapeutic intervention. However, since most of these approaches are targeted towards rescuing the rods, they would have to be applied prior to the loss of most rods. As previously discussed, diagnosis of RP at the initial stages of night

blindness is often rare, which limits the window of therapeutic intervention for these approaches.

2. Inhibition of secondary cone death:

Since rod death is always followed by cone death in humans and mice, and because cones are the neurons that mediate daylight vision, strategies that delay death of cone PRs would be an alternative option to extend vision. However, developing a strategy to delay cone death requires understanding of the mechanism(s) of secondary cone death. Since cone death occurs irrespective of the primary mutation in rods, the reason(s) for cone death is likely to be the same across various rod-specific mutations. Many theories have been proposed to explain the interdependence of cones on rods. Such theories include the secretion of toxic products by dying rods or overactive microglia recruited to remove dying rods secrete toxins that are harmful to cones[98,99]. However, the kinetics of rod and cone death suggest that this is an unlikely scenario, since cone death does not initiate until the final stages of rod death[13]. If cones were dying due to toxic byproducts, cone death should have initiated during the major phase of rod death and not after most rods have died. Another theory is the absence of a trophic factor that is secreted by rods and is required for cone survival[100-102]. There is also a proposition that once rods are lost, cones are exposed to higher levels of oxygen from the choroidal vasculature above, resulting in increased oxidative stress[103-105]. Our laboratory recently proposed a different theory suggesting that cones suffer from a nutrient shortage induced by disruption of the retinal architecture once most rods have been lost[13]. Our model as well as the oxidative stress

and trophic factor models are not mutually exclusive and we will elaborate further on these below.

A. Oxidative stress model:

Like all neurons, PRs require large amounts of ATP to re-equilibrate their membrane potential, since they constantly hyperpolarize in response to light[106,107]. This requirement is higher for cone PRs since they are active throughout the day, as opposed to rods. Concordantly, cones in mice have nearly twice the number of mitochondria as rods, while this number is increased ten-fold in primates[108,109]. The high rate of mitochondrial activity is accompanied by the generation of reactive oxygen species (ROS), which are formed as a byproduct of mitochondrial metabolism[110]. Further, PRs are constantly exposed to the ultraviolet radiation from sunlight and the reactions involving the chromophore as part of the visual cycle result in the generation of free radicals[111-113]. In order to counteract the oxidative stress, the inner segments of PRs are packed with antioxidant enzymes such as superoxide dismutase and glutathione peroxidase[8,112]. On the contrary, PR outer segments have evolved a natural mechanism to eliminate oxidized lipids and proteins. PRs shed about 10% of their OS daily, which is phagocytized by the RPE, through which they are able to remove the toxic byproducts of oxidative metabolism[20,21]. The importance of maintaining normal ROS levels in PRs is further supported by the fact removal of a subunit of NADPH oxidase, an enzyme complex that produces ROS, confers protection to PRs against light-induced degeneration[114].

Since rods constitute about 95% of the total PRs, they consume most of the oxygen in the outer retina. Therefore once the rods die, the remaining 3-5% of cones are now faced with an overload of oxygen[105,115,116]. The oxidative stress model for secondary cone death therefore suggests that the cell number in the PR layer is a critical determinant of cone death and may also explain why cone death is a rather slow process in RP, since oxidative damage may accumulate over a long period of time and eventually kill cones. In this regard, systemic delivery of antioxidants has prolonged cone survival in various models of RP[104,117]. Co-expression of anti-oxidant enzymes such as catalase and superoxide dismutase-2 also delayed cone death in the *rd10* mouse model of RP[118]. More recently, rAAV-mediated expression of the nuclear factor erythroid derived 2 like 2 (*Nrf2*), a transcription factor that regulates various antioxidant enzymes was shown to effectively delay cone death in three mouse models of RP[119]. rAAV-mediated delivery of antioxidant enzymes to cone PRs avoids the side effects of globally reducing ROS levels that can occur when antioxidants are administered orally or through other systemic routes[120].

B. Rod-derived cone viability factor:

Research efforts to determine trophic factors produced by rods led to the identification of the rod-derived cone viability factor (RdCVF) in 2004[102]. This factor is encoded by the nucleoredoxin-like 1 gene (*NXNL1*) and functions as a thioredoxin-like protein.[121] Since its discovery, various studies have demonstrated its protective effect in mouse models either by direct injection as a peptide[122] or as a gene therapy[123]. Consistent with the

thioredoxin nature of this factor, retinae of mice lacking the *Nxnl1* gene exhibit increased oxidative stress and progressive decline in cone and rod function[124]. Therefore, one could speculate that RdCVF protects cones in RP by reducing oxidative stress. However, a recent study led to the finding that the mechanism of RdCVF-mediated protection is its indirect interaction with glucose transporter-1, which increases glucose uptake in cone-enriched cultures thereby improving cone cell metabolism.[125] This is directly in line with our proposed model for secondary cone death, which suggests that cones suffer from a glucose shortage upon the loss of rods.

C. Metabolic model of cone death:

PRs are among the highest energy consuming cells in the human body[106]. First, they utilize large amounts of ATP in order to re-equilibrate membrane potential in response to photons of light, as previously discussed. Second, the PR OSs are very densely packed with lipids and proteins in order to facilitate the capturing of photons[5,6]. In fact, the average lipid content of a PR cell is about 15%, when compared to about 1% for 'normal' cells[6]. Under these circumstances, when a PR cell sheds about 10% of its OS daily, the amount of new lipid and protein that needs to be resynthesized every day is tremendous[126,127]. PRs have thus developed elegant mechanisms to enable them to achieve their high metabolic demands. PRs derive glucose primarily from the RPE cells and they have been shown to take up lactate from Müller Glia cells, with which they are in intimate contact in vivo[128,129]. While glucose is the predominant source of ATP in most cells, lactate can also be converted to pyruvate and enter the Kreb's cycle to fuel ATP

synthesis[130]. Glucose can therefore be utilized in other biosynthetic pathways to generate building blocks for membrane synthesis and this is a common feature of cells with a high rate of cell division[131]. Interestingly, there is a study which suggests that most of the glucose taken up by PRs does not enter the Kreb's cycle[129], which suggests that similar to proliferating cells, PRs may divert most of their glucose for anabolic functions[132].

The PR OSs are in intimate contact with the RPE cells and these RPE:OS interactions are critical for the transfer of nutrients like glucose from the RPE into PRs. Each RPE cell interacts with about 25-30 PR OSs[126,133]. However, because in humans and mice rods outnumber cones at a ratio of 20:1, most of these RPE:OS interactions are those of the RPE with rod OSs. Consequently, only one or two cone OSs are in contact with each RPE cell. During the initial phases of rod death, these interactions are still intact, however as the disease progresses, the massive death of rods causes a disturbance of the architecture of the PR layer. This is because rods are much more abundant than cones and upon their loss, the PR layer collapses (See Figure 1.4 for illustration). This perturbs the interactions of the remaining cone OSs with the RPE, which affects the flow of nutrients into cones. Thus, we hypothesized that once a critical ratio of rods to cones is breached per RPE cell, cone death initiates as a cell-autonomous event due to a reduction in nutrient flow from the RPE. To test this hypothesis, we compared the kinetics of rod and cone death across four different mouse models of RP, each of which have a mutation in a rod-specific gene that causes the rods to die at different rates[13]. We observed that regardless of the primary mutation in rods, cone death initiates only after about 90% of

rods have died. Therefore, the remaining 10% of rods could represent the critical ratio at which cone death initiates as a cell autonomous event. The gradual reduction in nutrient levels may also explain why cones survival for extended periods of time following death of rods.

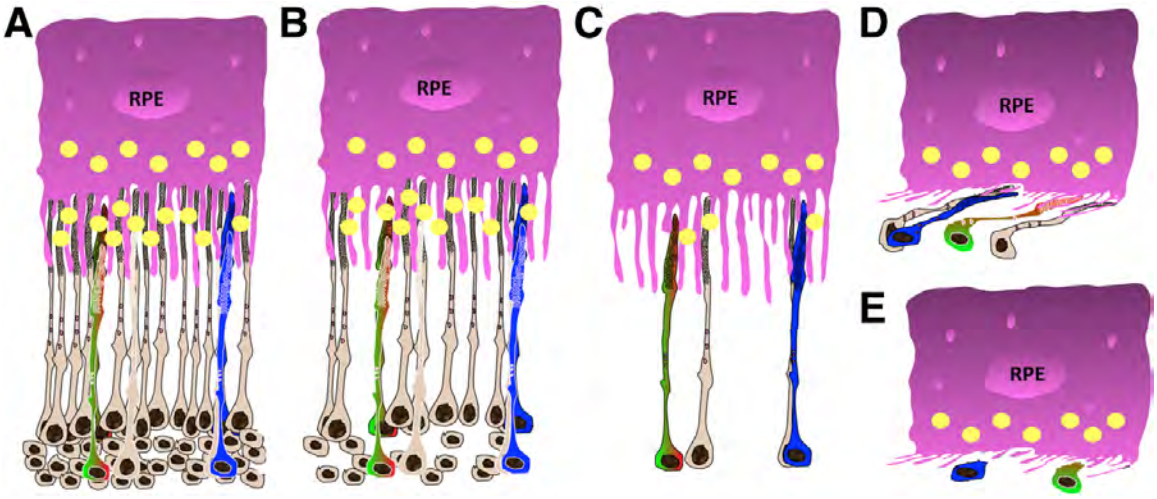

Figure 1.4: Starvation model for cone death in RP. **(A)** In a normal retina, rods and cones interact with the RPE via their outer segments allowing for transfer of nutrients (depicted as yellow dots). During early stages of rod loss, these interactions are still intact **(B)**, however once most rods are lost **(C)** these collapse of the PR layer results in the breaching of the RPE:cone OS interactions **(D-E)** reducing flow of nutrients into cones. Rods are depicted in white, while cones are shown in red-green and blue colors.

Since RPE is the primary source of glucose for PRs, loss of the RPE:cone OS interactions are likely to reduce glucose levels in cones and its subsequent divergence into biosynthetic pathways like the pentose phosphate pathway (PPP). The PPP generates NADPH as a byproduct, which is used as reducing agent for lipid synthesis. The shortening of cone OSs that is seen during degeneration may be indicative of a deficit of lipids due to insufficient NADPH that is required for their synthesis[13,134]. Further,

NADPH is also required for the regeneration of the visual chromophore necessary for PR function. The first step in chromophore recycling is the conversion of all-trans retinal into all-trans retinol and requires NADPH as a reducing equivalent[19]. Thus, the inability to efficiently regenerate of the chromophore could explain the reduction in cone function during disease. Lastly, NADPH also functions as a reducing agent for glutathione, which serves to counteract the effects of oxidative stress[135]. Therefore, a lack of NADPH is also consistent with increased oxidative stress in cones during disease.

In addition to the kinetics of rod and cone degeneration across the four mouse models of RP, the following evidences also encouraged us to propose that cones suffer from a nutrient shortage[13]. During cone degeneration, we found an upregulation of the hypoxia-inducible factor-1 alpha (HIF-1α) and its target gene the glucose transporter-1 (GLUT1). HIF-1α is a transcription factor that is normally increased during stress conditions such as hypoxia or starvation to improve glycolysis[136]. Since the loss of rods leads to hyperoxic conditions in cones, the increase in HIF-1α is likely to represent a shortage of glucose. Our hypothesis was further corroborated by microarray analysis carried out across the four mouse models of RP, which revealed an increase in the expression metabolic genes at the onset of cone death, particularly genes of the insulin/AKT/mammalian target of rapamycin (mTOR) pathway, a key pathway that regulates cell metabolism, growth and survival[137]. Concordantly, we found that cones showed increased phosphorylation of the ribosomal protein S6, a bona fide mTOR

target[137], suggesting that cones were increasing the activity of this pathway, to potentially adapt to the shortage of nutrients.

To test whether further activation of the insulin/mTOR pathway would enhance cone survival, we treated the *rd1* mouse model of RP with daily systemic injections of insulin. We found that cone survival did improve, however the therapeutic effect of insulin lasted only for a period of four weeks.[13] Prolonged treatment with insulin did not result in further improved survival, potentially due to the negative feedback loop within the insulin/mTOR pathway[137], leading to a state of insulin resistance. However, our results were encouraging and suggested that activation of pro-growth and/or pro-survival mechanisms downstream of the insulin receptor can prolong cone survival. This thesis is largely based on studying the events downstream of the insulin receptor that contribute to cone survival. We will further elaborate on the insulin/mTOR pathway in the following sections.

3. Restoration of visual sensitivity by optogenetics:

Optogenetics is an emerging field where transmembrane light-sensitive receptors are delivered to the eye either to restore visual sensitivity in PRs that have become non-functional or expressed in non-PR cells such as bipolar or ganglion cells to make them photosensitive[138]. These light receptors are opsin-like proteins such as channel rhodopsins and halorhodopsins, which are delivered using rAAV or lentiviral vectors[138-141]. While these proteins are activated in response to light photons, some of them produce an

excitatory current while some produce an inhibitory current[138]. Concordantly, individual or combinatorial expression of these proteins have been shown to produce either ON, OFF or a combination of the two responses in the inner retinal neurons following death of PRs[142-145]. Expression of halorhodopsin has also successfully restored visual sensitivity of dormant cones in mouse models of RP[141]. The strategy therefore allows for therapeutic intervention at late stages of disease. Further, optogenetics can be used to supplement approaches that extend PR survival discussed so far, thereby improving their functionality.

The large number of approaches as well as disease targets being pursued increase hope that there will be therapeutic strategies that will effectively prolong vision in people affected by inherited retinal degenerations. A combination of these approaches may be more beneficial than a single approach. However regardless of the results obtained in animal models, effectiveness in human patients will be the ultimate test for any therapy.

Background on the insulin/AKT/mTOR pathway:

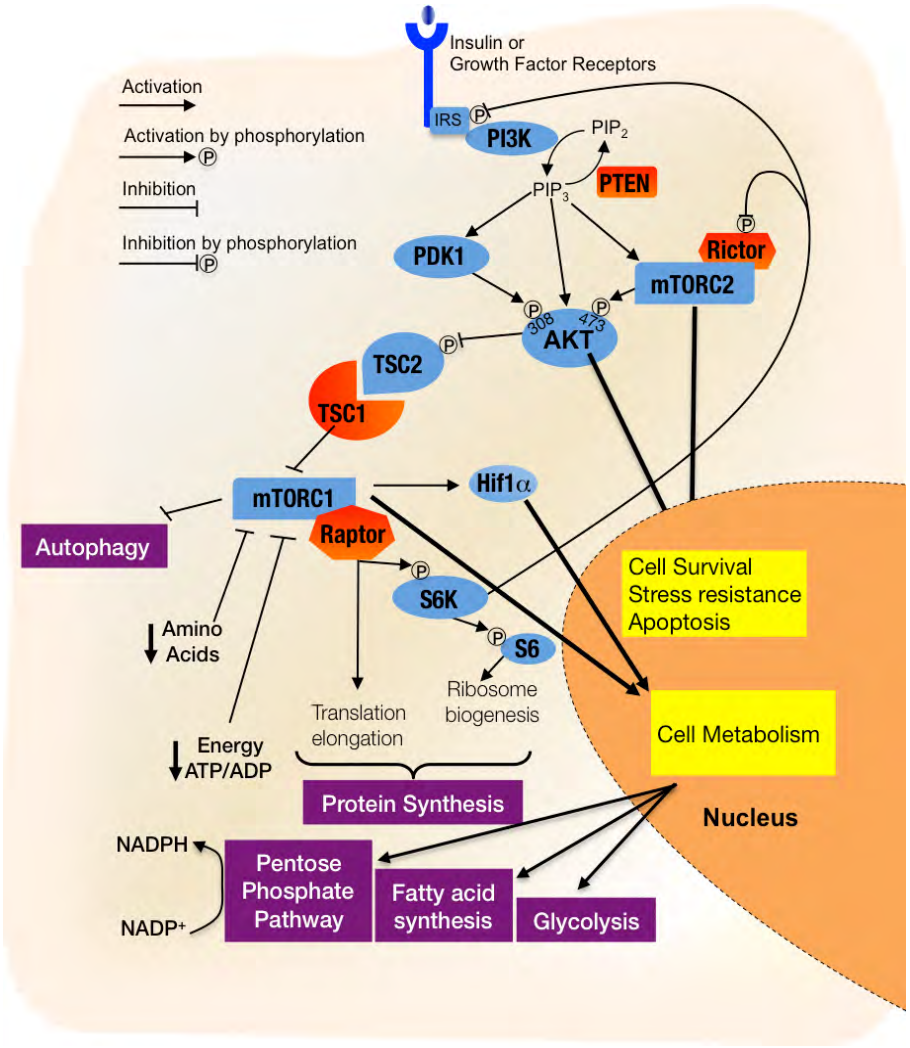

Figure 1.5: Schematic of the insulin/AKT/mTOR pathway. The schematic is a simplified version of the pathway and is focused on the components that are important to this study. mTOR exists as part of two complexes; mTORC1 which regulates pro-growth processes like protein synthesis, glycolysis, lipid synthesis and inhibits autophagy, while mTORC2 regulates mainly pro-survival process. Both mTOR complexes are activated in response to growth factors, while mTORC1 is also sensitive to amino acids and energy levels. See main text for more details on the pathway regulation.

Upon binding of growth factors like insulin, tyrosine kinase (TK) receptors such as the insulin receptor phosphorylate and recruit adaptor proteins such as the insulin receptor substrate (IRS)[146]. Phosphorylated IRS proteins in turn facilitate the recruitment of

phosphatidylinositol-3-kinase (PI3K) to the plasma membrane, which increases the levels of the secondary messenger phosphotidylinositol triphosphate (PIP3) that mediates various downstream functions of insulin. The effects of growth factor stimulation are counteracted by PTEN (phosphatase and tensin homolog), which converts PIP3 to PIP2, thereby reducing downstream signaling events.[147]

Two key kinases downstream of PIP3 that are central to the insulin/AKT/mTOR pathway are protein kinase B (PKB), also known as AKT, and the mammalian target of rapamycin, mTOR. AKT has a multitude of targets and 3 isoforms that are often cell-type specific[148]. In contrast, mTOR is found in 2 large protein complexes referred to as mTORC1 (mTOR complex 1), which is characterized by the accessory protein Raptor (regulatory-associated protein of mTOR) and mTORC2 (mTOR complex 2) characterized by the accessory protein Rictor (rapamycin-insensitive companion of mTOR)[149]. The two mTOR complexes possess a distinct set of functions and targets. Increased PIP3 levels promote 3-phosphoinositide-dependent protein kinase (PDK1) and mTORC2 activity[150]. In turn, PDK1 and mTORC2 phosphorylate AKT on Thr308 and Ser473 respectively. While phosphorylation on both AKT sites is required for full activation of AKT, phosphorylation of AKT at Thr308 is sufficient for its activity towards mTORC1, and does not require mTORC2-mediated phosphorylation at Ser473[149]. Activated AKT phosphorylates two distinct substrates that lead to activation of mTORC1. Phosphorylation of the tuberous sclerosis protein TSC2 known as tuberin, relieves the inhibitory effect of the tuberous sclerosis complex (TSC) on mTORC1[149,151].

The TSC is composed of TSC2 in association with two other proteins, TSC1 (hamartin) and TBC1D7 (Tre2-Bub2-Cdc16 (TBC) 1 domain family, member 7), both of which are required for complex stability to mediate to downstream effects of the complex[152]. The TSC acts as a GTPase activating protein (GAP) for Rheb (Ras-homolog enriched in the brain). In its GTP-bound form, Rheb promotes activation of mTORC1, and its conversion to GDP-Rheb by the GAP activity of the TSC complex results in inhibition of mTORC1[153,154]. The second mode of activation of mTORC1 by AKT is through phosphorylation of PRAS40 (proline-rich AKT substrate 40kDa). PRAS40 inhibits mTORC1 activation by binding to its accessory protein Raptor, and this is relieved by AKT-mediated phosphorylation[155]. Upon mTORC1 activation, the ribosomal protein S6-kinase (S6K), a target of mTORC1, phosphorylates the IRS and prevents further downstream signaling, thereby closing the feedback loop and preventing over-activation of the pathway[156,157]. This is also the feedback loop that we hypothesized was responsible for limiting the protective effect of insulin in our studies[13]. S6K also phosphorylates Rictor, the accessory protein of mTORC2, which results in the inhibition of mTORC2 activity towards its targets such as the serum and glucocorticoid-regulated kinase (SGK) and protein kinase C (PKC). However, S6K mediated phosphorylation of mTORC2 does not affect its activity towards AKT[137,158-161]. These feedback loops between mTORC1 and mTORC2 as well as between mTORC1 and the IRS allows cells to fine tune mTOR activity in response to growth factors and other signals.

mTOR complexes: Composition, functions and regulation

mTOR was identified as the target of rapamycin (also known as Sirolimus), an immunosuppressant and antiproliferative agent produced by the bacterium Streptomyces hygroscopicus in the Rapa Nui island, hence the name rapamycin[162-164]. mTOR has a C-terminal protein kinase domain that is similar to PI3K and thus, belongs to the family of PI3K-related protein kinases (PIKK). Other kinases in this family include proteins like ATM, ATR and DNA-PK, which are involved in regulating DNA damage and genotoxic responses[155]. In contrast, mTOR is mainly responsible for regulating responses to various other stresses such as nutrient, oxygen and energy deprivation.

As mentioned previously, mTOR is found in two distinct complexes, mTORC1 and mTORC2 that are characterized by their unique accessory proteins Raptor and Rictor, respectively[165,166]. These accessory proteins are indispensible for complex assembly and for the binding of mTOR to substrates and regulatory proteins[137]. Additionally, the two mTOR complexes also contain shared components such as mammalian lethal with SEC13 protein 8 (mLST8) and the DEP domain containing mTOR interacting protein (DEPTOR) as well as other proteins unique to each complex[137,167,168]. Rapamycin inhibits mTORC1 activity potentially by weakening the interaction of Raptor with mTORC1[169]. However, prolonged exposure to rapamycin has been also shown to reduce mTORC2 activity in certain systems and this is attributed to the sequestration of the pool of free mTOR, thereby reducing mTORC2 complex formation[137,170]. While both mTOR complexes are activated in response to growth factors as described above, mTORC1 is

additionally regulated by factors such as energy, nutrient and oxygen levels in cells. mTORC1 integrates these inputs and promotes various pro-growth process such as protein synthesis, ribosome biogenesis, lipid and mitochondria synthesis and inhibits catabolic processes like autophagy. In contrast, little is known about other modes of activation of mTORC2, which regulates mainly pro-survival processes[137,155].

Activation of mTORC1:

Nutrients: Amino acids are essential for synthesis of proteins, which are the building blocks of the cell. Additionally, amino acids are also required to generate substrates that feed into metabolic pathways such as the Kreb's cycle and hence also required for the synthesis of ATP[155]. mTORC1 is a master regulator of protein synthesis and therefore sensitive to the levels of amino acids in the cell. The activation of mTORC1 by amino acids is complex and involves various proteins, among which the Rag GTPases are key players[171,172]. These proteins belong to the Rag family of small GTPases and exist on the surface of the late endosome and lysosome as heterodimers of either RAGA or RAGB in combination with either RAGC or RAGD. Under conditions of sufficient amino acids, the Rag heterodimers assume an active conformation, where RAGA/B are bound to GTP, while RAGC/D are GDP bound. Under amino acid starvation, the GTP-GDP loading states are reversed. In their active conformation, the Rag heterodimers interact with Raptor, thereby recruiting mTORC1 to the surface of the lysosome. Therefore under conditions of amino acid availability, mTORC1 is localized at the lysosome. This step is critical because it facilitates interaction of mTORC1 with Rheb, which also resides on the

lysosome and this interaction is critical for the activation of mTORC1[171,172]. Amino acids were also shown to regulate TSC2 localization, where under conditions of amino acid starvation, TSC2 is recruited to the lysosome to inhibit Rheb, which consequently inhibits mTORC1 activity[173]. Together, the above studies establish that the lysosome is a critical site that integrates both growth factor as well as nutrient inputs to mediate activation of mTORC1.

Growth factors: The effect of growth factors such as insulin on activation of mTORC1 was previously discussed and Rheb, which in its GTP-bound form promotes mTORC1 kinase activity, is a critical mediator of these effects. Besides promoting phosphorylation and inhibition of TSC2 by AKT, growth factor stimulation also results in the dissociation of TSC2 from the lysosome, thereby relieving its inhibition on Rheb[174]. Growth factors can also activate mTORC1 through pathways outside of the PI3K-AKT axis. One such example is the activation of the Ras pathway by growth factors, which in turn activates the extracellular regulated kinase (ERK) that phosphorylates and inhibits TSC2[175]. Additionally, Wnt signaling can also activate mTORC1. Wnt inhibits glycogen synthase kinase 3β (GSK3β), which inhibits TSC2 by phosphorylation, thereby activating mTORC1[176].

Glucose, oxygen and energy levels: Glucose and energy levels are tightly linked because the energy from glucose is converted to ATP during glycolysis and oxidative metabolism and thus under low glucose conditions, ATP levels decline. mTORC1 detects the

reduction in ATP using a sensor known as the AMP-activated protein kinase (AMPK). The levels of AMP and ATP in the cell regulate AMPK allosterically[177] and upon low ATP levels, AMPK inhibits mTORC1 by two mechanisms. AMPK phosphorylates TSC2, stimulating its inhibitory effect on mTORC1[178]. Besides, it also phosphorylates Raptor and promotes its binding with the 14-3-3 proteins, thereby preventing its association with mTORC1[179]. Other than glucose starvation, stress such as hypoxia can also lead to an energetic imbalance by impairing mitochondrial metabolism leading to AMPK activation[137].

Functions of mTORC1:

Protein synthesis and ribosome biogenesis: Protein synthesis is an energy consuming process requiring ATP, GTP as well as synthesis of ribosomal units[155]. Being a sensor of nutrient and energy levels in the cell, it is not surprising that mTORC1 plays a critical role in regulating this energy-costly process. Two target proteins are predominantly responsible for mediating the effects of mTORC1 namely, S6 kinase (S6K) and eIF4E-binding protein 1 (4EBP1). eIF4E is the eukaryotic translation initiation factor 4E which recruits initiation factors at the 5' end of most mRNAs, and is inhibited upon binding to 4EBP1[180]. This inhibition is relieved upon phosphorylation of 4EBP1 by mTORC1, thereby initiating translation[181]. Phosphorylated S6K promotes mRNA translation by phosphorylating proteins such as eIF4B[182] and eEF2K[183] (eukaryotic elongation factor 2 kinase). Additionally, S6K is known to increase transcription of rRNA polymerase RNA polymerase 1 (RNAP1), which is involved in the synthesis of ribosomal RNAs and

proteins[184]. S6K also phosphorylates S6, which is a component of the 40S ribosome. While the role of this phosphorylation remains unclear, it is one of the most commonly used readouts of mTORC1 activity[137,154].

Metabolism: Gene-expression profiling of cells with constitutively activated mTORC1 signaling mediated by loss of the TSC revealed that mTORC1 increases the expression of various genes involved in glycolysis, lipid synthesis and the PPP[185]. These effects of mTORC1 are mediated by its activation of the sterol regulatory element binding proteins (SREBP) and the hypoxia-inducible factors (HIF). SREBP-1 is normally activated in response to low sterol and lipid levels and undergoes a processing step, which involves cleavage into the active form, which then binds to specific sterol regulatory DNA elements[186]. Activated mTORC1 promotes the posttranslational processing of SREBP-1, thereby increasing expression of various genes involved in lipid biosynthesis and the PPP[185]. mTORC1 also increases the translation of HIF-1α, which is known to improve glycolysis through increasing expression of enzymes such as hexokinase, phosphofructokinase and pyruvate dehydrogenase, besides improving glucose uptake by the cell through increased expression of the glucose transporter-1[185]. Activation of mTORC1 is also known to increase mitochondrial biogenesis and oxidative metabolism by promoting transcriptional activity of PPARϒ co-activator-1 (PGC1α), a co-activator of genes involved in mitochondrial metabolism[187]. Together, these examples show how mTORC1 impinges on various aspects of cell metabolism at the transcriptional, translational or post-translational levels.

Autophagy and the ubiquitin-proteosome system: Autophagy is a catabolic process by which cells degrade cytoplasmic proteins and organelles in lysosomes in order to maintain homeostasis, and is especially important for balancing cellular resources under conditions of nutrient or energetic stress[188]. The primary form of autophagy is macroautophagy (henceforth, referred to as autophagy) where cytoplasmic cargo is delivered to double-membrane organelles called autophagosomes that later fuse with the lysosome to form autolysosomes, leading to degradation of its contents[189]. mTORC1 functions as a major negative regulator of autophagy and under nutrient replete conditions, when mTORC1 is active, it inhibits the initiation of autophagy[190]. Consequently, constitutive activation of mTORC1 in tissues such as skeletal muscle and liver leads to accumulation of undigested proteins[191-195]. Conversely, inhibition of mTORC1 by rapamycin or other mTOR inhibitors induces autophagy[196]. mTORC1 directly phosphorylates ATG1 (autophagy-related gene 1) also known as ULK1 (unc-51 like autophagy activating kinase 1), and ATG13 (autophagy-related gene 13) proteins that are involved in the formation of the phagophore or the pre-autophagosome, thereby inhibiting the process at its inception[190,197]. Since autophagosomes are known to engulf portions of the cytoplasm, autophagy was typically known as a non-selective process[198]. However over the last decade, the identification of autophagy receptors and adaptor proteins points towards a great deal of selectivity in the degradation of autophagic cargo[199,200]. We will discuss selective autophagy and other autophagy regulatory mechanisms in the following sections.

The ubiquitin-proteosome system is involved in the recognition, targeting and degradation of ubiquitinated proteins by the proteasome and is the predominant pathway for non-lysosomal degradation in the cell[201]. A recent study showed that mTORC1 promotes proteosomal degradation by increasing the expression of the master transcription factor nuclear factor erythroid-derived 2-related factor 1 (NRF1; also known as NFE2L1), which regulates the expression of various proteosomal genes[202]. The increase in proteosomal degradation therefore serves as a resource for cells to maintain a constant supply of amino acids in order to keep up with the increased rate of protein synthesis that is seen upon activation of mTORC1. Thus, mTORC1 exerts opposing effects on the two major degradation systems in the cell, exemplifying its complex regulation of cell metabolism and homeostasis.

Functions of mTORC2:

mTORC2 is known to phosphorylate proteins belonging to the AGC family of kinases such as AKT, SGK and PKC through which it exerts its effects on cell survival[203-205]. Additionally, it is known to control proteins involved in the regulation of cytoskeletal organization and polarity[206,207]. While mTORC1 is localized to the lysosome, it is suggested that mTORC2 is found at the plasma membrane[208], consistent with its role in regulating cell polarity as well as phosphorylating AKT following activation by growth factors. The phosphorylation of AKT by mTORC2 at Ser473 enhances AKT phosphorylation on Thr308 by PDK1, and together they completely activate AKT.[137]

However, mTORC2-mediated phosphorylation of AKT is not required for its activity towards all substrates, as previously stated. For example, AKT-mediated inhibition of TSC2 does not require AKT to be phosphorylated at Ser473 by mTORC2. However, loss of mTORC2 suppressed the AKT-dependent phosphorylation of the forkhead box proteins FOXO1 and FOXO3[137,161]. The FOXO proteins are transcription factors that activate a variety of genes involved in apoptosis and cell cycle arrest[209]. mTORC2 causes exclusion of FOXO from the nucleus[210,211] through AKT-mediated phosphorylation of FOXO, thereby playing an indirect role in cell survival. However, the FOXO proteins are also known to transcribe other autophagy and lysosomal-related genes and therefore, the effects of FOXO translocation will have to be assessed based on the cellular context[212,213]. Besides AKT, the SGK family of proteins is also known to regulate FOXO translocation as well as the expression of ion channels, thereby also regulating cell size[214,215].

The insulin/AKT/mTOR pathway in PRs:

Given the high-energy demands of PRs, it is surprising that not many studies have focused on characterizing the role of this pathway in rods or cones. Loss of the insulin receptor, as well as one of the *Akt* isoforms, *Akt2* increases sensitivity to degeneration induced by light-stress in rod PRs[216,217]. With regard to cones, loss of three of five regulatory subunits of *Pi3k* in cones is known to induce cone degeneration[218,219]. While this suggests that PI3K activity is critical for cones, not much is known about the signaling events downstream of this kinase that are essential for cone metabolism. This is important because it is possible that the protective effects of insulin as well as growth

factors such as CNTF were mediated downstream of PI3K. My thesis work stems from these gaps in the field and is focused on the characterization of the insulin/mTOR pathway in mouse models of RP. Manipulation of cell metabolism generally influences autophagy and in our case hopefully also cell death (apoptosis: in particular caspase-2 mediated) thus we have also explored these aspects during the progression of cone death in RP. A brief introduction of these two processes is provided below.

Apoptosis and Caspase-2:

Apoptosis is a highly regulated form of programmed cell death where a series of biochemical events lead to the dismantling of a cell, without leakage of the cellular contents to the extracellular space[220]. Apoptosis is mediated by a family of cysteine proteases known as caspases, which can be broadly classified as initiator or executioner caspases depending on whether they initiate or partake in the cell death process[221,222]. Caspases are synthesized as pro-caspase zymogens, which are later activated to mediate apoptosis. Initiator caspases (examples are caspase-2, -8, and 9) are usually activated by proximity-induced oligomerization, aided by adaptor molecules, which bring procaspase molecules together, which is followed by autocatalytic processing to yield active caspase molecules[223]. Oligomerization of caspase precursor molecules is however, sufficient to activate initiator caspases and the subsequent cleavage only enhances caspase activity[224,225]. Once active, initiator caspases activate executioner caspases (examples are caspase-3, -6 and 7) by cleavage, which later mediate cell death by cleaving important cellular proteins[221]. Caspase activity can thus be detected by various methods such as

assessing cleavage of the caspase itself, or cleavage of its target proteins by western blot. Other methods include the use of peptides that harbor the amino acid sequence, usually 4-5 amino acids in length, that is recognized by a specific caspase[226]. When such a peptide is coupled with a fluorescent dye or streptavidin tag, it can be used either for in vivo imaging of caspase activity in cells/tissues or for immunoprecipitation experiments.

Caspase-2 has been regarded as the most evolutionarily conserved caspase because it shares about 43% amino acid identity with the *C.elegans* programmed cell death gene (CED-3)[227]. The precursor protein of caspase-2 has three regions; an N-terminal prodomain, which contains the CARD motif that facilitates interaction between procaspase molecules, followed by a large and small subunit, which together forms the catalytic unit of the caspase[224]. Adaptor proteins such as RAIDD (receptor-interacting protein associated CED-3 homologous protein with a death domain) and PIDD (p53 induced protein with a death domain) bring procaspase molecules together in a complex known as the PIDDosome, which facilitates interaction between precursor caspase-2 molecules, the first step in initiator caspase activation[228]. This step can be activated by stimuli such as heat shock, DNA damage or by mere overexpression of the precursor caspase[229]. This is followed by a series of autocatalytic processing steps resulting in removal of the prodomain and cleavage between the large and small subunits resulting in a stable heterodimer, which forms the fully active enzyme. However, it should be noted that the uncleaved procaspase dimer itself has catalytic activity, albeit to a lesser extent[224]. Once active, caspase-2 functions by cleaving molecules like Bid, a pro-

apoptotic protein, which disrupts the mitochondrial integrity, thereby releasing molecules like cytochrome c and AIF (apoptosis inducing factor) found in the mitochondrial intermembrane space[230,231]. Cytochrome c facilitates activation of other initiator caspases like caspase-9, while AIF promotes chromatin condensation and DNA fragmentation. Together, these events result in dismantling of the cell.

Metabolic regulation of caspase-2:

Signaling molecules that sense the existence of metabolites and communicate with the cell's survival machinery are key in deciding the future fate of metabolically compromised cells. Several studies have made an elegant connection between metabolism and cell fate. For example, low glucose levels result in AMPK-mediated phosphorylation of p53 and cell cycle arrest[232]. This ensures that cell division does not progress under conditions of insufficient nutrients. Additionally, glucose levels and/or growth factors also regulate various pro- and anti-apoptotic proteins of the Bcl-2 family[233-235] While these events may eventually trigger caspase activation, caspase-2 is the only known example where defects in cell metabolism directly result in caspase activation. Caspase-2 is activated specifically in response to low NADPH, but not low ATP levels, an elegant link that was established in studies performed in oocytes[236] Characterization of *Caspase-2*$^{-/-}$ mice revealed an increase in number of oocytes in female mice, due to which the caspase was thought to play an important role in the elimination of excess germ cells during development.[237] Later, using the *Xenopus laevis* system, Nutt et al. established that caspase-2 activation was regulated by the metabolic status of the

oocyte, particularly of NADPH, which is synthesized in the PPP[236]. The authors demonstrated that high NADPH levels result in the activation of Ca^{2+}/calmodulin-dependent protein kinase II (CaMKII), which phosphorylates caspase-2 at Ser135, facilitating binding of 14-3-3 proteins to the caspase and preventing its association with its adaptor protein RAIDD required for caspase activation[236,238]. Consequently unhealthy oocytes, which do not have sufficient nutrients to increase flux through the PPP to generate NADPH, die by a caspase-2 and cytochrome c dependent mechanism. Another study also established a link between metabolism and caspase-2 where the authors observed that neurons deficient in caspase-2 were more sensitive to nerve growth factor (NGF) deprivation[237].

Cell death pathways during retinal degeneration:

Rod cell death in RP has been shown to be predominantly executed by apoptosis and involves caspases such as caspase-3 and -7. However, loss of caspase-3 conferred almost no protection to rod death in the fast progressing *rd1* mouse model[239]. The redundancy among caspases may make it more challenging to inhibit cell death upon removal of a single caspase, especially in fast progressing *rd1* model. However, in models of autosomal dominant RP with slower degeneration kinetics, cell death has been efficiently delayed upon removal of caspase-7[240] or over-expression of XIAP[81]. While caspase-3 and caspase-7 were thought to have overlapping functions, recent studies suggest that they possess unique targets, which may explain the protective effect observed upon caspase-7, but not caspase-3 ablation[241]. On the contrary, the only cell death mechanism described in

cones so far is that of necrosis, the inhibition of which delayed early cone death in the *rd10* mouse model[242]. Necrosis is a form of cell death that is usually activated in response to acute stress and while previously thought to be an uncontrolled form of cell death, recent studies show that it also has programmed mechanisms[243]. The disturbance of the retinal architecture from the massive loss of rods is a structural insult to the retinal tissue that may induce necrosis in cones. Consequently, administration of necrotic inhibitors or loss of RIP3, a key protein in the necrotic pathway conferred protection to early cone death[242]. However besides this finding, there is no study that investigates if cone death also involves apoptotic mechanisms. Since our model for cone death suggests that glucose and thus NADPH levels are reduced in cones, we investigated if the NADPH-sensitive Caspase-2 plays a role during cone cell death. The results from this study are discussed in Chapter II.

Autophagy:

While autophagy was briefly introduced, we will now elaborate on this evolutionarily conserved process in the context of selective autophagy as well as complex regulation in neurons. The autophagy related gene (Atg) proteins constitute the core of the autophagy machinery and so far over 30 such proteins have been identified in yeast that are involved in various stages of the process from phagophore formation to autophagsosome expansion[244]. A critical step in the expansion of the autophagosome involves conjugation of the microtubule-associated protein 1 light chain 3 (LC3 or Atg8, denoted as LC3-I in its cytosolic form) to phosphoethanolamine (PE) present in the autophagosome

membrane. The LC3-PE conjugate is denoted as LC3-II. Due to the difference in molecular weights between LC3-I and LC3-II, the ratio of LC3-II:LC3-I is often assessed by western blot as an indicator of autophagic activity[189]. While autophagy was primarily regarded as a bulk, non-selective degradation process, research over the last several years indicates a great extent of selectivity in the process. Selectivity is mediated by the presence of autophagy receptors and adaptor proteins that are capable of recognizing specific types of cargo and interacting with the autophagy core machinery to deliver these components for degradation. The autophagy receptors are characterized by the presence of a WxxL motif, also known as the LC3-interacting region, which facilitates interaction with LC3[245-247]. p62 was the first autophagy receptor to be identified and remains the most well studied receptor till date[199]. The protein possesses an WxxL motif that allows it to interact with the autophagosome, in addition to an ubiquitin-interacting domain that facilitates its interaction with proteins/organelles that are marked with ubiquitin for degradation[200,248]. In fact, studies show that p62 is actually required for the formation of ubiquitinated aggregates in both dividing cells as well as neurons[249,250]. However, p62 can also recognize cargo that is not ubiquitinated and has been involved in the degradation of a wide range of substrates such as bacteria, viral particles in addition to organelles like mitochondria, which may or may not be ubiquitinated[200]. It is important to note that upon delivery of cargo to the autophagosomes, p62 also gets recycled and therefore, does not accumulate in the cell unless there is a defect in the autophagy process[251]. Consequently, an impairment of autophagy in accompanied by the accumulation of p62 and ubiquitin aggregates[199].

In addition to p62 and few other known autophagy receptor proteins, the autophagy-linked FYVE protein (ALFY) is a large, scaffold protein that has garnered attention over the last few years due to its role in the clearance of ubiquitinated aggregates. This protein is also called as WDFY3 due to the presence of WD repeats and FYVE domains. ALFY was found to colocalize with p62 and ubiquitin containing aggregates and its structural features strongly indicate that it plays a major role in autophagy[252]. The FYVE domain facilitates interaction with PI3P that is found in membranes[253], while the WD40 repeats are essential for interaction with Atg5[254]. Additionally, ALFY also possesses PH-BEACH (pleckstrin homology-beige and Chediak-Higashi) domains that mediate interaction with p62[255]. Together, these studies reveal that ALFY binds to p62-containing ubiquitinated aggregates and links them to the autophagosome through its interaction with Atg5 and PI3P. Further, over-expression of ALFY was shown to facilitate clearance of protein aggregates in neurodegenerative disease models in vivo, implying a fundamental role for this protein in the recognition and targeting of ubiquitinated proteins[254].

Regulation of autophagy:

Under nutrient-rich conditions when mTORC1 activity is increased, autophagy initiation is inhibited by mTORC1-mediated phosphorylation of Atg1/ULK1 at Ser757. ULK1 is also phosphorylated by AMPK at various sites (Ser555/317/777) and this serves to promote autophagy under conditions of energy crisis[190,256]. It is proposed that mTORC1-mediated phosphorylation of ULK1 prevents access to AMPK under nutrient-rich conditions. Nutrient starvation conditions lead to dissociation of mTORC1 from ULK1,

allowing access to AMPK to promote autophagy[256]. However, these studies were performed in dividing cells and a recent study in neurons revealed a rather interesting mechanism of autophagy regulation[194]. The study showed that upon loss of TSC in neurons, ULK1 is phosphorylated by mTORC1 at Ser757 as well as by AMPK at Ser555. mTORC1 is therefore unable to prevent the association of ULK1 with AMPK, which leads to the initiation of autophagy. Therefore unlike dividing cells, neurons with constitutive mTORC1 activity maintain an active autophagy flux, suggesting that the effects of mTORC1 on autophagy may largely be dependent on the cell type and its metabolic demands.

In several systems, the FOXO transcription factors have been shown to be the primary regulators of autophagy by transcriptionally increasing expression of genes like LC3 and Bnip3 (Bcl-2 19-kDa interacting protein 3), which are required for autophagosome maturation. In these studies, mTORC1 activity was dispensable for the induction of autophagy[212,213]. Further, some studies suggest that reduction of amino acids like leucine stimulates autophagy in an mTOR-independent manner, although the precise mechanism remains unknown[257].

mTORC1 and lysosomal regulation: mTORC1 also plays a critical role in the termination stages of autophagy and the regulation of lysosomal genes and enzymes. Recently, a role for mTORC1 was uncovered in regulating the localization of TFEB (transcription factor EB), a transcription factor that promotes expression of various lysosomal genes and

enzymes[258,259]. It was found that under nutrient-rich conditions, mTORC1 phosphorylates TFEB at the lysosomal surface and causes its retention in the cytoplasm. Under conditions of starvation, when mTORC1 localization at the lysosome is reduced, TFEB is not phosphorylated which allows its translocation to the nucleus to regulate expression of lysosomal genes. Consequently, inhibition of mTORC1 leads to TFEB translocation to the nucleus, while constitutive mTORC1 activation by over-expression of the Rag GTPase mutants, leads to retention of TFEB in the cytoplasm. In another study, the authors described a phenomenon where prolonged starvation, which induces autophagy through suppression of mTORC1, causes a reactivation of mTORC1 signaling over time since fusion of the autophagosome with the lysosome release free amino acids, which reactivate mTORC1[260]. This phenomenon known as autophagic lysosome reformation (ALR) prevents constitutive autophagy activation, which could have detrimental effects on the cell. Further, mTORC1 that is reactivated facilitates the recycling of the lysosomes membranes to resynthesize lysosomes, thereby placing a critical role for mTORC1 in lysosomal biogenesis and recycling.

Disease models used in the study:

With this understanding of the complex regulation of the insulin/AKT/mTOR pathway, we will now discuss in Chapters II and III, the results obtained upon manipulation of the pathway in mouse models of RP. The disease model extensively used in this work is the retinal degeneration-1 (*rd1*) mouse model, which harbors a loss of function mutation in the rod-specific phosphodiesterase-6β gene (*Pde6b*)[72]. The gene is part of the

phototransduction cascade in rods and its deficiency leads to rod death due to an accumulation of cGMP within the cell. The *rd1* model is one of the fastest progressing models of RP, where rod death peaks around P11-P13 and by P21, about 90% of rods have died and cone death initiates at this stage.[13] We have also employed a second model known as the rhodopsin-knockout (*Rho-/-*) mice, where rod death occurs due to incomplete formation of outer segments[261]. The model displays much slower degeneration kinetics, due to which it more closely resembles the progression of disease in humans[13]. However, due to the slower rate of degeneration, one can analyze cone death only after 17 weeks of age, which significantly reduces the pace of research. Therefore, the *rd1* mouse model is more advantageous in this regard since one can investigate the effects of manipulating cone death as early as 4-5 weeks of age. While it is challenging to prolong cone survival efficiently in this model due to its fast degeneration kinetics, any mechanism that protects cones in this model is likely to also function in a slower model.

CHAPTER II

mTORC1 activation is both required and sufficient to promote cone survival in Retinitis Pigmentosa mice

Introduction:

The inter-neuronal relationship between rod and cone PRs in humans and mice is that rod death always leads to loss of cones, while cone death has only a minimal effect on rods[24-27]. This phenomenon plays a central role in RP, since mutations in a few rod-specific genes affect disproportionately a large number of patients (RetNet: https://sph.uth.edu/retnet/)[29]. Because cones are essential for daylight, color, and high-acuity vision, it is their loss that leads to blindness. The fact that cone death always follows rod death independently of the underlying mutation in a rod-specific gene suggests that the reason(s) for cone death might be similar across various forms of RP. Thus, targeting the common mechanism(s) of cone death may allow for the development of vision therapies with broad clinical significance.

Previous research in our laboratory comparing the kinetics of rod and cone death across four mouse models of RP led to the proposition that cones suffer metabolic imbalances following the loss of rods[13]. Further, at the onset of cone death, we observed gene expression changes in many metabolic genes and genes of the insulin/mTOR pathway, a key pathway controlling cell metabolism. To test whether activation of the insulin/mTOR

pathway alters cone survival, we treated the fast-progressing *rd1* mouse model of RP with daily systemic injections of insulin, which activates the pathway[13]. While cone survival did improve, the therapeutic effect of insulin lasted only for a period of 4 weeks, possibly due to the negative-feedback loop within the insulin/mTOR pathway (Figure 2.1). Our findings, though encouraging, left many questions unanswered regarding the role of mTOR and its potential as a therapeutic target to promote cone survival in RP. As such, it remained unclear whether insulin acts directly on cones to improve cone survival, or whether it stimulates other cells such as RPE cells or retinal Müller glia cells to release neuroprotective factors, as its administration was systemic. It was also unclear whether the protective effect of insulin requires mTOR activity and whether, by circumventing the feedback mechanism within the insulin/mTOR pathway, cone survival can be prolonged to the point of being therapeutically relevant to humans. Last, it remained to be tested whether the effect of insulin can be extended to other mouse models of RP, giving it a broader clinical significance.

To evaluate the long-term therapeutic potential of the insulin/mTOR pathway on cone survival and to test whether insulin acts directly on cones through this pathway, we have now constitutively activated this pathway in cones. Through the use of various conditional alleles of genes downstream of the insulin receptor (Figure 2.1, highlighted in red) that were deleted using a cone-specific Cre recombinase line[262], we uncover a novel role for mTORC1 as being required as well as singularly sufficient to promote long-term cone survival in RP mice.

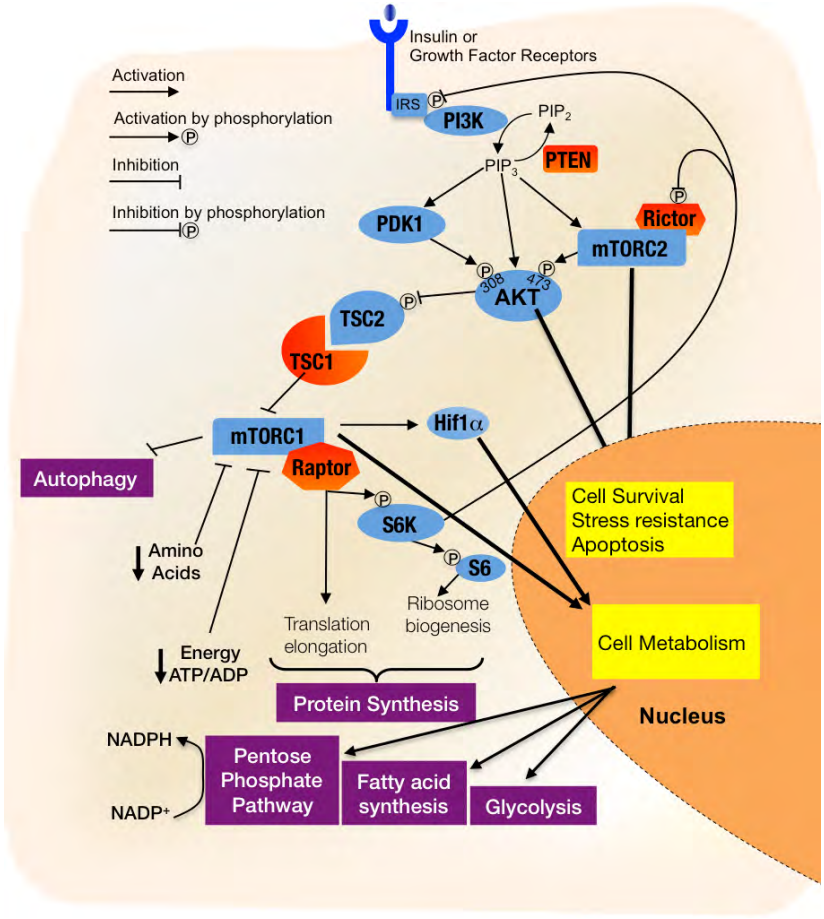

Figure 2.1: Schematic of the insulin/AKT/mTOR pathway. Conditional knockout alleles that were used in the study are denoted in red. A detailed description of the pathway and regulation are found in Chapter I.

Results:

mTORC1 is required and sufficient to promote cone survival in RP: To evaluate whether insulin acts directly on cones through the insulin/mTOR pathway and to test whether continued stimulation of the pathway significantly prolongs cone survival, we constitutively activated the pathway in cones of *rd1* mice by conditional deletion of the tumor-suppressor gene phosphatase and tension homolog (*Pten*) using the Cre-lox system[263]. The Cre driver line used in all our studies is the M-opsin Cre, which uses the

human medium wavelength opsin promoter to achieve cone-specific expression[262]. This Cre driver line has been tested in various studies to achieve deletion of various conditional alleles in cones[264-266]. The *rd1* M-opsin-*Cre Pten*$^{c/c}$ mice that were generated will hereafter be referred to as *rd1-Pten*^{cKO} mice (cKO denotes cone-specific knockout; in all instances, *Cre*$^{+}$ denotes cKO of the gene indicated). *Pten* counteracts the action of growth factors such as insulin by decreasing intracellular levels of the second messenger phosphatidylinositol-trisphosphate (PIP_3). Therefore, activation of the pathway by loss of *Pten* is not sensitive to the negative-feedback loop of the insulin/mTOR pathway, as PIP_3 levels remain high even after growth factor receptors are turned off by the feedback loop[147]. As a consequence of sustained pathway activity, we found that cone survival was significantly improved in retinae of *rd1-Pten*^{cKO} mice up to 8 months of age when compared with cone survival in *Cre*$^{-}$ littermate control retinae or with that observed in retinae following insulin injections in our previous study (Figure 2.2 A and B)[13]. Cone ARRESTIN, a protein that is enriched in cones was used as a proxy to evaluate cone survival. The surface area of the retina that is covered by cone arrestin signal was first calculated and then extrapolated to percentage of cone survival. This method provides an unbiased, accurate estimation of cone survival during disease and is described in detail in Chapter V. All cone survival quantification data are representative of at least 8 retinae per genotype, unless specified.

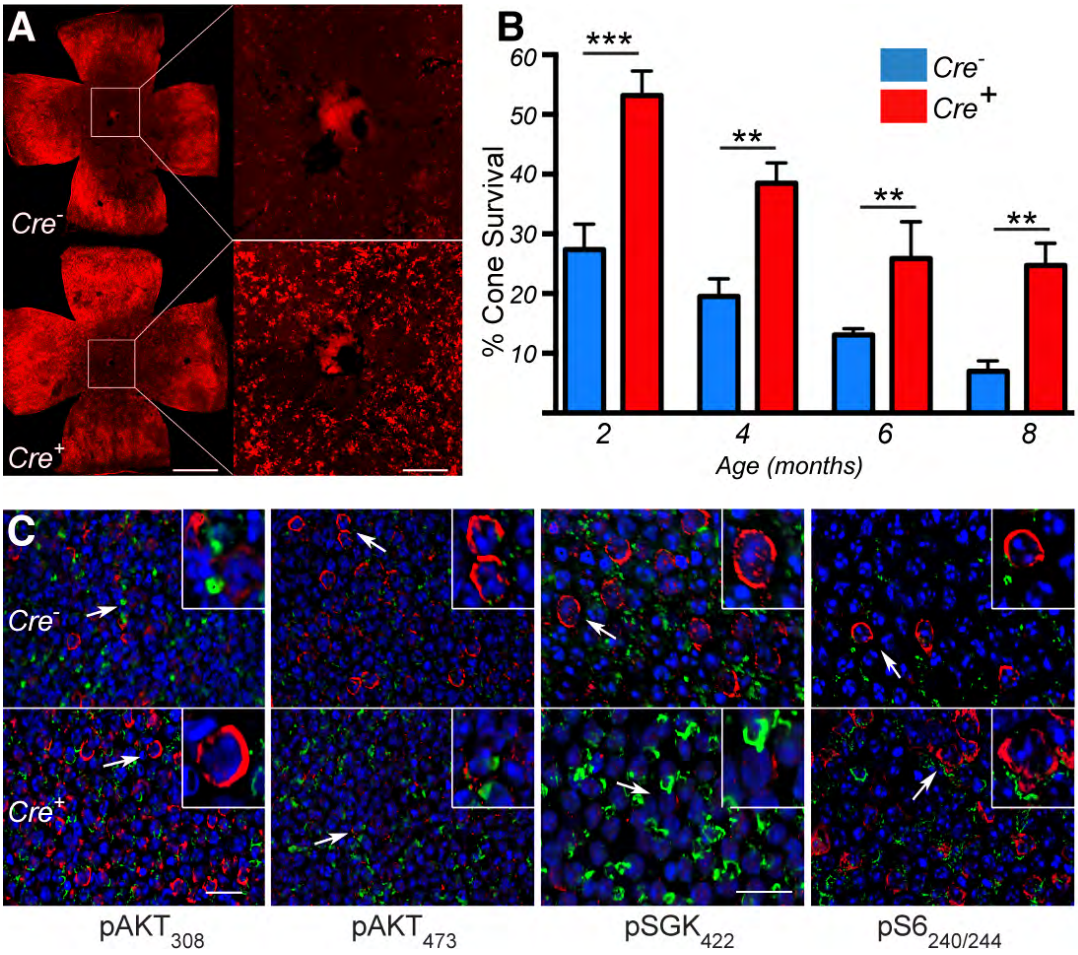

Figure 2.2: Loss of *Pten* promotes cone survival in *rd1* mice. Data shown are from *rd1*-mutant mice harboring the *Pten*$^{c/c}$ allele. (**A**) Representative retinal flat mounts of *rd1*-mutant mice at 2 months of age showing more central cones in *Cre*$^{+}$ animals (red signal indicates cone arrestin). Scale bar: 1 mm (left); 200μm (right). (**B**) Quantification of cone survival at the indicated time points. $^{**}P < 0.01$ and $^{***}P < 0.005$ by Student's *t* test. (**C**) Immunofluorescence analyses at P21 of retinal flat mounts to detect phosphorylation of sites on the indicated proteins (red signal). Upper right of each panel shows magnification of the area indicated by an arrow. Cone layer is identified by PNA staining (green signal indicates PNA; blue signal indicates nuclear DAPI). Scale bars: 20μm (magnifiction for insets, 2.5X original).

The improved cone survival obtained upon loss of *Pten* suggests that sustained cell-autonomous activation of the pathway in cones can serve as a long-term therapeutic strategy to prolong cone survival in RP.

Loss of *Pten* activates various downstream signaling pathways and kinases; however two key kinases downstream of PTEN that are central to the insulin/mTOR pathway are mTOR, which exists in two complexes, and AKT[137,149]. To identify which kinase(s) downstream of PTEN promote(s) cone survival, we first assessed the phosphorylation status of AKT and other bona fide targets of both mTOR complexes. Immunofluorescence on retinal flat mounts at P21 revealed an increase in the number of cones positive for PDK1 dependent phosphorylation of AKT at Thr308 and a decrease in the number of cones positive for mTORC2-mediated phosphorylation of AKT at Ser473. Consistent with this finding, the number of cones positive for phosphorylated SGK-1, another mTORC2 target, was also reduced, while the number of cones phosphorylated on ribosomal protein S6 (p-S6), an indirect mTORC1 target, was increased (Figure 2.1 C). Since phosphorylation of AKT on both sites is required for most AKT-mediated prosurvival functions, but phosphorylation on Thr308 is sufficient to activate mTORC1, the data suggest that cone survival upon loss of PTEN is mediated mainly by increased mTORC1 activity[149,161]. The reduction in mTORC2 activity upon loss of PTEN is likely due to the inhibitory effect of mTORC1 on mTORC2[158,160].

We were not able to detect any of the above phosphorylation changes by western blot on whole retinal extracts (Figure 2.3 A). This result could be explained by the low

proportion of cones in the retina (3%)[2] and/or the high expression levels of these phosphorylated proteins in other retinal cell types (Figure 2.3 B), which makes it difficult to detect cone-specific changes in whole retinal extracts. Therefore, immunofluorescence analyses on whole retinal mounts or sections will be the preferred method of detection of cone-specific changes.

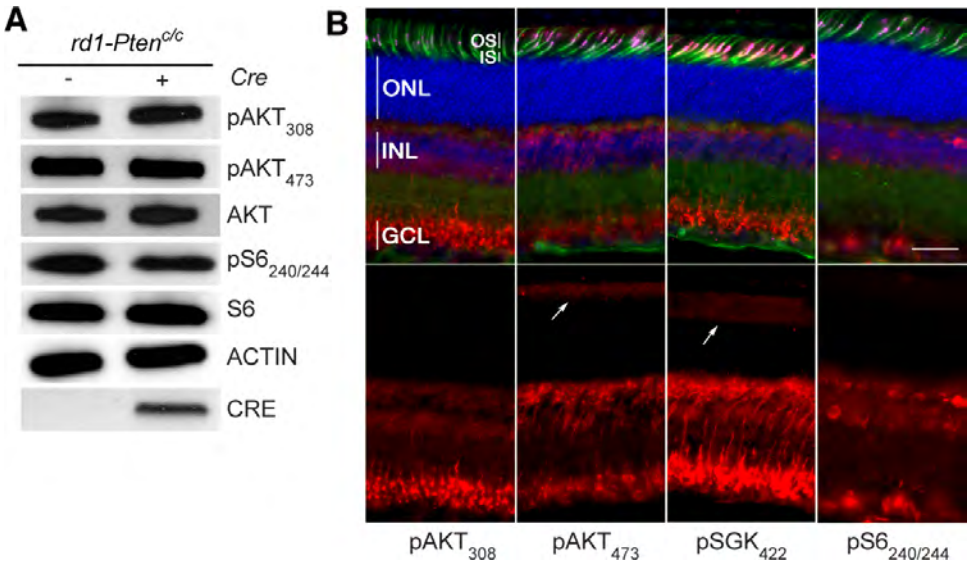

Figure 2.3: Challenges in detecting cone–specific changes by western blot. (**A**) Western blot analyses from whole retinal extracts at P21 from *Pten*$^{c/c}$ mice in the *rd1* background. Proteins of interest are indicated on the right. (**B**) Immunofluorescence analysis at P21 on retinal cyrosections of *Pten*$^{c/c}$ mice for phosphorylation on sites of proteins indicated (red signal). Arrows show possible low level of expression or background noise of phospho (p) AKT_{473} and SGK_{422} in PRs, while $pAKT_{308}$ and $pS6_{240}$ appear almost undetectable in PRs. In contrast, robust expression is seen in the inner nuclear layer (INL) and/or ganglion cell layer (GCL). This makes it difficult to detect phosphorylation changes of these proteins by western blot using whole retinal extracts as *Pten* is lost only in cones. Additionally, after the loss of most rods, retinal extracts contain mainly proteins of INL and GCL cells (green: PNA; magenta: short-wave opsin; blue: nuclear DAPI; IS: inner segment; ONL: outer nuclear layer; OS: outer segment). Scale bar: 50µm.

To test whether increased mTORC1 activity is responsible for the survival effect mediated by loss of *Pten*, we generated *rd1* mice with simultaneous deletion of *Pten* and *Raptor* (*Raptor*$^{c/c}$ allele[267]) in cones (*rd1* M-opsin-*Cre* *Pten*$^{c/c}$*Raptor*$^{c/c}$) and quantified cone survival in these mice at 2 months of age, a time point at which the difference in cone survival was quite large following loss of *Pten*. Interestingly, concurrent loss of *Pten* and *Raptor* not only abolished the survival effect seen upon loss of *Pten*, but also accelerated cone death (Figure 2.4 A and B). A similar acceleration of cone death was seen upon loss of *Raptor* alone, while loss of *Rictor* (*Rictor*$^{c/c}$ allele[267]) in cones had no effect on cone survival in *rd1* mice (Figure 2.4 A and B). Loss of *Raptor* and *Rictor* was verified by phosphorylation changes in their downstream targets S6, AKT, and SGK1 (Figure 2.4 C). The results show that mTORC1 activity is not only required for the improved cone survival seen upon loss of *Pten*, but is also critical for cone survival under the stress conditions encountered during disease. Furthermore, the data suggest that known mTORC2- and AKT-mediated prosurvival mechanisms do not contribute to cone survival upon loss of *Pten*.

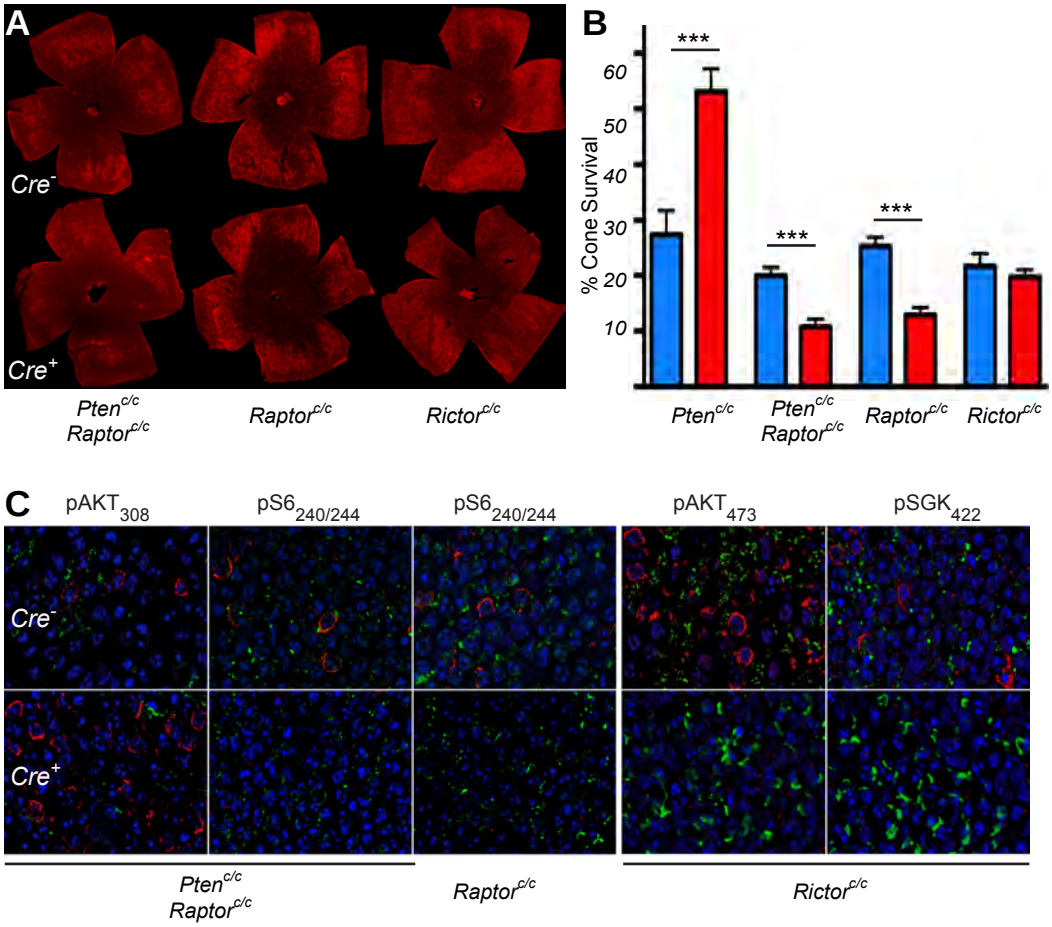

Figure 2.4: *Raptor* but not *Rictor* is required for loss of *Pten*-mediated survival. Data shown are from *rd1*-mutant mice harboring the indicated conditional alleles. (**A** and **B**) Representative retinal flat mounts (**A**) and quantification of cone survival (**B**) at 2 months of age (red signal indicates cone arrestin). ***$P <$ 0.005 by Student's *t* test. (**C**) Immunofluorescence analyses (red signal) of retinal flat mounts at P21 to detect phospho-specific sites on the indicated proteins (green signal indicates PNA; blue signal indicates nuclear DAPI).

It is important to note that while loss of *Raptor* accelerated cone death in *rd1* mice, neither loss of *Raptor* nor *Rictor* had any effect on cone survival of wild type mice (Figure 2.5) suggesting that mTOR activity is not required to keep cones alive in a wild type background.

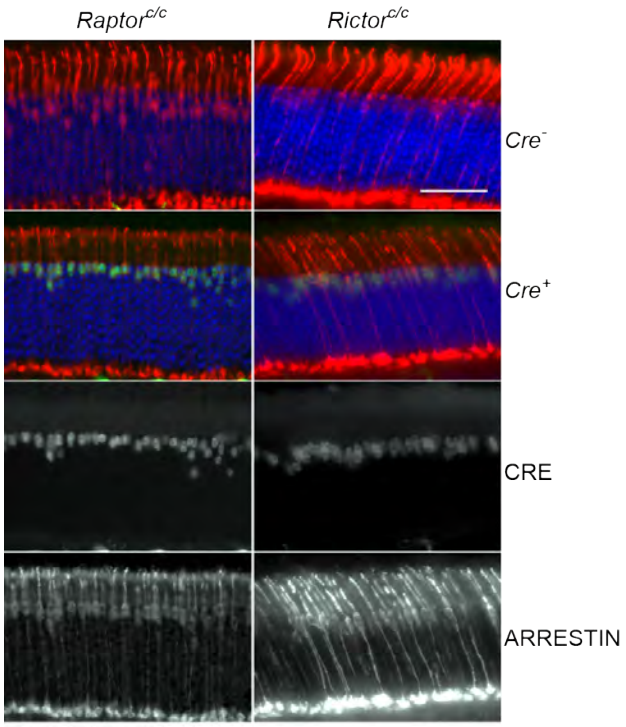

Figure 2.5: Neither loss of *Raptor* nor *Rictor* affects cone survival in wild type mice. Immunofluorescence analysis on retinal cryosections from mice harboring either the *Raptor*$^{c/c}$ or *Rictor*$^{c/c}$ conditional allele showing normal distribution of cones. (Red signal: cone arrestin; green: CRE recombinase; blue: nuclear DAPI) CRE and cone-arrestin staining are shown separately below in grayscale for *Cre*$^{+}$ mice.

To corroborate whether increasing mTORC1 activity alone is sufficient to prolong cone survival, we disrupted the tuberous sclerosis complex (TSC) by ablation of *Tsc1*, which results in robust and constitutive activation of mTORC1. This was achieved by using mice with conditional allele for *Tsc1* to disrupt the TSC in cones of *rd1*-mutant mice (*rd1* M-opsin-*Cre* *Tsc1*$^{c/c}$ mice[268], herein referred to as *rd1*-*Tsc1*^{cKO}). At 2 months of age, loss of *Tsc1* in these mice resulted in a more pronounced rescue of cones when compared with loss of *Pten*. Many of the retinae displayed almost wild type distribution of cones in central areas. The protective effect was significant up to 8 months of age (Figure 2.6 A and B). Cone function in these mice at 2 months of age, as evaluated by full-field electroretinography (ERG), was maintained at the levels recorded at the onset of cone death (P21), while it declined in *Cre*$^{-}$ animals (Figure 2.6 C). ERG recordings are low in the *rd1* mutant at the onset of cone death when compared with those in WT mice (~20% of WT), because rod degeneration starts before eye opening and before outer segments (OSs) have fully matured[104,269,270]. When compared with loss of *Pten*, S6 was uniformly phosphorylated in cones, demonstrating a robust activation of mTORC1 in *rd1* *Tsc1*^{cKO} retinae (Figure 2.6 D).

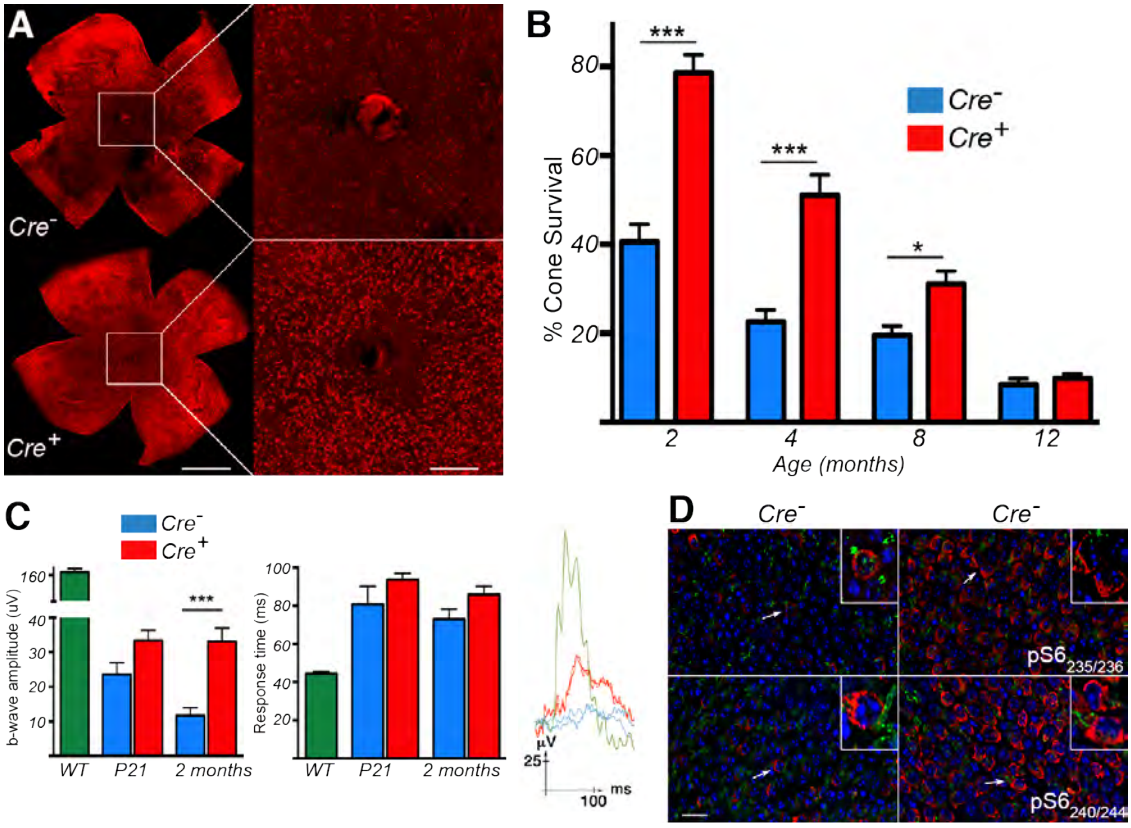

Figure 2.6: Activation of mTORC1 promotes cone survival and maintains cone function in *rd1*-mutant mice. (**A**–**D**) *rd1*-mutant mice harboring the *Tsc1*$^{c/c}$ allele. (**A**) Representative retinal flat mounts from *rd1*-mutant mice at 2 months of age showing a higher concentration of central cones in *Cre*$^{+}$ animals (red signal indicates cone arrestin). Scale bars: 1 mm (left); 200 μm (right). (**B**) Quantification of cone survival at the indicated time points. **P* < 0.05 and ****P* < 0.005 by Student's *t* test. (**C**) Evaluation of cone function by photopic ERG recordings in mice at P21 and 2 months of age showing b-wave amplitude, the average response time of the b-wave peak, and representative recordings in animals at 2 months of age (left to right). The same ERG protocol was used for WT and *rd1* animals. The data are representative of recordings in at least 5 animals per genotype. ****P* < 0.005 by Student's *t* test. (**D**) Immunofluorescence analyses to detect p-S6 on 2 different mTORC1-dependent sites (red signal) at P21 (green indicates PNA; blue indicates nuclear DAPI). Scale bar: 20 μm (magnification for insets, 2.5X original).

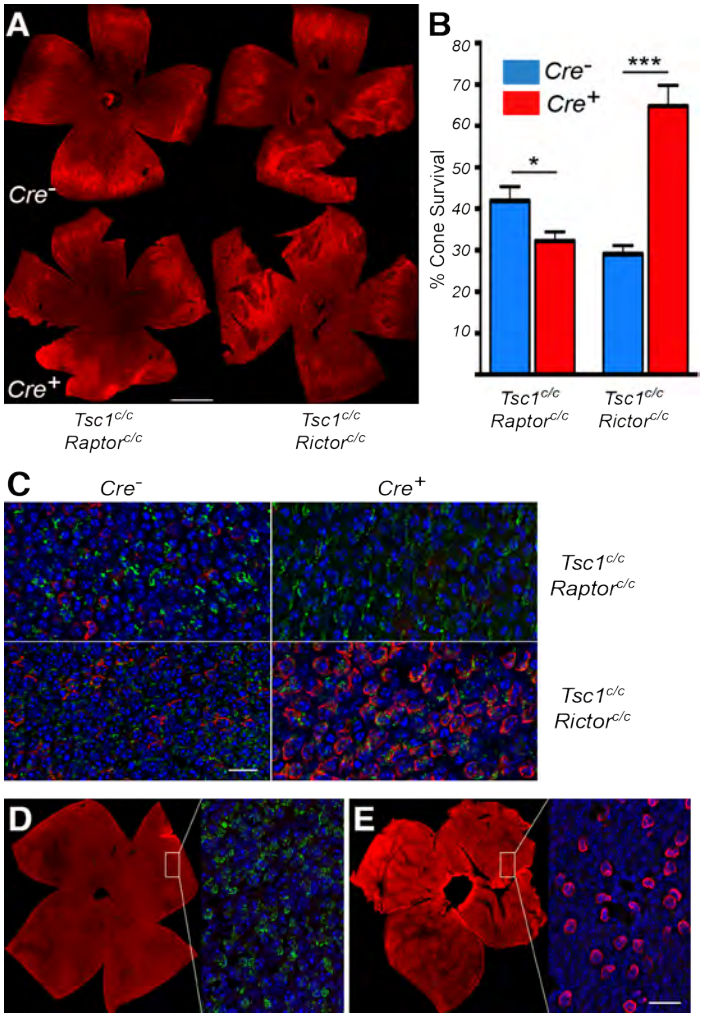

Figure 2.7: mTORC1 is sufficient to prolong cone survival in RP. (**A**–**C**) Data shown are from mice on an *rd1*-mutant background harboring the indicated conditional alleles. (**A**) Representative retinal flat mounts from mice at 2 months of age (red signal indicates cone arrestin). Scale bar: 1 mm. (**B**) Quantification of cone survival in mice at 2 months of age. **P* < 0.05 and ****P* < 0.005 by Student's *t* test. (**C**) Immunofluorescence analyses of retinal flat mounts to detect pS6 at P21. pS6 was absent from the cone layer (green signal indicates PNA) upon loss of *Tsc1* and *Raptor*, while the number of cones positive for pS6 increased upon loss of *Tsc1* and *Rictor* (blue signal indicates nuclear DAPI). Scale bar: 20μm. (**D** and **E**) Ki67 staining (red signal) in retinae of *rd1 Tsc1*^{cKO} mice at 2 months of age (**D**) and WT mice at P0 (**E**), when cell division is ongoing (green signal indicates PNA; blue signal indicates nuclear DAPI). Higher magnification (30X) is shown on the right side of each panel. Scale bar: 20 μm.

Loss of the protective effect by simultaneous ablation of *Tsc1* and *Raptor*, but not *Tsc1* and *Rictor*, confirmed that mTORC1 activity was both required and sufficient to promote cone survival (Figures 2.7 A-C). Importantly, while mutations in TSC cause benign tumors in tissues such as the kidney and brain[271], loss of *Tsc1* in cones did not induce cone proliferation as assessed by the proliferation marker Ki67, indicating that the protection was due to improved cone survival and not cone numbers (Figures 2.7 D and E).

mTORC1 prolongs cone survival by improving cell metabolism: As discussed in Chapter I, PRs are among the most metabolically active cells in the human body, since they need to replenish membranes and proteins lost due to the daily shedding of their OSs[106,272]. Consequently, PRs require large quantities of glucose to synthesize sufficient amounts of NADPH to keep up with daily membrane synthesis. mTORC1 is at the center of cell growth and proliferation, regulating genes involved in glycolysis, the PPP, and de novo lipid synthesis[185]. We therefore investigated whether sustained mTORC1 activity increases the expression of key metabolic target genes that increase NADPH production in cones, thereby improving survival and function. As such, we analyzed the expression of glucose transporter 1 (GLUT1), which increases glucose uptake, hexokinase-II (HKII), which phosphorylates glucose more effectively, and glucose-6-phosphate dehydrogenase (G6PD), which shunts glucose into the PPP for NADPH synthesis[273]. Immunofluorescence analysis revealed an increase in the expression of all 3 aforementioned genes in cones of 2-month-old *rd1 Tsc1*^{cKO} mice (Figure 2.8 A). We did

not observe this increase in immunofluorescence upon the concurrent loss of *Tsc1* and *Raptor* (Figure 2.8 A), indicating that the increase was mTORC1 dependent.

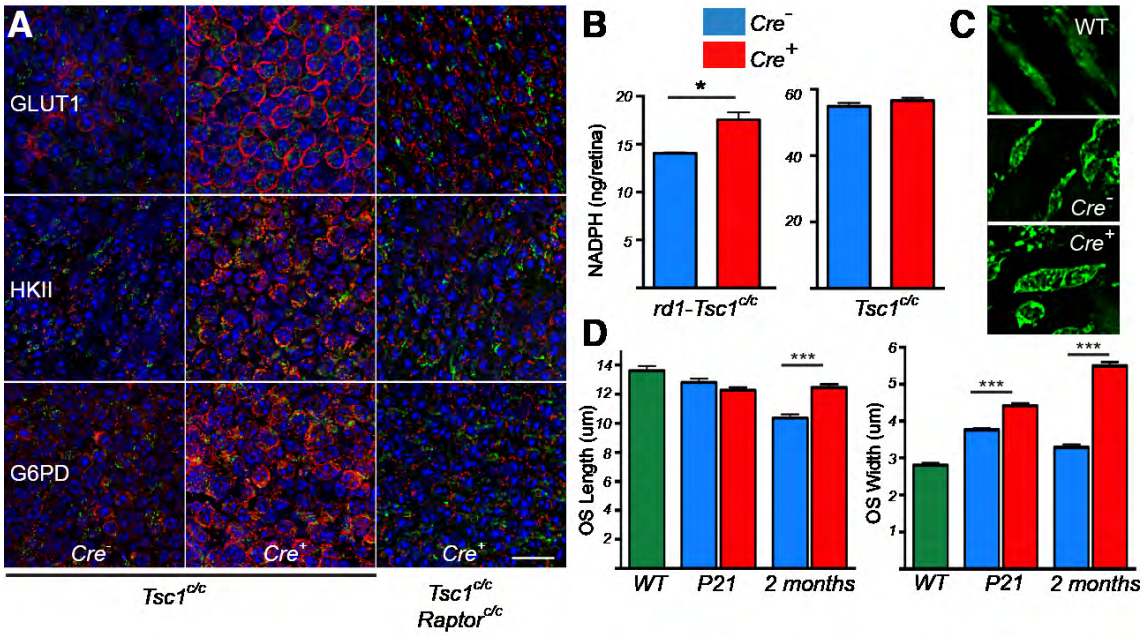

Figure 2.8: mTORC1 activation improves glucose metabolism in cones. (**A**) Immunofluorescence analyses to detect the indicated proteins (red signal) on retinal flat mounts from 2-month-old *rd1* mice harboring the indicated conditional alleles. Concurrent loss of *Tsc1* and *Raptor* abolished the increase in immunoreactivity seen upon loss of *Tsc1* alone (green signal indicates PNA; blue signal indicates nuclear DAPI). Scale bar: 20 μm. (**B**) NADPH measurements on whole retinal extracts at P21 from $Tsc1^{c/c}$ mice in *rd1*-mutant and WT backgrounds (ng/retina, nanogram per retina). **P* < 0.05 by Student's *t* est. Data are representative of 3 biological replicas, with 3 retinae per replica. (**C**) Representative images of outer segments (OS) from WT (top panel) and *rd1* $Tsc1^{c/c}$ mice (middle and bottom panels) at 2 months of age. (**D**) Quantification of OS length and width at the indicated time points. ****P* < 0.005 by Student's *t* test. Data represent 40 measurements performed on 2 animals in each genotype.

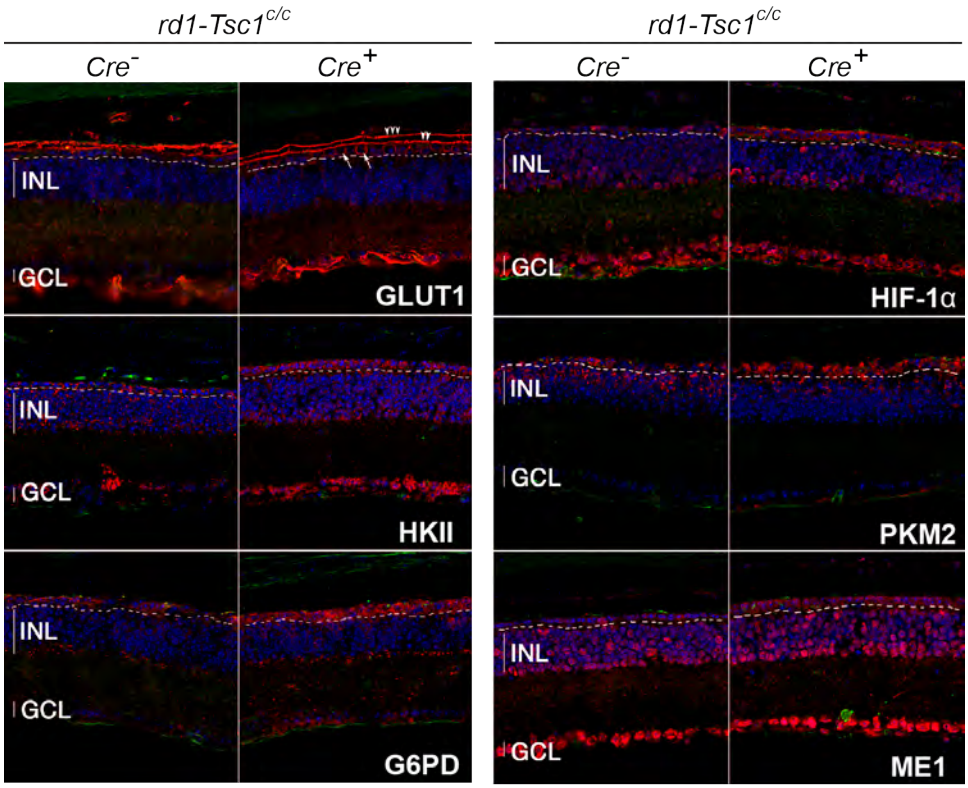

Figure 2.9: Increase in expression of metabolic genes upon loss of *Tsc1* during disease. Immunofluorescence analysis for proteins indicated (red signal) on retinal cryosections from *rd1* mice harboring the *Tsc1*$^{c/c}$ allele at 2 months of age. Dotted lines depict the border between the cone layer and the INL. In *rd1* mice all 6 proteins are expressed at higher levels in the cone layer upon loss of *Tsc1* (see also **Figure 2.8** for immunofluorescence analysis on flat mounts for GLUT1, HKII and G6PD). Arrows show expression of glucose transporter-1 (GLUT1) on cone membrane, while double and triple arrowheads show expression on the apical and basal side of the RPE respectively (green: PNA; blue: nuclear DAPI, INL: inner nuclear layer, GCL: ganglion cell layer)

The increase in expression of GLUT1, HKII and G6PD in *rd1-Tsc1*^{cKO} cones suggests that glucose uptake, retention, and divergence to the PPP are improved. Other glycolytic genes that contribute to an increase in NADPH production, such as pyruvate kinase

muscle isoform 2 (PKM2) and malic enzyme 1 (ME1), were also seen by immunofluorescence to be upregulated in cones of *rd1 Tsc1*^{cKO} mice at 2 months of age, as was an increase in the transcription factor hypoxia-inducible factor 1 α (HIF-1α), which regulates the transcription of many glycolytic genes (Figure 2.9)[185,274]

In agreement with these findings, we detected significantly higher levels of NADPH in whole retinal extracts from *rd1 Tsc1*^{cKO} mice at P21 (Figure 2.8 B), a time point at which cone death initiates but at which cone distribution was still similar between *Cre*$^{-}$ and *Cre*$^{+}$ littermate controls. The cone death kinetics upon *Tsc1* loss from P21 to 2 months of age is represented later in Figure 2.11. Interestingly at this time-point, among the aforementioned metabolic genes, immunofluorescence showed that only ME1 expression was increased at P21 (Figure 2.10 A). This suggests that while mTORC1 signaling is active at P21 (Figure 2.6 D), the expression of these metabolic genes increases gradually over time. To further test this finding, we performed quantitative RT-PCR (qRT-PCR) analysis at P21 and P24 and found that most metabolic genes started to display a modest but statistically significant difference between *Cre*$^{-}$ and *Cre*$^{+}$ retinae by P24 (Figure 2.10B)

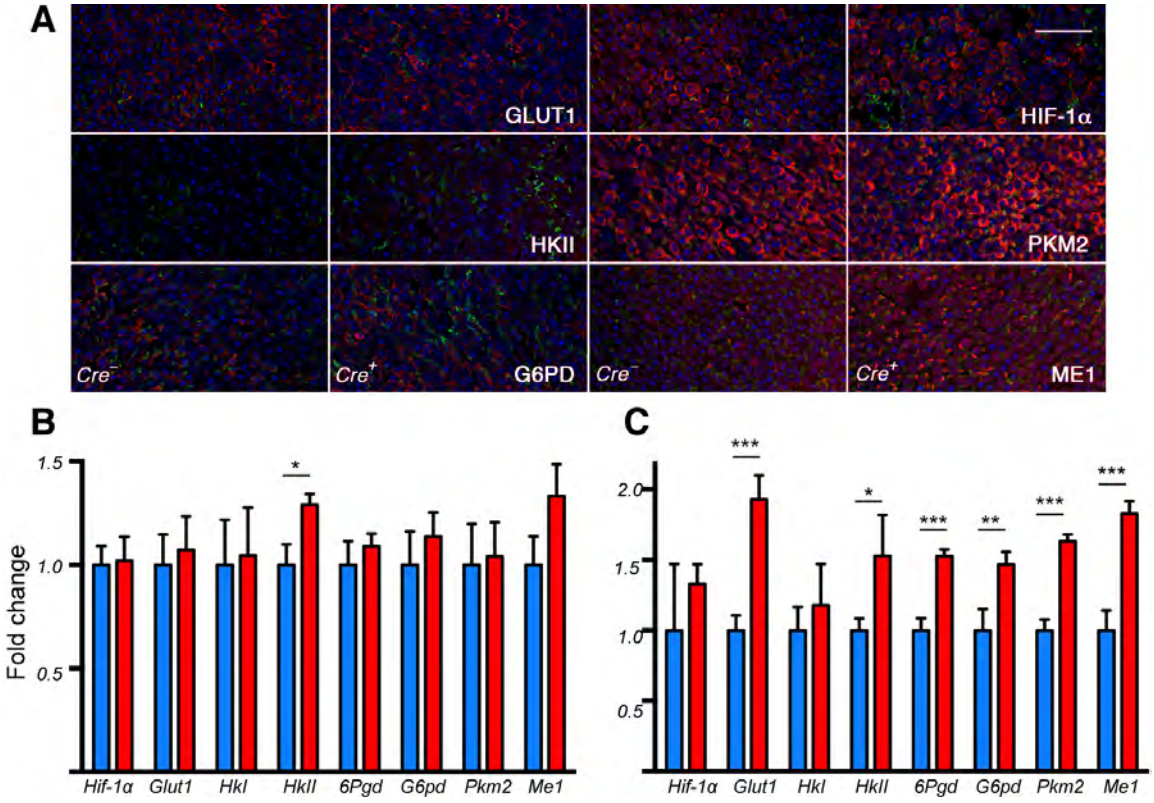

Figure 2.10: Increased expression of mTORC1 targets over time. (**A-C**) Immunofluorescence analysis on retinal flat mounts (**A**) and quantitative real-time polymerase chain reaction (qRT-PCR) (**B**, **C**) on *rd1* mutant mice harboring the *Tsc1*$^{c/c}$ allele. (**A**) Immunofluorescence analyses at P21 for proteins indicated (red signal). Apart from ME1, none of the other genes showed a clear increase in expression upon loss of *Tsc1* at P21 when compared to 2 months (**Figure 2.8A** and **2.9**) (green: PNA; blue: nuclear DAPI). Scale bar: 20μm. (**B**, **C**) qRT-PCR analysis for genes indicated on cDNA synthesized from retinal extracts at P21 (**B**) or P24 (**C**). Error bars: SD. P-values: ***<0.005; **<0.01; *<0.05; ns: not significant, calculated by *t*-Test. Data represents average of 3 biological samples run in duplicates with two animals per sample (HKI: hexokinase I; 6PGD: 6-phosphogluconate dehydrogenase).

Performing the qRT-PCR or NADPH assay at a later time point would have complicated the interpretation of the data, as the differences in cone density between *Cre*$^{-}$ and *Cre*$^{+}$

retinae becomes statistically significant after P24 (Figure 2.11), and thus any difference could be attributed to the greater number of cones.

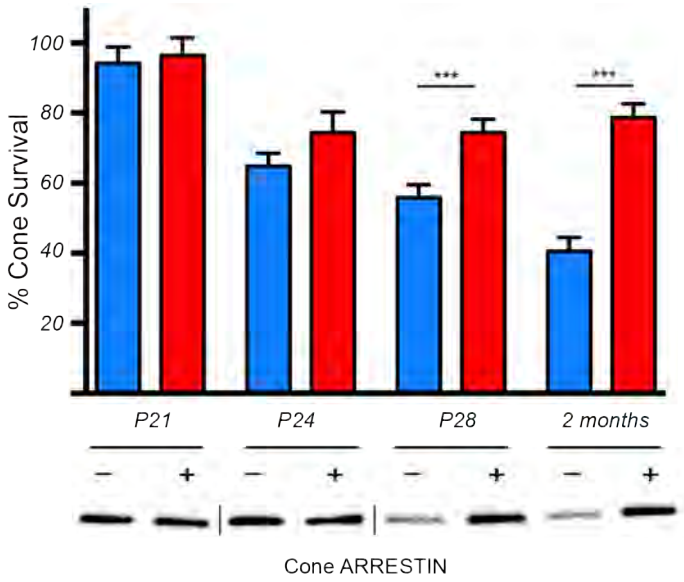

Figure 2.11: Early cone death kinetics. (**A**) Quantification of cone survival in *rd1* mice harboring the *Tsc1*$^{c/c}$ allele at time points indicated. P-values: ***<0.005; ns: not significant, calculated by t-Test. (**B**) Western blot for cone-arrestin from whole retinal extracts at time points indicated (Lanes separated by vertical lines of the time point P24 were run on a separate gel and inserted into the figure).

In agreement with an improvement in NADPH synthesis as well as a progressive increase in metabolic gene expression, we found that OS length was maintained in *Cre*$^{+}$ mouse retinae between P21 and 2 months of age (Figure 2.8 C and D). Since NADPH is also essential for chromophore recycling[19], its increase, in conjunction with maintained OS length and a higher number of cones, may account for the higher ERG recordings in *Cre*$^{+}$ animals at 2 months of age (Figure 2.6 C).

Interestingly, we did not detect any significant increase in NADPH in retinal extracts from WT mice in which *Tsc1* was ablated in cones by the same Cre driver line (Figure 2.6 B). This is consistent with the finding that loss of *Tsc1* did not cause an increase in the expression of any of these genes in the cones of WT mice by 2 months of age (Figure 2.12, only GLUT1 and HIF-1α are depicted, however no difference was observed in any of the other metabolic genes), which suggests that mTORC1 only regulates the expression of these genes under disease conditions.

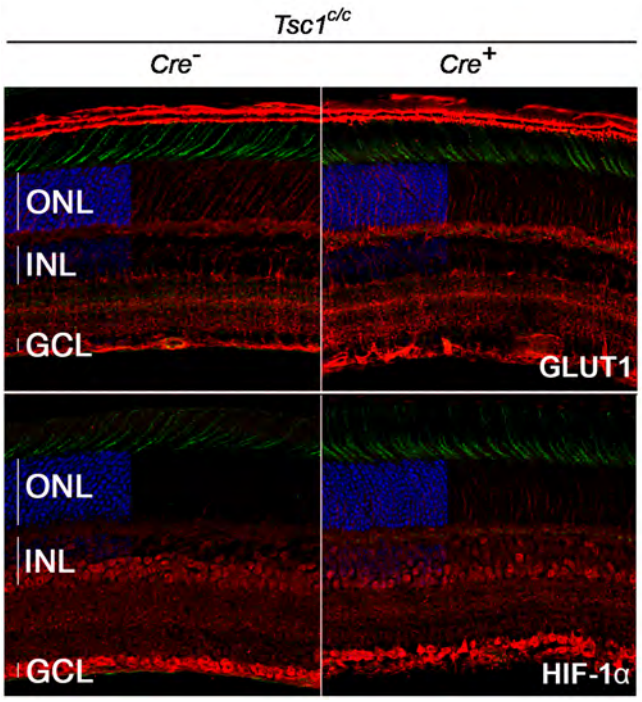

Figure 2.12: Loss of *Tsc1* induces expression of metabolic genes only under disease conditions. Immunofluorescence analysis for proteins indicated (red signal) on retinal cryosections from mice harboring the *Tsc1*$^{c/c}$ allele at 2 months of age. Compared to *rd1* mice (**Figure 2.9**), none of the metabolic genes show an increase upon loss of TSC1. (Green: PNA; blue: nuclear DAPI; 3/5 of DAPI signal has been removed to visualize the expression of the protein indicated to the right) ONL: outer nuclear layer, INL: inner nuclear layer, GCL: ganglion cell layer

In summary, sustained activation of mTORC1 in cones improves cone survival and function under disease conditions by gradually increasing the expression of genes involved in glucose uptake, retention, and utilization.

To further test whether NADPH levels are crucial for cone survival during disease, we examined the role of the initiator caspase, caspase-2 (CASP2), a protease that initiates apoptotic cell death and has been shown to be activated under low intracellular NADPH levels but not low ATP levels[236]. Caspases are commonly activated by cleavage, thus the identification of a cleavage product is generally used to assess caspase activity[275]. Western blot analysis using retinal extracts from *rd1* mice revealed no cleaved CASP2 products, while cleaved CASP2 was readily detectable after transfection of HEK239 cells with full-length *Casp2* (Figure 2.13 A), suggesting that CASP2 is not cleaved during cone degeneration. However, because dimerization of initiator caspases is sufficient to activate the protease, albeit to a lesser extent, the absence of a cleavage product does not necessarily mean that a caspase is not active[224]. To further test whether CASP2 was activated in cones, we performed immunofluorescence analyses using 6 different CASP2 antibodies, none of which revealed any specific pattern of loss of CASP2 expression in the retinae of *Casp2*$^{-/-}$ mice, making it difficult to determine whether CASP2 was actually expressed and activated in cones (data not shown). However, Western blot analyses using extracts of the photoreceptor-enriched retinoblastoma cell line Y79 revealed an immunoreactive band (Figure 2.13 A), suggesting that CASP2 may be present in photoreceptors.

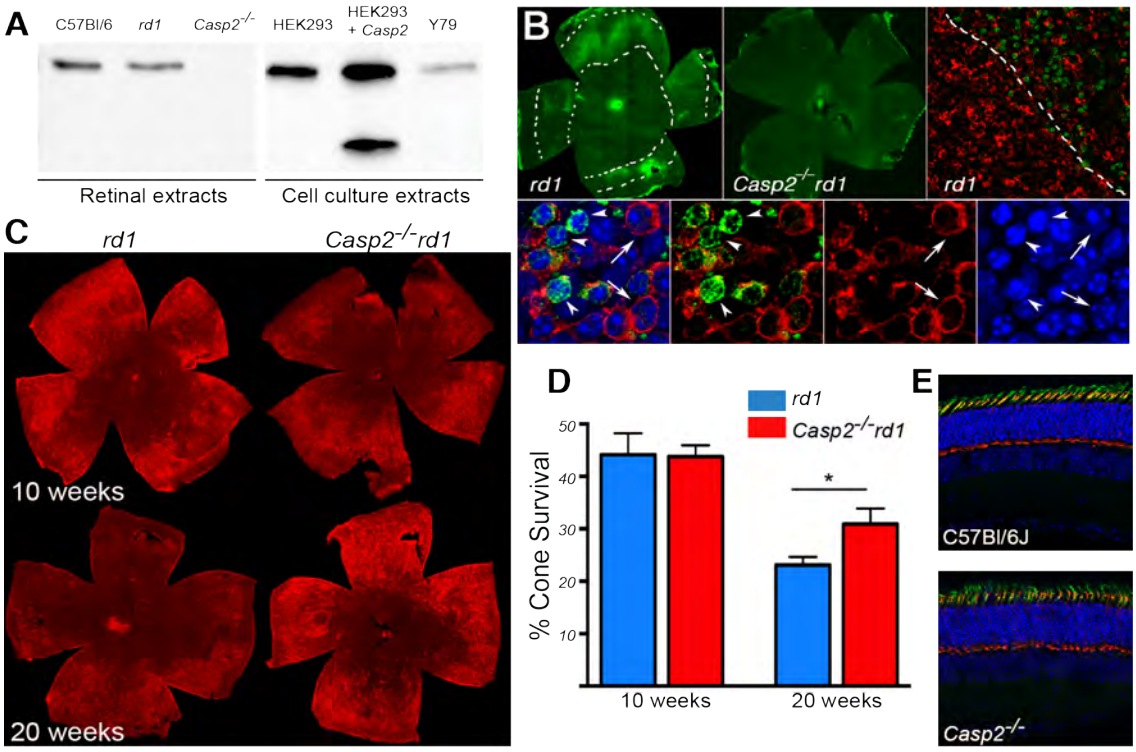

Figure 2.13: Loss of *Casp2* slows cone death. (**A**) Western blot analyses of full-length and cleaved CASP2 with retinal extracts of indicated genotypes (left) and with cell culture extracts (right) of HEK293 cells, HEK293 cells transfected with full-length *Casp2*, and extracts of the photoreceptor-enriched retinoblastoma cell line Y79. (**B**) Immunofluorescence to detect active CASP2 (green signal indicates FITC-labeled CASP2 activity peptide) and red-green opsin (red signal) in retinae of 2-month-old *rd1* animals. Top row, left to right: Retinal flat mount showing the CASP2-active zone (between the dotted lines) of cell death progressing toward the periphery. Middle panel: No CASP2 activity was detected in the absence of *Casp2*. Right panel: Higher magnification of central-to-peripheral death wave is demarked by the dotted line. To the left of the line, little CASP2 activity was seen, and many cells still expressed red-green opsin (red signal), while to the right of the line, there were few red-green opsin–positive cells and many cells positive for activated CASP2. Bottom panels: higher magnification showing that cells with more CASP2 activity (arrowheads) had pyknotic nuclei and less red-green opsin immunoreactivity as opposed to cells with more red-green opsin immunoreactivity (arrows; blue signal indicates nuclear DAPI).

(**C**) Representative retinal flat mounts from mice of the indicated genotypes at 10 and 20 weeks of age. (**D**) Quantification of cone survival in *rd1* and *Casp2*$^{-/-}$ *rd1* mice at the indicated time points. *$P < 0.05$ by Student's *t* test. (**E**) Immunofluorescence analyses to detect cone arrestin (red signal) and PNA (green signal; blue signal indicates nuclear DAPI) in retinal cryosections from 20-week-old WT and *Casp2*$^{-/-}$ mice.

To determine whether CASP2 was activated in cones without cleavage, we used a peptide bearing the CASP2 target sequence (VDVAD) conjugated with the fluorophore FITC. The peptide becomes covalently linked once bound to the active site of the protease, facilitating the clearance of unbound excess peptide. Using this assay, we found that CASP2 activity occurred mainly in cones that lacked red-green opsin expression and displayed pyknotic nuclei, a key characteristic of apoptotic cells (Figure 2.13 B). Moreover, the pattern of cells positive for CASP2 activity reflected the central-to-peripheral progression of cone death, suggesting that we were indeed capturing dying cones across the retina. However, because the sequence of caspase-binding peptides is rather short, false-positives can occur. To test for specificity of the activity assay and to determine whether *Casp2* plays a role in vivo during cone degeneration, we crossed the *Casp2*$^{-/-}$ allele onto an *rd1*-mutant background (*Casp2*$^{-/-}$ *rd1*). Loss of CASP2 not only abolished any CASP2 activity seen in *rd1* retinae (Figure 2.13 B), but also significantly improved cone survival in the retinae of these mice at 20 weeks of age (Figure 2.13 C and D), while loss of CASP2 in WT mice did not affect PR survival (Figure 2.13 E). In summary, the data suggest that removal of an NADPH-sensitive cell death mechanism can delay cone death in RP, further supporting the notion that cone death in RP is

intimately linked to glucose and NADPH levels and indicating that cone death is likely a result of nutrient deprivation.

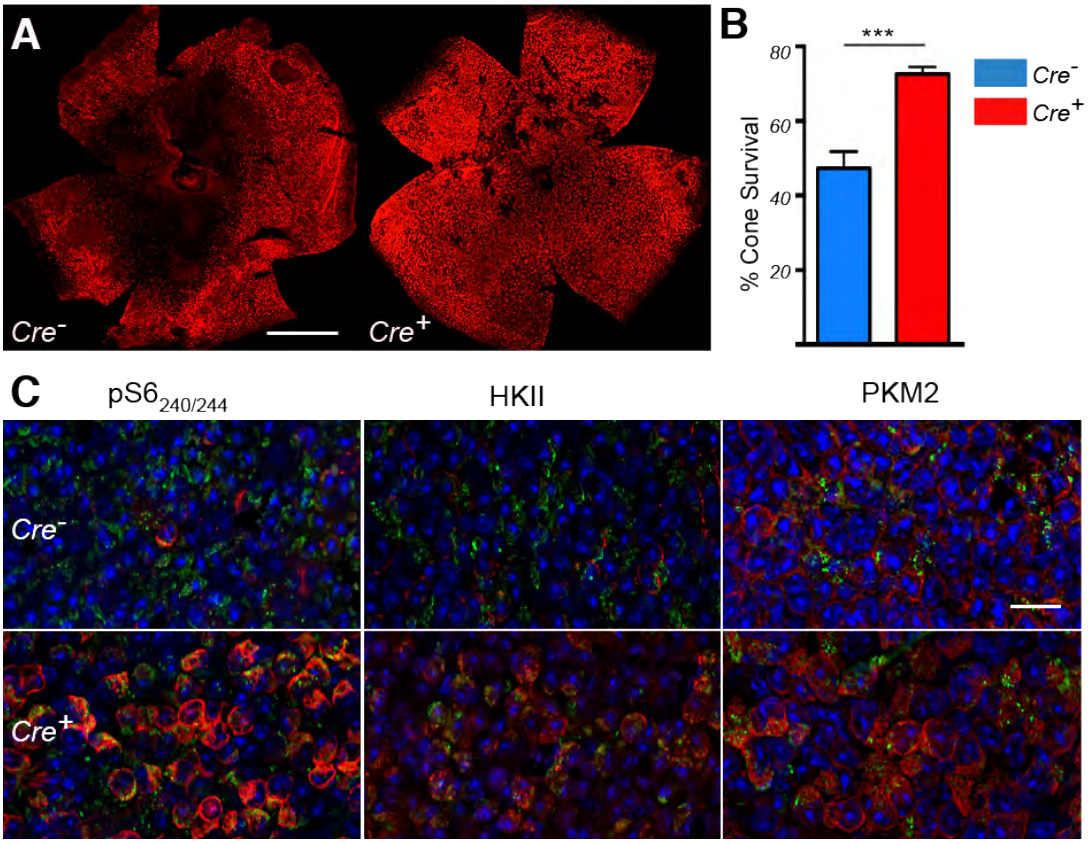

Figure 2.14: Cone protection mediated by loss of *Tsc1* is conserved in RP. Data shown are from *Rho*$^{-/-}$ mice harboring the *Tsc1*$^{c/c}$ allele. (**A**) Representative retinal flat mounts from mice at 30 weeks of age (red signal indicates cone arrestin). Scale bar: 1 mm. (**B**) Quantification of cone survival in mice at 30 weeks of age. ***P < 0.005 by Student's t test. (**C**) Immunofluorescence analyses to detect the indicated proteins (red signal) on retinal flat mounts (green signal indicates PNA; blue signal indicates nuclear DAPI). Scale bar: 20 μm.

Constitutively activated mTORC1 delays cone death in rhodopsin-KO mice: To test whether improved cone survival mediated by increased mTORC1 activity is applicable to other models of RP, we used the rhodopsin-KO (*Rho*$^{-/-}$) mouse[261], which displays slower degeneration kinetics. Cone death initiates at around 17 weeks of age, and by 30 weeks of age, *Rho*$^{-/-}$ retinae show a degree of cone degeneration equivalent to that of 2-month-old *rd1* mouse retinae. Similar to the observations made in the *rd1* mouse model, loss of *Tsc1* in the cones of *Rho*$^{-/-}$ mice was able to significantly prolong cone survival at 30 weeks of age (Figure 2.14 A and B). Moreover, increased immunoreactivity against metabolic genes such as HKII and PKM2 in cones, as well as an increase in the number of cones positive for p-S6 (Figure 2.13 C), indicates that the mechanism of protection is similar to that observed in *rd1* cones. These findings suggest that this approach is independent of the mutation in a rod-specific gene, allowing for therapeutic intervention at the mTORC1 level to prolong vision in RP.

CHAPTER III

mTORC1 activation that maintains autophagy is more beneficial for long-term cone survival of RP mice

Introduction:

In Chapter II we demonstrated that constitutive activation of the mammalian target of rapamycin complex 1 (mTORC1), mediated by loss of either of the two negative regulators, *Pten* or *Tsc1*, promoted cone survival for a period of up to 8 months in *rd1* mice (Figures 2.2 and 2.5). Because *Tsc1* is a direct upstream negative regulator of mTORC1, its removal promoted a more robust rescue of cones at 2 months of age, with many retinae displaying almost a wild type distribution of cones. The protective effect of mTORC1 activation was conserved in two mouse models of RP and promoted survival of nutrient stressed cones by improving glucose uptake and utilization. However, while cone protection remained initially stable, cone loss eventually resumed beyond 2 months of age. Since activation of mTORC1 affords a mutation independent approach to prolong vision, we investigated why in *rd1* mice with loss of *Tsc1*, cone death resumed between 2-4 months of age. mTORC1 is a critical negative regulator of autophagy and to study if loss of *Tsc1* in *rd1* cones, while promoting cone survival through strong activation of mTORC1, may have simultaneously introduced an unwarranted secondary problem, we analyzed the process of autophagy at 2 months of age, a time point just prior to when cone death resumes upon loss of *Tsc1*.

We show that loss of *Tsc1* in cones causes a defect in autophagy leading to an accumulation of autophagic aggregates in both wild type and *rd1* mice. We demonstrate that this defect was not due to an inhibition of autophagy initiation, but due to an accumulation of autolysosomes, suggesting a defect in the end-stage of the process. The incomplete digestion of proteins caused an amino acid shortage in cones thereby hampering long-term cone survival. To facilitate autophagy, we administered the allosteric mTORC1 inhibitor rapamycin, which enhanced survival of cones with *Tsc1* loss at 4 months of age. Interestingly, improved cone survival did not depend on the clearance of autophagic aggregates, rather on maintaining autophagy at a steady state. In this regard, we found that moderate activation of mTORC1 by loss *Pten*, while initially less efficient at promoting cone survival, maintained autophagy and protected cones for up to 1 year, when the protective effect by *Tsc1* removal was lost. This suggests that therapeutic interventions with mild mTORC1 activators that maintain autophagy or gene therapy with selected mTORC1 targets are achievable objectives to delay vision loss in patients with RP.

Results:

Impaired autophagy upon loss of *Tsc1* in wild type mice leads to a progressive decline in cone function and cone specific proteins. To study the long-term effect of *Tsc1* loss in cones of mice with retinal degeneration (*rd1-Tsc1*^{cKO} mice) we first analyzed the effect of its loss in wild type mice (*Tsc1*^{cKO} mice). In Chapter II, we demonstrated that *Tsc1*^{cKO} mice did not show an increase in metabolic gene expression in cones by 2 months

of age (Figure 2.12) however; we did not further characterize its effect on cone function and survival. Electroretinogram (ERG) recordings on mice with *Tsc1* loss showed a strong reduction in cone function over a period of one year with a statistically significant decline as early as 3 months of age (Figures 3.1 A and B). In agreement with the decline in cone function, a cone count, using an antibody directed against the cone specific protein cone ARRESTIN, showed significant loss of cone-arrestin positive cones over-time (Figure 3.1 C). To count cones, retinae were divided into two sectors of radii 1mm and 2mm respectively, and cones were manually counted in four squares per sector, each square measuring 40,000 μm^2. More details about cone quantification are provided in Chapter V.

mTORC1 is a critical negative regulator of autophagy and impaired autophagy due to constitutive activation of mTORC1 has been shown to affect cellular function and survival in various tissues[191,192,194]. We therefore examined the status of autophagy in cones of $Tsc1^{cKO}$ mice, by evaluating the expression of p62, an adaptor protein that is involved in the recognition and targeting of autophagic cargo, such as ubiquitinated proteins, to the lysosome for degradation[276]. We observed an accumulation of both p62 and ubiquitin in cones of $Tsc1^{cKO}$ mice, suggesting a defect in the clearance of ubiquitinated proteins (Figure 3.1 D and E). Taken together, our observations suggest that loss of *Tsc1* in cones leads to a defect in autophagy, which could in part, be responsible for the decline in cone function and associated loss in cone specific proteins.

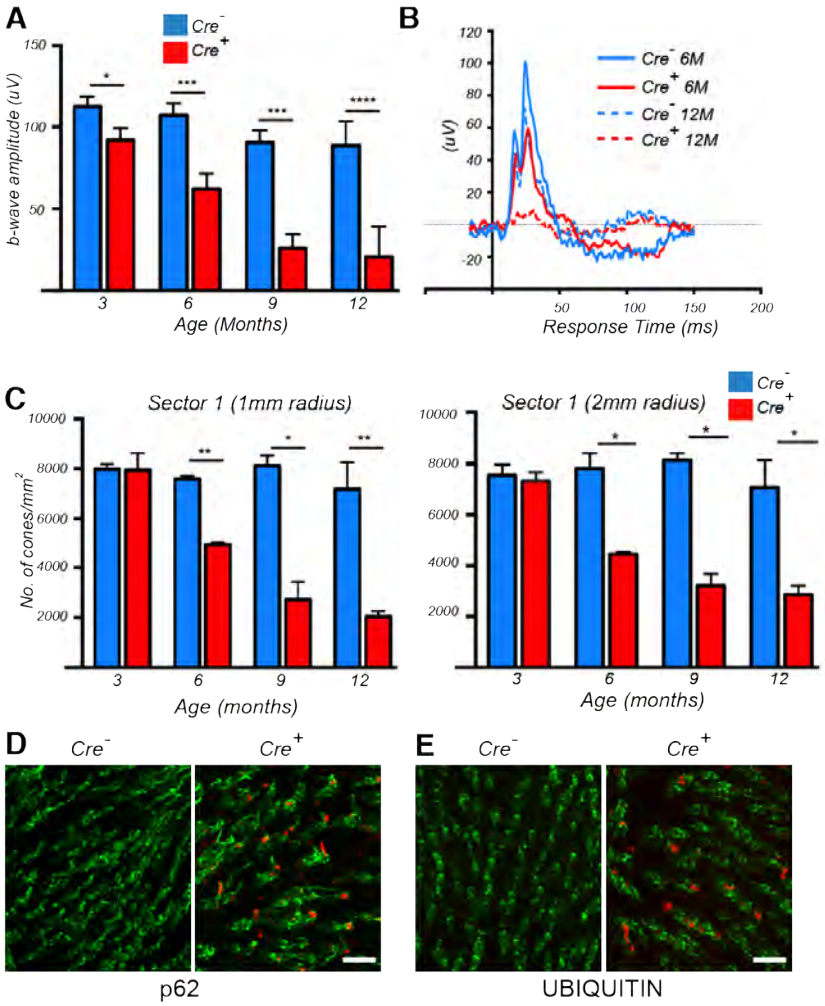

Figure 3.1: Loss of *Tsc1* in cones of wild type mice leads to defective autophagy and progressive decline of cone function. Data shown are from mice harboring the *Tsc1*$^{c/c}$ allele. (**A-B**) Evaluation of cone function over time showing average b-wave amplitudes (left) and representative photopic ERG traces (right) at indicated time points. Data are representative of recordings from at least 6 mice per genotype. $^{*}P < 0.05$, $^{***}P < 0.001$, $^{****}P < 0.0001$ by Student's *t* test. (**C-D**) Evaluation of cone survival: Bar graphs representing the average number of cone arrestin positive cones/mm^2 in Sector 1 & 2 over a period of 1 year. Data are representative of at least 2 mice in each group. $^{*}P < 0.05$, $^{**}P < 0.01$ by Student's *t* test. (**D-E**) Immunofluorescence analysis on retinal whole mounts of p62 and UBIQUITIN (red signal) at 2 months of age. Cones are marked in green by PNA. Scale bars: 20μm

Loss of *Tsc1* in cones of RP mice causes an accumulation of autolysosomes. The findings in wild type mice led us to assess if loss of *Tsc1* also impairs autophagy in RP mice (*rd1-Tsc1*^{cKO}) where cones are subject to conditions of nutrient deprivation. Similar to our observations in wild type mice, *rd1-Tsc1*^{cKO} mice showed an accumulation of p62 and ubiquitin aggregates in cones (Figure 3.2 A). The prevalent model for mTORC1-mediated inhibition of autophagy is through its direct phosphorylation of ULK1 (Unc-51 like autophagy activating kinase-1) at Ser757, a protein that forms part of the autophagy initiation complex[190]. To test if loss of *Tsc1* did indeed inhibit autophagy initiation we injected *Cre*$^{-}$ and *Cre*$^{+}$ *rd1-Tsc1*$^{c/c}$ littermates subretinally at birth with a recombinant adeno-associated virus (rAAV9) that expresses a tandem-tagged mCherry-GFP-LC3 gene[189]. LC3 (Microtubule-associated protein 1 light chain 3) is part of the autophagosomal membrane and remains associated with it even after fusion with the lysosome[189]. Therefore, besides assessing for autophagy initiation, the vector also allows monitoring autophagic flux since the GFP portion of the LC3 reporter construct is pH sensitive. Consequently, autophagosomes appear yellow expressing both red and green fluorescence (mCherry^{+}/GFP^{+}), while autolysosomes appear only red (mCherry^{+}/GFP^{-}) as GFP is quenched by the low pH of the autolysosome. At 2 months of age we found a significant increase in the number of autolysosomes in *rd1-Tsc1*^{cKO} cones (Figure 3.2 B and C), while the number of autophagosomes was similar between *Cre*$^{-}$ and *Cre*$^{+}$ littermates. The data also point towards the existence of an active autophagy flux in *rd1-Tsc1*^{cKO} cones.

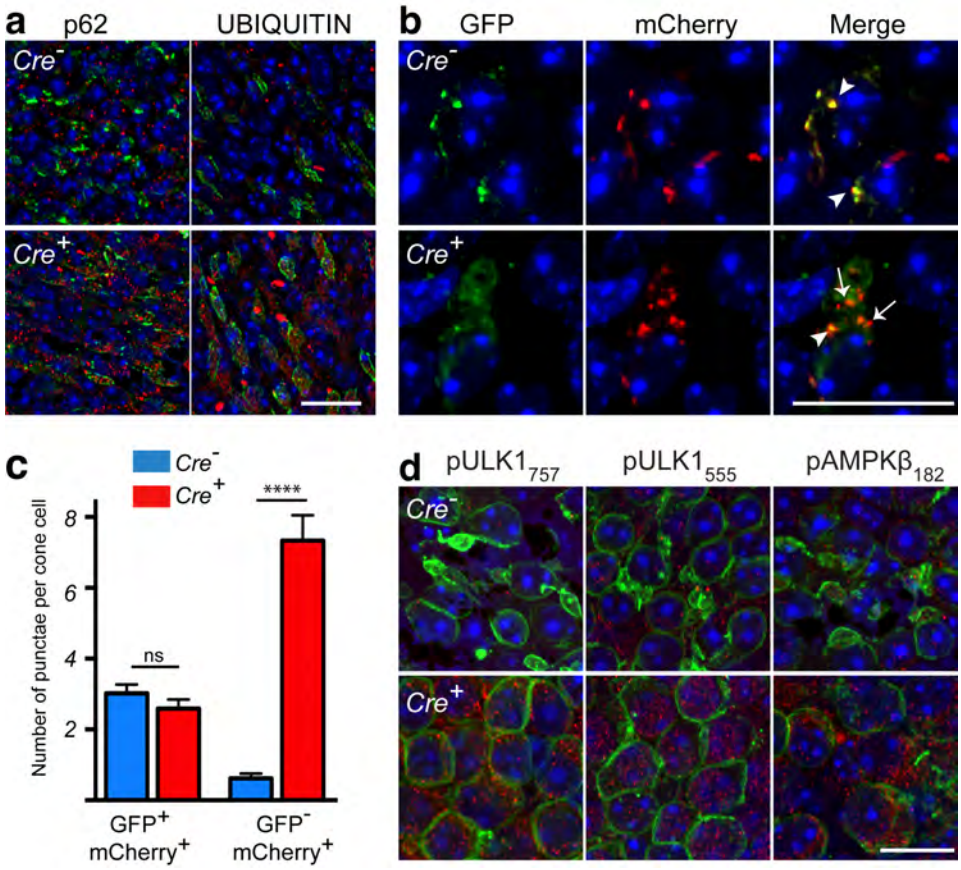

Figure 3.2: *Tsc1* loss maintains autophagic flux in cones of *rd1* mice and causes an increase in autolysosomes. Data shown are from *rd1* mutant mice harboring the *Tsc1*$^{c/c}$ allele at 2 months of age. (**A**) Immunofluorescence analyses on retinal flat mounts for proteins indicated (red signal). Cone layer was identified by PNA staining (green). (**B-C**) Immunofluorescence analyses on retinal flat mounts of retinae infected with the AAV9-mCherry-GFP-LC3 vector at birth. (**B**) Representative images showing increased mCherry^{+}/GFP^{-} punctae (arrows) in cones of *Cre*$^{+}$ mice indicating an increase in number of autolysosomes. Arrowheads indicate GFP^{+}/mCherry^{+} autophagosomes. (**C**) Bar graphs representing average number GFP^{+}/mCherry^{+} punctae (autophagosomes) and GFP^{-}/mCherry^{+} punctae (autolysosomes) per cone cell. Data are representative of measurements in at least 60 cones over 3 different animals per genotype.

****P < 0.0001 by Student's *t* test. (**D**) Immunofluorescence analyses (red signal) on retinal flat mounts for phosphorylation sites on indicated proteins. Cones were detected by SW OPSIN (short wave length opsin: green signal) staining. In all panels blue is nuclear DAPI. Scale bars: 20μm

Therefore, while the data contradict the notion that activated mTORC1 inhibits autophagy, they are in agreement with a recent report which showed that unlike proliferating cells, post-mitotic neurons with TSC loss maintain autophagy through an AMP kinase dependent mechanism that activates ULK1 by phosphorylation at Ser555[194]. Consistent with that we observed increased phosphorylation in *rd1-Tsc1*^{cKO} cones of both ULK1 sites, Ser757 and Ser555, as well as increased phosphorylation of AMPK (Figure 3.2 D), suggesting that the mTORC1-dependent inhibition of ULK1 was overridden through activation of ULK1 by AMP-kinase.

In agreement with an increased number of autolysosomes, proteins required for autophagosome formation such as ATG12 (Autophagy Gene 12), and ALFY (autophagy-linked FYVE protein), a scaffold protein implicated in the selective degradation of ubiquitinated proteins were upregulated in cones (Figure 3.3 A)[199,277]. Moreover, quantification of lysosomes by counting the punctae positive for the lysosomal marker proteins LAMP1/2 (Lysosomal associated membrane protein 1 or 2) indicated an increase in the number of lysosomes in *rd1-Tsc1*^{cKO} cones (Figure 3.3 B and C), corroborating the increase in number of autolysosomes. The increase in the number of lysosomes also coincided with increased nuclear translocation of the forkhead box protein O3 (FOXO3A), a transcription factor that regulates the transcription of various autophagy-related genes (Figure 3.3 D)[212,213].

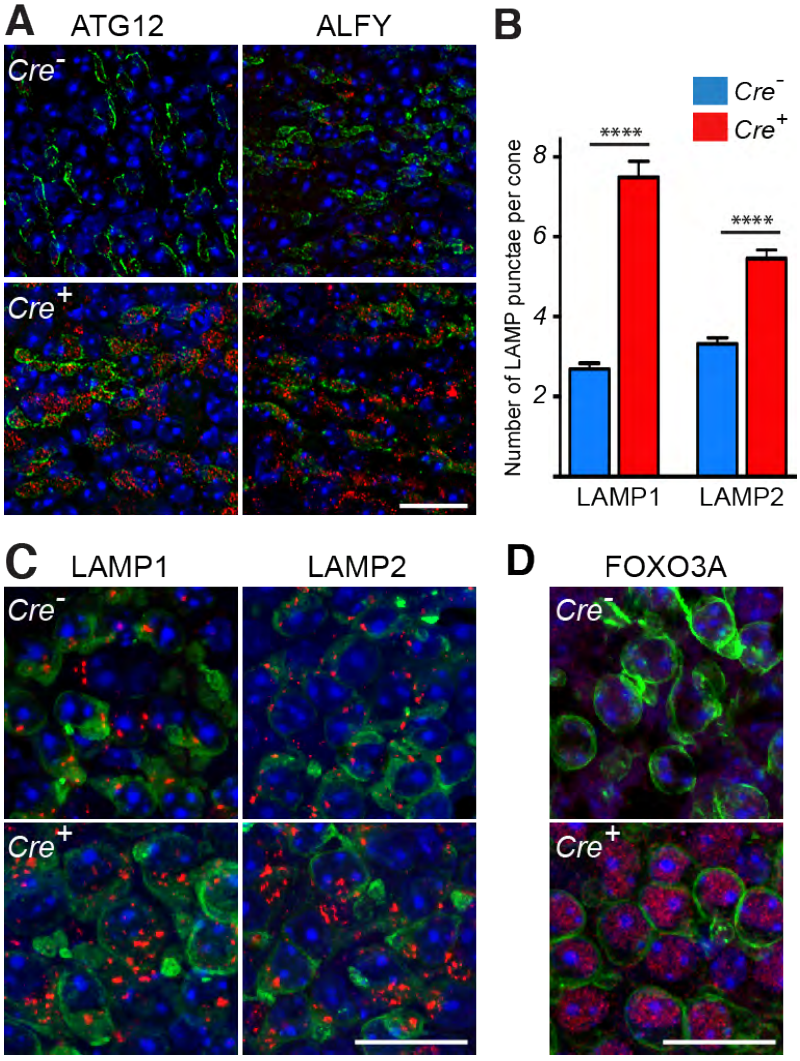

Figure 3.3: Loss of *Tsc1* in cones of *rd1* mice leads to an upregulation of autophagy and lysosomal genes. Data shown are from *rd1*-mutant mice harboring the *Tsc1*$^{c/c}$ allele at 2 months of age. (**A**) Immunofluorescence analyses on retinal flat mounts for the indicated proteins (red signal). Cone layer was identified by PNA staining (green). (**B**) Bar graphs representing average number of LAMP1 and LAMP2 punctae per cone. Values are representative of measurements performed in at least 60 cone cells across 2 animals per genotype. $^{****}P < 0.0001$ by Student's *t* test. (**C**) Representative immunofluorescence on retinal flat mounts for LAMP1 and LAMP2 (red signal). Cones were detected by cone ARRESTIN staining (green signal). (**D**) Immunofluorescence analysis of FOXO3A (red signal). Cones were detected by SW OPSIN staining (green signal). In all panels blue signal is nuclear DAPI. Scale bars: 20μm

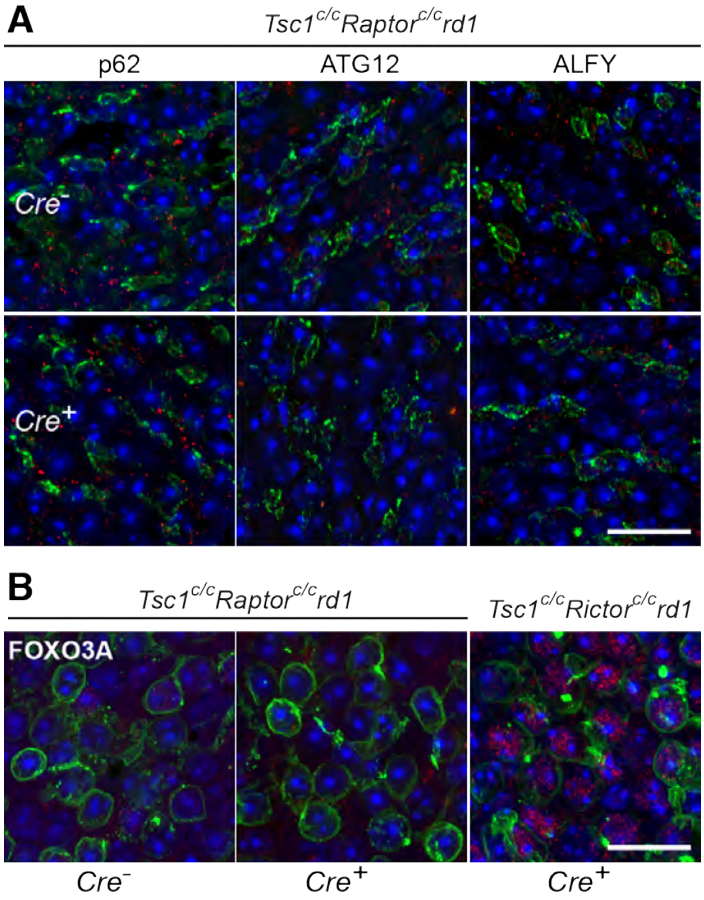

Figure 3.4: Increase in expression of autophagy genes is dependent on mTORC1. Immunofluorescence analyses on retinal flat mounts for indicated proteins (red signal) in *rd1* mice harboring the conditional alleles as indicated at 2 months of age. No difference is observed in the expression of autophagy genes (**A**) or FOXO3A (**B**) between *Cre*$^{-}$ and *Cre*$^{+}$ littermates of *Tsc1*$^{c/c}$*Raptor*$^{c/c}$ mice while nuclear FOXO3A is increased in *rd1-Tsc1*^{cKO}*Rictor*^{cKO} cones. Green is PNA in (**A**) and SW OPSIN in (**B**). Scale bars: 20μm

The accumulation of p62 as well as the upregulation of ATG12 and ALFY were mTORC1 dependent, as they were unchanged in *rd1-Tsc1*^{cKO} cones that lacked the mTORC1 accessory protein RAPTOR (Figure 3.4 A). The increased nuclear translocation of FOXO3A upon *Tsc1* removal has been reported previously as well and could be a result of the inhibitory effect of activated mTORC1 on mTORC2[158,160,278].

Reduced mTORC2 activity would then reduce AKT activity, which is a key kinase that regulates FOXO3A localization[279]. In this regard, nuclear FOXO3A staining was maintained in *rd1-Tsc1*^{cKO}*-Rictor*^{cKO} cones which lack an active mTORC2 complex, absent in *rd1-Tsc1*^{cKO}*-Raptor*^{cKO} cones (Figure 3.4 B), and we demonstrated previously a reduction in AKT (Ser473) phosphorylation upon activation of mTORC1 (Figure 2.1 C).

In summary, our data suggest that the defect in autophagy does not arise from autophagy initiation, autophagosome maturation or fusion with the lysosome. Since mTORC1 is a negative regulator of the transcription factor EB (*Tfeb*)[258,259], a master transcription factor of lysosomal enzymes, the increased accumulation of autolysosomes could result from a deficiency of lysosomal enzymes due to increased mTORC1 activity.

***Tsc1* loss induces a shortage of free amino acids in cones.** The autophagy defect in *rd1-Tsc1*^{cKO} cones could cause an imbalance in cellular homeostasis if the increase in protein synthesis is not accompanied by a corresponding increase in protein turnover depleting the cell of free amino acids. To test this notion, we performed an experiment that exploits the mechanism of amino acid sensing by mTORC1. Under amino acid-replete conditions, mTORC1 is recruited by the Rag GTPases to LAMP2 containing compartments where it encounters *Rheb* for activation[280]. Therefore, colocalization of mTORC1 with LAMP2 can be used to assess if the cell has a sufficiency of amino acids.

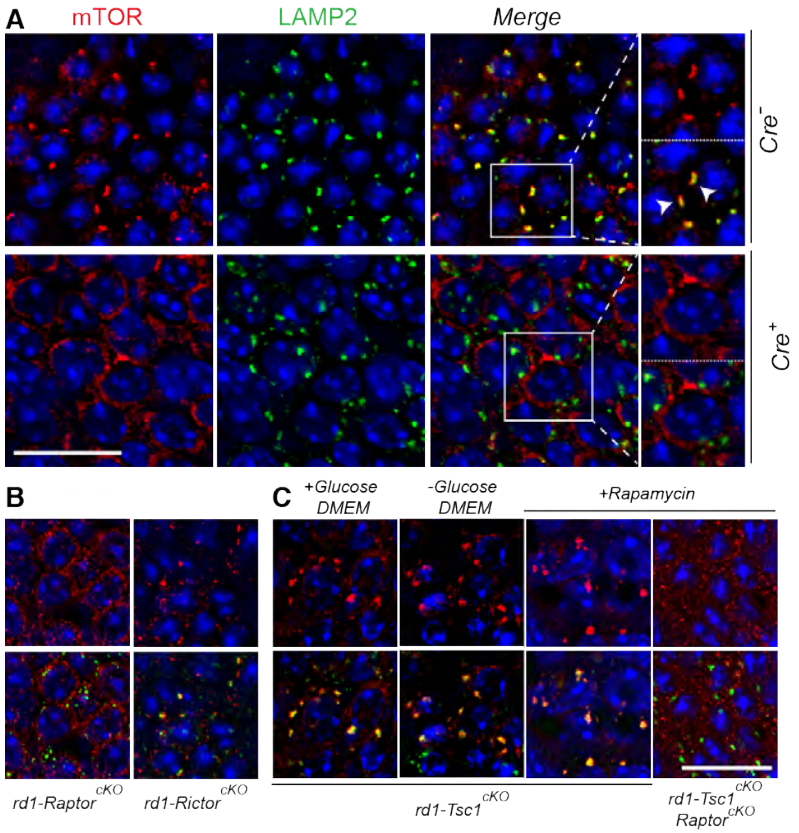

Figure 3.5: mTOR and LAMP2 colocalization analysis reveals a shortage of amino acids upon *Tsc1* loss in cones. Immunofluorescence analyses on retinal whole mounts of *rd1* mutant mice harboring the conditional alleles indicated at 2 months of age. (**A**) Localization of mTOR to LAMP2-containing compartments in retinae of *rd1-Tsc1*$^{c/c}$ *Cre*$^{-}$ mice (arrowheads in higher magnification view). Localization is lost in *Cre*$^{+}$ mice (lower row in **A**). Higher magnification view: the upper panel mTOR, lower panel mTOR and LAMP2. (**B** and **C**) Only *Cre*$^{+}$ retinas of genotype indicated are shown with the upper row showing mTOR staining and lower row showing both mTOR and LAMP2. (**B**) mTOR:LAMP2 colocalization is lost in *rd1-Raptor*^{cKO}mice, but retained in *rd1-Rictor*^{cKO} mice. (**C**) mTOR:LAMP2 colocalization in *rd1-Tsc1*^{cKO} mice can be restored by incubating retinas in DMEM media with or without glucose for 2 hours or by systemic administration of rapamycin (intraperitoneal), but not in retinae from *rd1-Tsc1*^{cKO} mice upon concurrent removal of *Raptor*. Retinae were harvested two hours post-Rapamycin injection. In all panels red staining indicates mTOR, green LAMP2 and blue nuclear DAPI. Scale bars: 20μm. Higher magnification images in (**A**): 1.5X original

We observed at 2 months of age in *Cre*$^{-}$ cones distinct focal mTOR staining that is strongly associated with LAMP2. However, in age-matched *rd1-Tsc1*^{cKO} cones mTOR staining was diffuse and showing almost no colocalization with LAMP2 (Figure 3.5 A). To verify that the mTOR staining at the lysosome observed in *Cre*$^{-}$ cones was reflective of mTORC1, we repeated the experiment with *rd1-Raptor*^{cKO} retinae, where colocalization was lost, and with *rd1-Rictor*^{cKO} retinae, where colocalization was maintained, indicating that the mTOR staining that colocalized with LAMP2 was in fact mTORC1 (Figure 3.5 B).

To test if the absence of mTOR:LAMP2 colocalization in *rd1-Tsc1*^{cKO} cones was caused by a shortage of amino acids, we explanted retinas from *rd1-Tsc1*^{cKO} mice and incubated them in glucose-rich and glucose-free DMEM media (Figure 3.5 C). In both cases, short-time exposure to regular media containing amino acids restored the mTOR:LAMP2 colocalization. Similarly, a single injection of rapamycin, an allosteric mTORC1 inhibitor, was also able to restore mTOR:LAMP2 colocalization in *rd1-Tsc1*^{cKO} cones, but not in *rd1-Tsc1*^{cKO} cones that also lacked *Raptor* (Figure 3.5 C).

Together, the data suggest that loss of *Tsc1* in cones of RP mice induces an imbalance in the supply and demand of amino acids, which could be responsible for the demise of cones seen between 2 and 4 months of age.

Rapamycin reverses the autophagy defect and improves cone survival upon *Tsc1* loss.

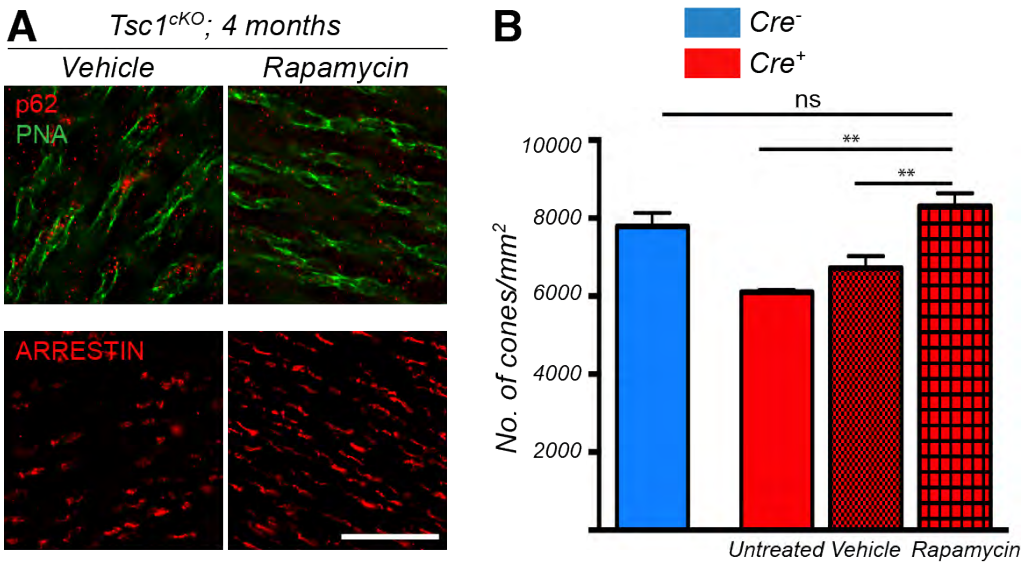

Figure 3.6: Rapamycin reverses the autophagy defect and improves cone survival upon *Tsc1* loss in wild type mice. (**A**) Immunofluorescence analysis on retinal flat mounts from *Tsc1*^{cKO} mice showing clearance of p62 aggregates in cones (upper panel, red signal; green: PNA) and recovery of cone arrestin (lower panel, red signal) expression upon delivery of rapamycin between P28 to 4 months of age. Images were acquired at 1mm radius from the optic nerve (Sector 1) Scale bars: 20μm. (**B**) Quantification in Sector 1 (1mm radius, as in **Figure 3.1**) of cone-arrestin positive cones in wild type mice at 4 months of age. Data are representative of at least 3 mice in each case. $^{**}P < 0.01$ by Student's *t* test.

The restoration of colocalization between mTOR and LAMP2 in *rd1-Tsc1*^{cKO} cones upon rapamycin administration (Figure 3.5 C) indicates that autophagy was restored resulting in the release of free amino acids. To test whether the p62 and ubiquitin aggregates or the lack of free amino acids cause cones to die in *rd1-Tsc1*^{cKO} mice, we performed a long-term rapamycin treatment. In Chapter II, we showed that *rd1-Tsc1*^{cKO} mice display a

decline in cone survival between 2 and 4 months of age. Similarly, removal of *Tsc1* in cones of wild type mice (*Tsc1*^{cKO}) causes loss of cone arrestin expression by 4 months of age (Figure 3.6 B). Because loss of mTORC1 activity did not affect cones in a wild type background but accelerated cone death during disease, we first administered rapamycin to *Tsc1*^{cKO} mice, where repeated injections between 1-4 months of age (18 in total) did clear p62 and ubiquitin aggregates and also restored cone arrestin expression in *Tsc1*^{cKO} mice (Figure 3.6 A and B).

In *rd1-Tsc1*^{cKO} mice where mTORC1 activity is critical to promote cone survival, we first tested the effect of rapamycin between 1-2 moths of age, a time window in which cone survival remains stable at around 78% (Figure 2.11). While one injection of rapamycin at 2 months of age was not able to clear p62 and ubiquitin aggregates, repeated injections at an interval of 5 days were sufficient to clear p62 and ubiquitin aggregates without affecting cone survival (Figure 3.7 A and B). The 5 days interval period was based on the time window it took for pS6 levels to recover in cones of *rd1-Tsc1*^{cKO} mice after one rapamycin injection (Figure 3.7 C and D).

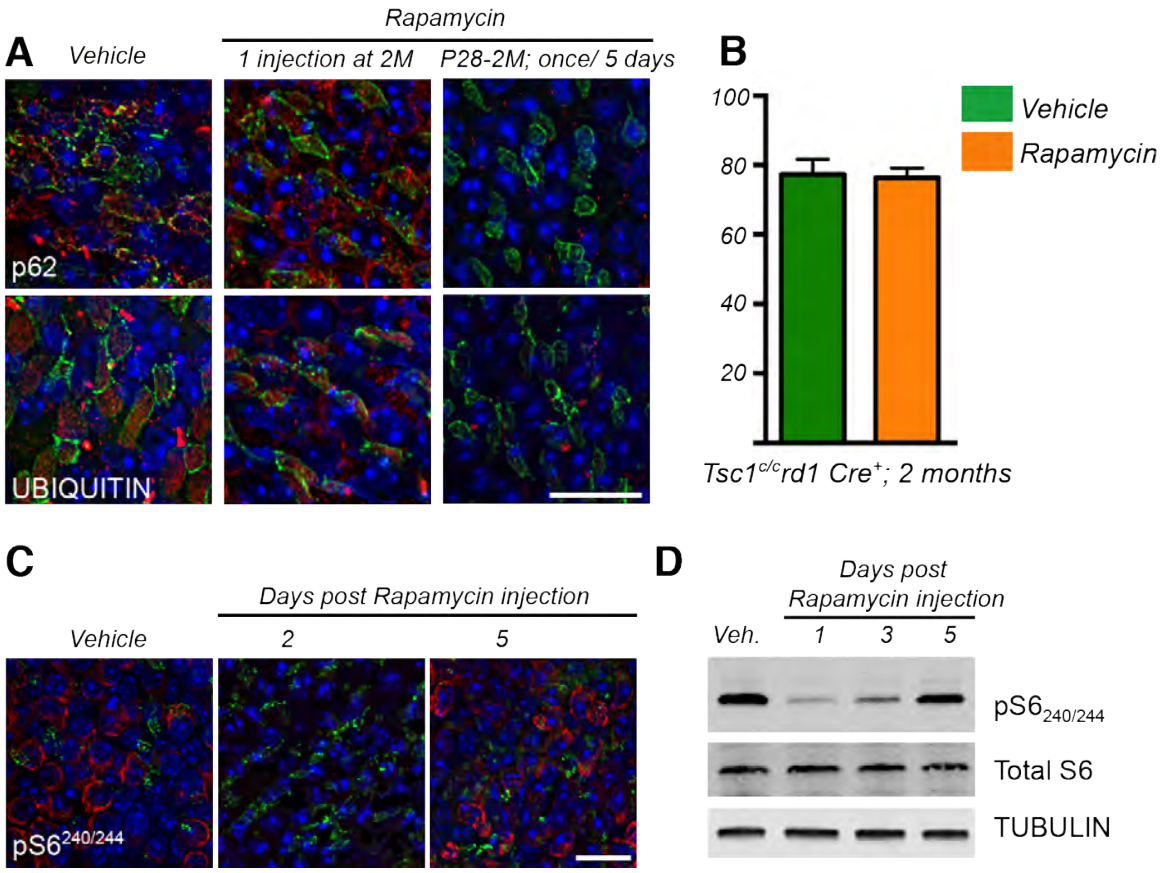

Figure 3.7: Effect of rapamycin administration in *rd1-Tsc1*$^{c/c}$ mice. (A) Immunofluorescence analyses on retinal flat mounts for p62 and UBIQUITIN (red signal, as indicated) in *rd1-Tsc1*^{cKO} mice at 2 months of age upon vehicle or rapamycin administration. **(B)** Quantification of cone survival in *rd1-Tsc1*^{cKO} mice at 2 months of age when administered with vehicle or rapamycin once every five days from P28 to 2 months. (**C-D**) Kinetics of recovery of phosphorylation of S6 on retinal flat mounts of *rd1-Tsc1*^{cKO} mice when administered with vehicle or rapamycin. (**C**) Immunofluorescence for phospho-S6 (red signal) on retinal flat mounts harvested 2 or 5 days after injection with vehicle or rapamycin. Green is PNA. Scale bar: 20µm (**D**) Western blot for phospho-S6 on mice harvested 1, 3 or 5 days after injection with rapamycin. The data show that S6 phosphorylation is almost fully recovered by day 5 after injection. Green signal in (**A**) and (**C**) is PNA. Scale bar: 20µm

Extended injections of rapamycin (18 in total) up to 4 months of age, however, led to a drop in cone survival when compared to vehicle-injected mice (Figure 3.8 A), suggesting that mTORC1 was inhibited too often over the 3 months time period. We therefore performed two additional treatment regimens reducing the frequency of administration by three-fold each time. This led to a dose dependent increase in cone survival with 6 injections being at par with vehicle treated mice and 2 injections showing a significant improvement in cone survival by 4 months of age (Figure 3.8 A and B). Post-injection analysis of p62 aggregates at 4 months showed that neither 6 nor 2 injections of rapamycin were sufficient to clear p62. (Figure 3.8 C, only data from 6 injections is shown) The data therefore suggests that clearance of p62 is not required to improve cone survival, since 2 or 6 single injections of rapamycin was not sufficient to clear p62 (Figure 3.7 A and 3.8 C), however one injection was sufficient to facilitate autophagy releasing free amino acids that directed mTOR to the lysosome for at least 14 days (Figure 3.8 D).

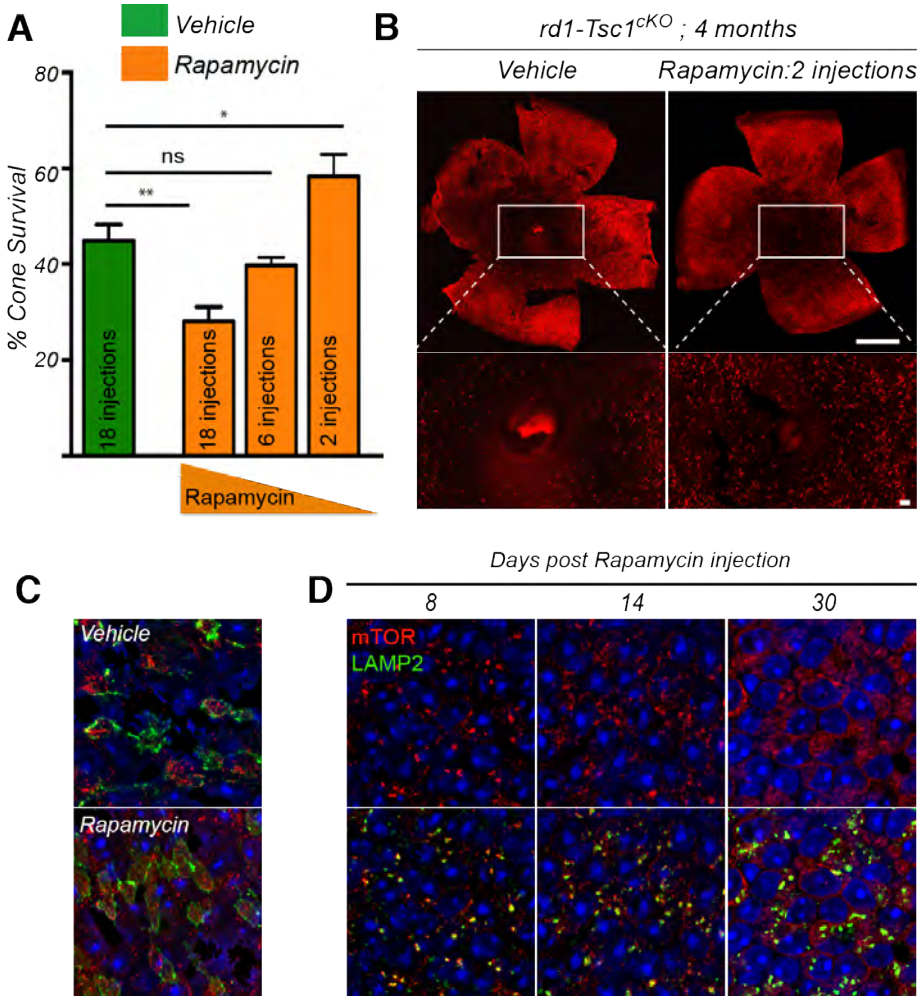

Figure 3.8: Dose-dependent effect of rapamycin administration on cone survival of *rd1-Tsc1*$^{c/c}$ mice. (**A**) Quantification of cone survival in *rd1-Tsc1*^{cKO} mice at 4 months of age upon injection with vehicle or rapamycin starting at P28. Number of rapamycin injections is indicated in bar. Data are representative of at least 6 mice in each group. $^{*}P < 0.05$, $^{**}P < 0.01$ by Student's *t* test. (Scale bars: Upper panel: 1mm and lower panel: 50um) (**B**) Representative retinal flat mounts of *rd1-Tsc1*^{cKO} mice at 4 months of age showing more central cones when two injections of Rapamycin were administered (red signal: cone arrestin; Scale bars: 1mm). (**C**) Immunofluorescence analyses for p62 (red signal) at 4 months of age in *rd1-Tsc1*^{cKO} mice treated with vehicle or 6-injections of rapamycin. (**D**) Dynamics of mTOR (red signal) localization with LAMP2 (green signal) post rapamycin injection in *rd1-Tsc1*^{cKO} mice with upper row showing mTOR staining and lower row showing both mTOR and LAMP2.

Increased mTORC1 activity by loss of *Pten* maintains autophagy and is more beneficial for long-term cone survival. Since intermittent inhibition of constitutively activated mTORC1 improved cone survival at 4 months of age when compared to constitutively activated mTORC1 alone we investigated the effect of lower levels of mTORC1 activation on autophagy, mTORC1 localization and long-term cone survival. We showed in Chapter II that loss of *Pten* in cones activates mTORC1 to a lesser extent than *Tsc1* loss. Consequently, *Pten* loss in cones of RP mice (*rd1-Pten*^{cKO} mice) results in a smaller cone survival effect at 2 months of age than seen with *Tsc1* loss. Interestingly, in *rd1-Pten*^{cKO} retinae we found no accumulation of p62 or ubiquitin in cones at 2 months of age, suggesting that autophagy is not impaired with lower mTORC1 activation (Figure 3.9 A). Concordantly, mTOR:LAMP2 colocalization in cones was similar between *Cre*$^{-}$ and *Cre*$^{+}$ littermates (Figure 3.9 B), with only a moderate increase in lysosomes per cone as assessed by LAMP1 positive punctae (Figure 3.9 C). The data suggest that while autophagy is increased, it is not impaired maintaining a free amino acid pool despite the increase in protein translation predicted to occur upon loss of *Pten*. In agreement with these findings, we did not observe any increase in ULK1 phosphorylation at both sites nor in AMP kinase phosphorylation (Figure 3.9 D), suggesting that autophagy is maintained at a steady state.

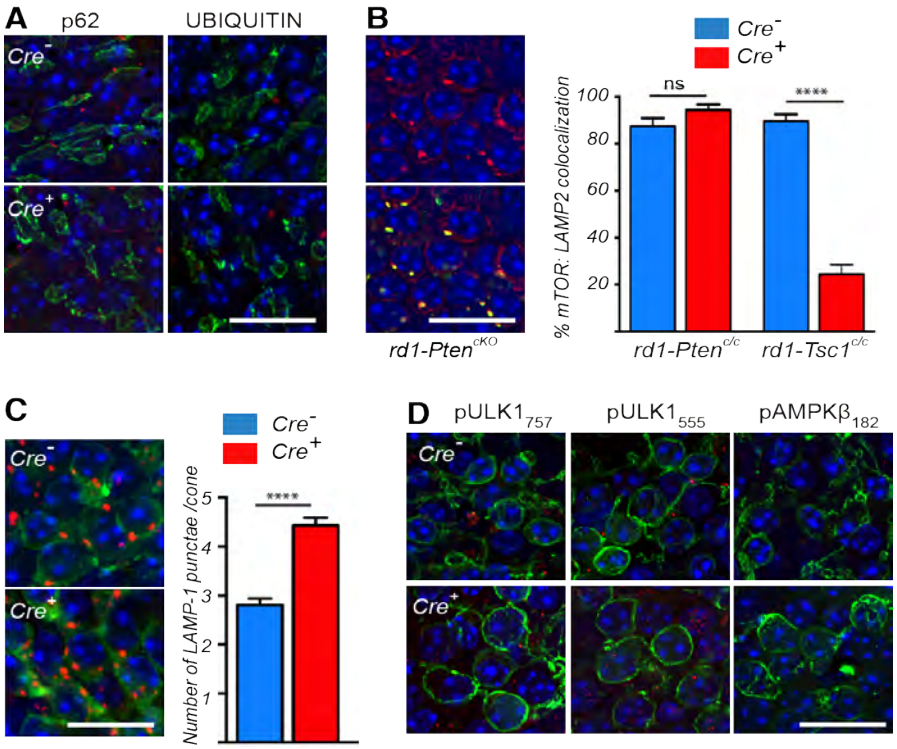

Figure 3.9: Moderate increase in mTORC1 activity by loss of *Pten* does not cause a defect in autophagy. Data shown are from *rd1-Pten*$^{c/c}$ mice, unless indicated otherwise. (**A**) Immunofluorescence analysis on retinal flat mounts for indicated proteins (red signal) at 2 months of age (green: PNA). (**B**) Immunofluorescence analysis on retinal flat mounts for mTOR (red signal) and LAMP2 (green signal) in *Cre*$^{+}$ mice at 2 months of age. Upper panel shows only mTOR, lower panel shows colocalization with LAMP2 (Scale bar: 20μm). Bar graphs represent percentage of mTOR punctae that colocalize with LAMP2 per cone. Data from *rd1-Tsc1*^{cKO} mice (representative images in **Figure 3.5 A**) is provided for comparison. The data represent values obtained from at least 60 cones across 2 animals per genotype ($^{****}P < 0.0001$ by Student's *t* test). (**C**) Immunofluorescence analysis on retinal flat mounts for LAMP1 (red signal) in *Cre*$^{-}$ and *Cre*$^{+}$ mice at 2 months of age. Cones were identified by cone arrestin antibody (green signal; Scale bar: 20μm). Bar graphs showing number of LAMP1 punctae per cone. Data represent values obtained from at least 60 cones across 2 animals per genotype ($^{****}P < 0.0001$ by Student's *t* test). (**D**) Immunofluorescence analysis on retinal flat mounts for indicated proteins (red signal) at 2 months of age (green: SW OPSIN) Scale bars: 20μm

In wild type mice, we observed only occasional accumulation of p62 in cones of *Pten*^{cKO} mice when compared to mice where *Tsc1* was removed in cones (Figure 3.10 A). This accumulation was not detrimental to cone function and survival up to 1 year of age (Figure 3.10 B and C).

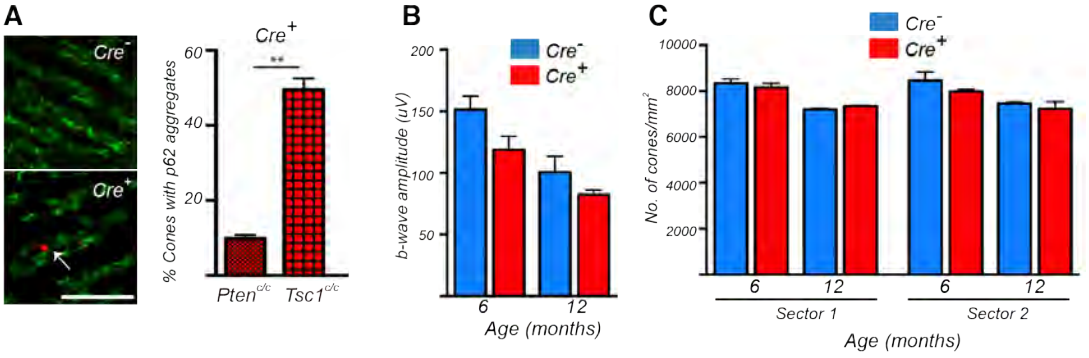

Figure 3.10: Loss of *Pten* does not affect cone survival or function in a wild type background. Data presented are from *Pten*$^{c/c}$ mice, unless indicated. (**A**) Immunofluorescence analysis (red signal) on retinal flat mounts for p62 in cones of *Pten*$^{c/c}$ mice at 2 months of age. Arrow indicates p62 aggregate in cone segment of *Cre*$^{+}$ mice. Green is PNA. Scale bar: 20μm. The bar graph represents quantification of percentage of cones with p62 aggregates in retinae from *Pten*^{cKO} and *Tsc1*^{cKO} (representative image in **Figure 3.6A**) mice at 2 months of age. p62 aggregation was not detected in *Cre*$^{-}$ mice in either genotype and hence was not included in the graph. Data are representative of measurements in at least 100 cone segments across 2 animals per genotype. $^{**}P < 0.01$ by Student's *t* test. (**B**) Evaluation of cone function by photopic ERG recordings showing average b-wave amplitudes. We did not measure a significant difference between *Cre*$^{-}$ and *Cre*$^{+}$ littermates at any time point. Data are representative of at least 6 mice in each group. (**C**) Quantification of cone number based on cone arrestin staining in two retinal sectors as described in **Figure 3.1**. No difference was observed up to 1 year of age between *Cre*$^{-}$ and *Cre*$^{+}$ littermates. Data are representative of at least 2 mice in each group.

Together these findings led us to test if long-term protection of cones is improved upon loss of *Pten* when compared to loss of *Tsc1*. In Chapter II, we evaluated the protective effect of *Pten* and *Tsc1* loss in cones of RP mice up to 8 and 12 months of age, respectively. At one year of age there was no cone protection upon loss of *Tsc1,* however; there was more than a 2-fold increase in cone survival in *rd1-Pten*^{cKO} mice when compared to *Cre*$^{-}$ littermates and cone survival was also significantly higher when compared to loss of *Tsc1* (Figure 3.11 A and B). A linear regression analysis shows that while the initial effect upon loss of *Pten* is less robust, the decline over time is not as steep when compared to loss of *Tsc1* (Figure 3.11 C).

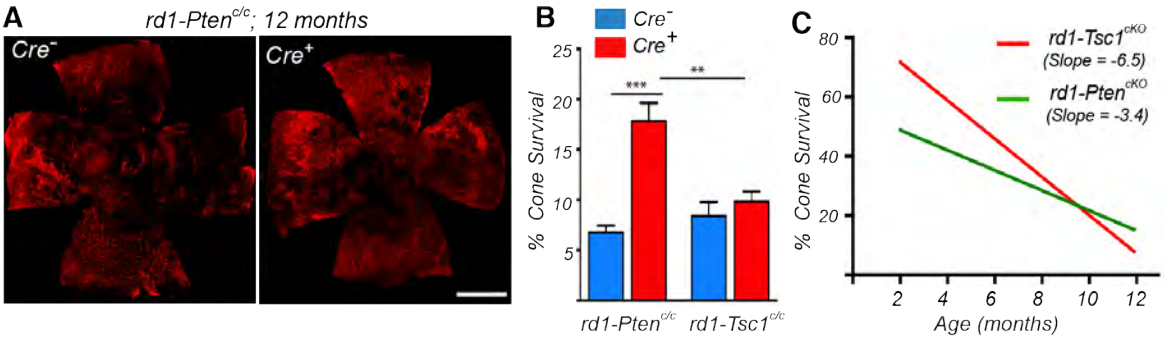

Figure 3.11: Moderate increase in mTORC1 activity by loss of *Pten* is more benefical for long-term cone survival. (A) Representative retinal flat mounts of *rd1-Pten*$^{c/c}$ mice at 12 months of age showing improved cone survival in *Cre*$^{+}$ mice (red: cone arrestin; Scale bar: 1mm). (**B**) Quantification of cone survival at 12 months of age comparing data obtained from *rd1-Pten*^{cKO} mice with *rd1-Tsc1*^{cKO}. $^{*}P < 0.05$ by Student's *t* test. (**C**) Linear regression of cone survival over time in *rd1-Tsc1*^{cKO} and *rd1-Pten*^{cKO} mice. Loss of *Pten* results in a more gradual decline in cone survival, as seen by the smaller slope.

In summary the data indicate that moderate mTORC1 activation that does not impair autophagy is more beneficial for long-term cone survival as both, glucose and amino acid metabolism are balanced, suggesting that therapeutic intervention with few mTORC1 target genes or mild mTORC1 activators is an obtainable goal for long-term vision stabilization in individuals with RP.

CHAPTER IV

Discussion

Loss of vision can drastically impact the quality of life. While RP has been studied for several decades, and many of the genes that cause the disease are known, there is still no treatment available for patients affected by the disease. This may partly arise from the fact that not many research efforts have focused on understanding how cones, which have highly specialized structural and functional requirements, regulate their metabolic demands. In this study, we show that cell autonomous activation of mTORC1 mediated by loss of either *Tsc1* or *Pten* is sufficient to promote long-term survival of cones in RP. Our data showing almost a wild type distribution of cones at 2 months of age upon loss of *Tsc1* in the *rd1* mouse model (Figure 2.6 A and B) holds great promise, since this model is one of the fastest progressing models of RP. Because cone death is also significantly delayed in the $Rho^{-/-}$ model (Figure 2.14), our approach is mutation-independent and can be applied to a broad spectrum of rod-specific mutations in RP. Our research also addresses a longstanding question of non-autonomous cone death and suggests that the secondary loss of cones in RP is principally caused due to a shortage of nutrients, particularly of glucose in cones. While unwarranted secondary effects such as the inhibition of autophagy accompany constitutive mTORC1 activation, our data suggest that it is possible to overcome this drawback by regulating the extent of mTORC1 activation (Figure 3.8). In this regard, activation of mTORC1 by loss of *Pten*, promotes

cone survival for up to 1 year of age without hampering autophagy (Figures 3.9 and 3.11). Thus far, no other study has reported significant protection of cones in the *rd1* mouse model at this late time point. Our comprehensive characterization of the role of the insulin/mTOR pathway members in cone PRs also highlights how neurons may differentially utilize this pathway under normal and nutrient stress conditions encountered during disease, which may have implications in other neurodegenerative diseases as well. We will now elaborate on the significance of our findings.

Role of mTOR in cone homeostasis and disease: Various growth factors that promoted cone survival in RP models[13,88,89,93] may act through increasing PI3K activity, since the kinase functions as a common upstream component of various signaling pathways[281]. PI3K activity is critical for cones as its loss leads to progressive decline of cone survival and function[218,219]. In this study we show that removal of mTORC1, which is downstream of PI3K, causes approximately a 50% decline in cone survival during disease (Figure 2.4 A and B), suggesting that mTORC1 is critical to allow cones to adapt to conditions of nutrient stress. However, loss of mTORC1 did not have any effect in wild type mice where cones do not encounter nutrient stress (Figure 2.5). While we presented data up to 2 months of age, a parallel study characterizing the long-term effect of mTORC1 ablation in wild type cones performed in our laboratory found that neither cone survival nor function is affected upon loss of mTORC1 for up to 1 year of age[282]. Most tissues are severely affected upon removal of *Raptor*, given the central role for mTORC1 in regulating the metabolic transcriptome, especially in cells with high metabolic

demands[283-285]. It is therefore surprising that this kinase was not required for survival of cones under normal conditions, suggesting that PI3K-dependent pro-survival signals are independent of mTORC1 in wild type cones. Consistent with these data, we do not observe an increase in the expression of mTORC1-target genes involved in cell metabolism in wild type cones upon constitutive activation of mTORC1 (Figure 2.12). Therefore, our data suggests that mTORC1 functions only under conditions of stress to increase expression of critical glycolytic genes. This is further supported by the finding that the expression of these genes increases gradually over time from P21 to 2 months of age, suggesting that the increase was in response to the progression of the disease (Figure 2.10).

Cones have considerably shorter outer segments (OS) when compared to rods and therefore, the requirement to synthesize membrane is lesser. Cones may therefore utilize less NADPH and consequently consume less glucose than rods. It however, remains to be determined if rods utilize mTORC1 to fulfill their metabolic requirements. On the contrary, the requirement for ATP may be higher in cones, since they function throughout the day and hence need ATP to constantly re-equilibrate membrane potential. However, under disease conditions, there is a shortening of cone OSs, which necessitates cones to diverge more glucose into biosynthetic pathways to maintain their OS, since PR function is tightly linked to OS integrity. The fact that cones may depend more on glucose during disease is demonstrated by the finding that mTORC1 activity, as evaluated by phosphorylation of S6, is barely detectable in cones under normal conditions, while it is

increased in cones of *rd1* mice (Compare Figure 2.3B with *Cre*$^{-}$ images from Figure 2.2C or 2.6D). Similarly, the expression of mTORC1 target genes like GLUT1 and HIF-1α is increased during disease in cones when compared to wild type cones (Compare *Cre*$^{-}$ in Figure 2.9 with Figure 2.12). Concordantly, removal of mTORC1 severely affects cones in RP since they are not able to synthesize NADPH to maintain their OSs. Cones can still generate ATP from lactate derived from Müller glia cells, since cone-glial interactions are not predicted to be affected in RP, unlike cone:RPE interactions[129]. In fact, neurons have been reported to use lactate to fuel oxidative metabolism[286,287]. Cones are known to remain dormant or non-functional in RP for extended periods of time following the loss of their OS[288]. This may be due to the fact that they still have sufficient ATP that affords survival in the absence of an OS. Together, the data suggest that the energy requirements for cones vary under nutrient replete and nutrient stressed conditions, which results in the differential utilization of mTORC1 under the two scenarios.

Loss of mTORC2 generally has a milder phenotype than loss of mTORC1 and this was also mirrored in our study, where its loss did not affect cone survival in either wild type or RP mice[267,289].

Constitutive activation of mTORC1 upon loss of the TSC in cell culture systems has been shown to render cells sensitive to complete withdrawal of glucose[290]. Loss of TSC increases the rate of glycolysis, which causes cells to become addicted to glucose. Under conditions of glucose withdrawal, the increased demand of TSC-null cells is not balanced

by a corresponding increase in supply, which decreases the ATP:ADP ratio, leading to the activation of an energetic stress response mediated by AMPK and subsequent induction of apoptosis. Under these conditions, inhibition of mTORC1 by rapamycin confers a survival advantage to cells with loss of TSC. Interestingly, low glucose conditions (as opposed to complete withdrawal) confer a survival advantage to TSC null cells[291]. This is because increased mTORC1 activity allows for the expression of transporters and other metabolic genes that allow cells to counterbalance the shortage of glucose. Similar to findings in cell culture, we find that loss of TSC confers a survival advantage to cones in RP mice (Figure 2.6 A and B). Retinae from *rd-Tsc1*^{cKO} mice have increased NADPH levels (Figure 2.8 B) suggesting that glucose uptake and divergence into the PPP was increased. Since NADPH is required for lipid and membrane synthesis, the increase in NADPH may have facilitated the synthesis of OSs thereby preventing the shortening of cone OSs normally seen during disease. Consequently, OS length and width are maintained between P21 and 2 months of age in *rd1-Tsc1*^{cKO} cones (Figure 2.8 D), which also improves cone function (Figure 2.6 C). NADPH is also required to recycle the visual chromophore that is required for PR function. Therefore, an overall healthier and better functioning cone PR is also likely to survive longer. Our data however, does not establish that the increase in NADPH and thus, improved cone survival was due to elevated expression of metabolic genes like HKII or G6PD. Further, we also do not show that glucose uptake was indeed increased in cones upon loss of *Tsc1*. Loss of the protective effect upon concurrent loss of *Tsc1* and *HkII* or any other metabolic gene, or measuring uptake of fluorescent or radiolabelled glucose analogs would unequivocally

address if improved cone survival was mediated by improving glycolytic metabolism of cones.

Besides glucose, amino acids and growth factors are also critical to maintain mTORC1 activity, and the lysosome is the site where these inputs converge to regulate mTORC1. Amino acids mediate the recruitment of mTORC1 to the lysosome, where GTP-bound Rheb, which in turn is regulated by growth factors, activates it[196]. Recent studies in cell culture have shown that TSC2 localization is also sensitive to amino acids[173]. A deficiency in amino acids promotes TSC2 localization to the lysosome, where it inhibits Rheb, subsequently inhibiting mTORC1 activity. Amino acids therefore exert a dual regulation of mTORC1 activity through mTORC1 and TSC2 localization. Consequently upon loss of TSC, cells are sensitive to amino acid withdrawal since they are unable to completely turn off mTORC1 activity. Under these conditions, mTORC1 is not completely withdrawn from the lysosome, thereby being still active despite the shortage of amino acids. Therefore, loss of TSC results in an inhibition of autophagy even under amino acid starvation conditions. What do these studies tell us about the situation in cones? We reported that upon loss of *Tsc1*, the mTOR staining is diffuse and predominantly not colocalized with the lysosome. However, our quantification revealed that about 20% of LAMP-2 puncate are still positive for mTOR upon loss of *Tsc1* (Figure 3.9 B). This residual mTORC1 at the lysosome may be sufficient to mediate an inhibition of autophagy. Therefore, while loss of *Tsc1* confers an initial survival advantage to cones,

the efficiency of cone survival eventually declines over time, since they are not able to regulate mTORC1 activity in order to promote autophagy.

The reduced localization of mTORC1 at the lysosome upon loss of *Tsc1* is also indicative of a shortage of amino acids because short-term incubation of retinae in glucose-free media is sufficient to restore mTOR:LAMP2 colocalization (Figure 3.5). Does the lack of amino acids arise because of reduced flow from the RPE, similar to glucose or is it the inhibition of autophagy that in turn, causes a shortage of amino acids or a combination of both? To address this question, we evaluated mTOR localization from P21, when cone death just initiates.

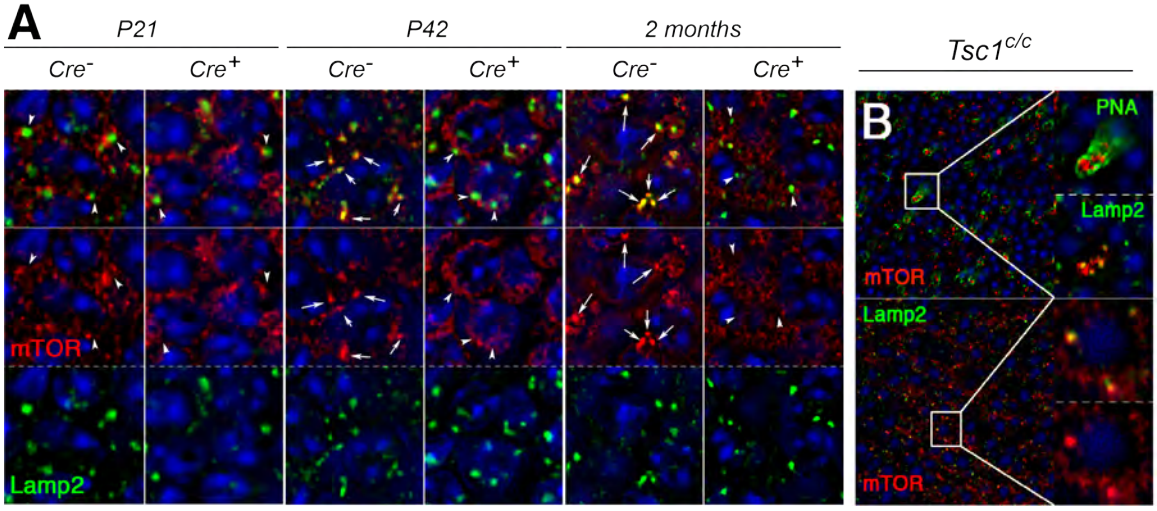

Figure 4.1: Dynamics of mTOR localization during disease. Immunofluorescence analyses on retinal whole mounts from *rd1-Tsc1*$^{c/c}$ (**A**) or *Tsc1*$^{c/c}$ (**B**) mice. Arrowheads in (**A**) indicate absence of mTOR (red signal) and LAMP2 (green signal) colocaliation, while arrows are used to depict colocalization. Green signal in (**B**) represents either the cone marker PNA or LAMP2, as indicated

Interestingly, we found that mTOR was not localized to the lysosome in either *Cre*$^{-}$ or *Cre*$^{+}$ cones at P21, by P42 however; mTOR localization is restored to the lysosome in *Cre*$^{-}$ cones, while it continued to remain diffuse in *Cre*$^{+}$ cones (Figure 4.1 A). In cones of wild type mice, mTOR was found at the lysosome, suggesting that its primary localization in the absence of nutrient stress in cones is at the lysosome (Figure 4.1 B). The data therefore suggest that cones also experience a shortage of amino acids at the onset of cone death. Cones of *Cre*$^{-}$ mice are able to initiate and maintain autophagy, which releases amino acids resulting in relocalization of mTOR to the lysosome, unlike *Cre*$^{+}$ cones, which furthers adds to the shortage of amino acids upon loss of *Tsc1*. Therefore, while glucose metabolism is improved on one hand, there is an amino acid crisis on the other hand. The reduction is ERG responses as well as progressive loss of cone-arrestin expression in wild type mice (Figure 3.1 A-C) further suggest that chronic activation of mTORC1 is not beneficial to cone PRs.

In contrast to *Tsc1* null cells, *Pten* null cells are able to turn off mTORC1 activity[173], which allows for the induction of autophagy in response to amino acid withdrawal. This is because upon loss of *Pten*, TSC2 is able to localize to the lysosome and inhibit mTORC1 under conditions of amino acid starvation. This may explain why loss of *Pten* results in a more sustained survival effect in *rd1* cones (Figure 3.11). While loss of *Pten* increased the number of cones positive for phospho-S6 in *rd1* mice at the onset of cone death (Figure 2.2), it would be interesting to determine if there is eventually a reduction in mTORC1 activity to adapt to the nutrient shortage, which allows for the maintenance

of autophagy, as reported in cell culture studies[173]. The challenge in evaluating the kinetics of S6 phosphorylation over time is that cell death is constantly ongoing in *rd1* mice and hence, a reduction in S6 phosphorylation may not necessarily indicate a reduction in mTORC1 activity over time. However, while *Pten* or *Tsc1* are principally deleted in every cone cell in their respective cases, loss of *Pten* still induces S6 phosphorylation in fewer cones when compared to loss of *Tsc1* (Compare Figure 2.2C with Figure 2.6D), which suggests that cones with loss of *Pten* are more proficient at regulating mTORC1 activity. Moreover, since we barely observe an accumulation of p62 or ubiquitin upon loss of *Pten* (Figure 3.9), the data suggest that mTORC1 activity is regulated in a manner that affords cone survival as well as maintains autophagy. Consequently, mTOR is retained at the lysosome, indicating a sufficiency of amino acids.

In summary, while of our findings parallel observations made in cell culture systems, they also provide new insights into how neurons may regulate mTOR activity in response to stress conditions. It is important to appreciate that cells in vivo may never experience conditions that are used in cell culture studies. Signaling events may be more dynamic (such as change in mTOR localization in *Cre*$^{-}$ mice) and hence, need to be examined over the course of the disease progression. Our studies also report other cell-type specific differences in the regulation of insulin/mTOR signaling. For example, loss of *Pten* usually activates both mTOR complexes and AKT, and *Pten*-null tumors are often dependent on mTORC2 activity[137,292]. We report that loss of *Pten* leads to a reduction of

mTORC2 activity (Figure 2.2 C) and also that mTORC2 was dispensable for cones (Figure 2.4).

Metabolic model of cone death and its relation to oxidative stress and rod-derived cone-viability (RdCVF) factor models: Cellular redox potential is tightly linked to nutrient availability. For example, NADPH is used to reduce oxidized glutathione, which serves to scavenge many free radicals[135]. Therefore, in addition to maintaining cone OS length and function, the increase in NADPH may also be used to reduce glutathione to counteract oxidative stress. The metabolic model of cone death is thus also consistent with oxidative stress as being causative for cone death in RP. However, oxidative stress alone is unlikely to be the main factor for cone death since antioxidants or over-expression of genes that counteract oxidative stress have not achieved the same protective effect as seen by loss of *Tsc1* in the *rd1* mouse model at 2 months of age[104,118,119].

RdCVF is a trophic factor that is secreted by rods and shown to have protective effects on secondary cone death in RP. Recently, a study found that RdCVF binds to basigin-1, a receptor that is present in PRs, which in turn stimulates GLUT1 activity[125]. The authors showed that RdCVF treatment improved glucose uptake and aerobic glycolysis in cone-enriched cultures and a mutant version of RdCVF that is unable to bind basigin-1 does not mediate cone survival in *rd1* mice. Therefore, RdCVF and mTORC1 seem to promote cone survival through the same mechanism of improving glucose levels in cones. However, we argue that the kinetics of rod and cone death in various models of

RP[13] exclude the possibility that a tropic factor secreted by rods plays a major role in cone survival. This is because cone survival continues for extended periods of time even in the absence of rods, which questions the extent to which the factor is important for cone survival. Nonetheless, these new findings on the mechanism of RdCVF action suggest that improving cone metabolism is ultimately the key factor to extend their survival, which suggests that the overall cause of cone death is a shortage of metabolites, particularly of glucose.

Apoptosis linked to low NADPH levels in cones: An understanding of the cell death mechanisms for cone death in RP remains largely elusive. Identifying a cell death mechanism may shed light on the overall cause of cell death, as some mechanisms require specific stress conditions or triggers. In this regard, the identification of *Casp2* as the first apoptotic mechanism for cone death in RP further corroborates the notion that low NADPH levels are a contributing factor to cone death and supports the overall idea of a nutrient shortage in cones. However, a delay in cone death in only seen at late stages, by 20 weeks of age (Figure 2.13 C and D). This could be due in part to the involvement of necrosis during the initial phase of cone death. A recent report showed that early cone death in the *rd10* mouse model of RP includes necrotic cell death[242]. Rod death progresses slightly slower in the *rd10* model than in the *rd1* model, yet it is still faster than in the *Rho*$^{-/-}$ model. The electron microscopic analyses performed in that study revealed several cone nuclei with necrotic features at early stages of cone death. Additionally, the study showed that inhibition of necrosis reduces the number of necrotic

nuclei and delays early cone death. Nonetheless, a greater number of cone nuclei showed signs of apoptotic cell death, even at early stages. Early necrotic cone death could be due to the rapidly occurring structural insult on the retina because of the rather rapid loss of rods. Once the necrotic phase ceases, the remaining cones may die by apoptotic mechanisms, including the activation of CASP2 induced by low NADPH levels. Interestingly, preliminary data from our laboratory shows that loss of *Rip3* in the *rd1* model shows no protective effect on cones by 6 weeks of age, when it conferred protection in the *rd10* model. The lack of protection in the *rd1* model may be attributed to the fact that the necrotic phase is rather short lived and cone death progresses very rapidly during this period (94% cones at P21 to 65% by P24 in Cre^- mice, Figure 2.11). Therefore, any approach including loss of *Tsc1* is unable to prevent this initial rapid decline (97% cones at P21 to 74% by P24 in Cre^+ mice, Figure 2.11). However, once the necrotic phase ceases, the metabolic gene regulatory network that is progressively activated by mTORC1 effectively prolongs cone survival.

In combination with early necrosis and *Casp2* mediated apoptosis, there are likely additional, as yet unidentified cell death mechanisms that contribute to cone death. These could explain why loss of CASP2 does not result in a more profound effect. One would expect these mechanisms to be linked either directly or indirectly to low intracellular energy levels, as improving cell metabolism through activation of mTORC1 effectively delays cone death. For example, reduced NADPH levels could induce cell death through oxidative stress before CASP2 is activated. Thus, removal of one of the cell death

mechanisms such as loss of CASP2, or treatments with antioxidants, is not sufficient to achieve the same effect that is seen with treating the overarching problem of starvation through loss of *Tsc1*.

Autophagy upon loss of *Tsc1* in cone PRs and implications in Tuberous Sclerosis: Loss of function mutations in *TSC1*/*TSC2* genes lead to tuberous sclerosis complex (TSC), a multi-system disorder characterized by benign tumors and dysfunction of the central nervous system causing various developmental and behavioral problems[271]. Since mTORC1 is a positive regulator of growth, giant cells with increased mitochondria and abnormal lysosomes are a hallmark of TSC[293]. Previous studies have shown that loss of *Tsc1/2* in neurons and other cell types increases endoplasmic reticulum and oxidative stress and induces autistic-like behavior in mice[195,294]. While the increase in mitochondria may result in oxidative stress, the aberrant lysosomes may be attributed to the inhibition of autophagy. Loss of *Tsc1* in cones results in phosphorylation of ULK1 at Ser757, which inhibits autophagy initiation, however, autophagy is promoted in neurons due to phosphorylation of ULK1 at Ser555 by AMPK (Figure 3.2 D). Unlike proliferating cells, neurons cannot divide to dilute undigested cellular contents and hence, they continue to accumulate it resulting in the gradual buildup of lysosomal stress. How AMPK gains access to ULK1 in the presence of mTORC1 is not known, nonetheless phosphorylation of ULK1 by AMPK appears to be a quality control feedback mechanism to promote autophagy in order to counteract stress in neurons. Brain tumors (cortical tubers) of patients with TSC also display an increase in LC3-II, the lipidated form of LC3, which

forms part of the autophagosome, suggesting an accumulation of autophagic cargo[194]. While the small percentage of cones cells in the retina may complicate the assessment of the ratio of LC3-I to LC-II by western blot, our LC3 reporter assay convincingly demonstrates an active autophagy flux (Figure 3.2 B and C). It is interesting to note that the total number of yellow and red punctae (autophagosomes and autolysosomes, respectively) is higher in *rd1-Tsc1*^{cKO} cones, indicating an overall increase in the total number of autophagy vesicles. On one hand, this could be due to an increase in autophagy initiation, since we also observe an increase in expression of autophagy and lysosomal genes (Figure 3.3 A-C). However on the other hand, the number of autophagosomes remains the same between *Cre*$^{-}$ and *Cre*$^{+}$ retinae, suggesting that there is only a shift towards more number of autolysosomes and that autophagy initiation is not increased per se (Figure 3.2 C). Nonetheless, the accumulation of autolysosomes suggests that *rd1-Tsc1*^{cKO} cones are unable to properly digest the autolysosomal contents, resulting in their accumulation over time. This could result from either a defect in lysosomal pH and/or a shortage of lysosomal enzymes. The first scenario is unlikely because if lysosomal pH were altered, we would not observe quenching of the GFP signal in our LC3 reporter assay. In order to test if the accumulation of autolysosomes resulted from a deficiency of lysosomal enzymes, we examined the expression of *Tfeb*, a master transcription factor of lysosomal genes and enzymes, since activation of mTORC1 excludes *Tfeb* from the nucleus, thereby preventing its transcriptional activity[258,259]. Use of two commercial antibodies against TFEB did not show any expression changes between *Cre*$^{-}$ and *Cre*$^{+}$ retinae. As a control, we performed the staining on cones lacking

Raptor, where *Tfeb* should constitutively localize to the nucleus. However, we did not detect any change with either antibody (data not shown). Therefore, we can only speculate that a lack of TFEB activity may be responsible for the autophagy defect. In the event that our hypothesis is right, over-expression of *Tfeb* using rAAV vectors may be the most straightforward approach to correct this defect. In addition to examining TFEB expression, lysosomal activity can be evaluated in colorimetric or fluorometric lysosomal activity assays, which assess the activity of lysosomal enzymes such as Cathepsin B/D, in retinal tissue extracts or following isolation of retinal lysosomes. The small percentage of cones in the retina would however, make it more complicated to perform and interpret these assays. Therefore, fluorescent activity assays that assess real-time lysosomal activity in vivo, similar to the fluorescent caspase activity assay that we have used, may be a feasible approach.

On the contrary, cones in *Cre*$^{-}$ mice may suffer from a shortage of lysosomal genes because they have very low number of autolysosomes when compared to the number of autophagosomes (less than 1:3, Figure 3.2 C). In neurons that maintain a normal autophagy flux, the ratio between autophagosomes and autolysosomes should ideally be 1:1[194]. Therefore, while the requirement for lysosomal genes is fulfilled by activation of mTORC1, it introduces a defect in the termination stages of the process. In contrast, loss of *Pten* mediates a small increase in lysosomal genes (Figure 3.9 C), which may be sufficient to promote autophagy without affecting the termination stages.

Are there other mechanisms one could harness to sustain the survival effect obtained upon loss of *Tsc1* beyond 2 months of age? Elimination of autophagy genes or p62 may not be the right approach because while this may prevent the formation of protein aggregates, removal of autophagy altogether may have detrimental consequences on the cell[198]. In line with this, tumorigenesis of TSC tumors was lost upon removal of *Atg5* or *p62*[193]. Further, the detection of selective autophagy adaptor proteins like ALFY in cones suggests that the process is highly specific for degradation of ubiquitinated proteins/organelles. Therefore, facilitating another degradation mechanism such as the ubiquitin proteasome system cannot compensate for a defect in autophagy. Based on a recent report on the regulation of the proteasome by mTORC1, proteosomal activity may in fact be elevated in cones upon loss of *Tsc1*[202]. Therefore, while both mechanisms are involved in the degradation of ubiquitinated proteins, each may have exclusive targets that accumulate upon impairment of the corresponding degradation mechanism.

Disaccharides like trehalose have been shown to enhance autophagy and improve neuronal survival in mouse models of diseases like amyotrophic lateral sclerosis, which are caused due to abnormal aggregation of proteins[295,296]. This sugar is interesting because unlike rapamycin, it induces autophagy without affecting mTORC1 activity. We therefore administered trehalose to *rd1-Tsc1*^{cKO} over a 4-month period. However, it did not result in any significant improvement in cone survival (53.2±3.3%), compared to control animals (51.1±4.5%). The reason why trehalose may not be effective in our case is that it is believed to promote autophagy by increasing expression of FOXO1 and other

autophagy genes[295]. Therefore, while its administration may promote autophagy in neurons with a functional TSC complex, cones that lack TSC already have an elevated expression of FOXO and autophagy genes. Therefore, trehalose and other agents that increase the basal level of autophagy may not be an effective strategy to correct the problem of autolysosome accumulation. While on one hand, the increased nuclear translocation of FOXO3A provides an explanation for the increase in autophagy and lysosomal genes in *rd1-Tsc1*^{cKO} cones; on the other hand, FOXO activation is also known to promote expression of various pro-apoptotic proteins of the Bcl-2 family[209]. One study performed in *Drosophila melanogaster* eye-antennal disc tissue showed that concurrent loss of *Tsc1* and *Foxo* resulted in an increase in organ size when compared to loss of *Tsc1* alone, suggesting that increased *Foxo* activation restricts pro-growth functions of mTORC1[278]. Therefore, the role of increased FOXO activation in *rd1-Tsc1*^{cKO} cones needs to be further investigated in order to determine whether it is beneficial or detrimental to cones.

Another potential strategy to extend survival of *rd1-Tsc1*^{cKO} cones would be to investigate the cell death mechanism that leads to the eventual loss of *rd1-Tsc1*^{cKO} cones. While *Caspase-2* is activated in cones of *rd1* mice in response to low NADPH levels, loss of *Tsc1* may induce activation of caspases such as caspase-3, -9 and -12, as previously reported due to activation of endoplasmic reticulum (ER) and other stress responses[297]. Therefore, gene therapy to silence caspases or over-expression of XIAP may be a potential strategy to extend survival of *rd1-Tsc1*^{cKO} cones. Since caspase

inhibitors are not efficient at crossing the blood-retinal barrier[242], gene therapy or intravitreal delivery of caspase inhibitors would be the only means to suppress caspase activity in *rd1-Tsc1*^{cKO} cones.

We employed a straightforward approach of inhibiting mTORC1 activity using rapamycin to promote autophagy in *rd1-Tsc1*^{cKO} cones. Similar to studies in various tissues with TSC loss[191,192,195], rapamycin treatment completely eliminated p62 accumulation and restored cone-arrestin expression in wild type mice (Figure 3.6). However, under conditions of disease, rapamycin demonstrated a dose-dependent effect on cone survival. These results are fascinating because they indicate how cell survival can be controlled by manipulation of mTORC1 activity. While studies so far have only shown how rapamycin reduces tumorigenesis of TSC tumors[192], it is possible that sporadic administration of rapamycin may enhance tumor survival since it allows tumor cells to rebalance their metabolic demands under conditions of low nutrients and hypoxia that cells in tumors experience[274]. The chronic effects of constitutive mTORC1 activation may also explain why TSC tumors are mostly benign, as opposed to tumors with loss of function mutations in *Pten,* which are highly aggressive and metastatic[147,271]. *Pten* is also further upstream in the insulin/mTOR pathway and therefore, its loss may alter additional signaling pathways that aggravate tumorigenesis, however the efficient balancing of cell metabolism through mTORC1 may also be a contributing factor to the difference in their tumorigenic effects. This point is exemplified in the linear regression analysis of cone

survival over a period of one year, where loss of *Tsc1* causes a very sharp decline in cone survival, as opposed to *Pten* loss (Figure 3.11).

Limitations of the mouse model in vision research: While the mouse is an excellent model organism to perform elegant genetic analyses due to shorter gestation times when compared to other mammals, they may not be the best system to study vision. This is because mice are primarily nocturnal animals and rely more on olfaction for navigation, as opposed to vision. Therefore, our laboratory has not had any success in using behavior tests such as the Cliff test to assess if loss of *Tsc1* improves visual behavior. The ERG serves as the only mode of assessment of visual function, which also become difficult to perform in *rd1* mice because degeneration progresses very rapidly. Further, mice lack the macula at the center of the retina, which harbors the cone-rich foveal pit. However, outside the macula the distribution of rods and cones is similar between humans and mice. Therefore, while the progression of cone death is from the center to the periphery in mice, in humans the central region that is most abundant in cones is always the last area to degenerate. Therefore, humans RP patients almost always retain some amount of central vision even at the end stages of the disease. Therefore, approaches that delay cone death may at least serve to preserve central vision in humans if administered at late stages of the disease.

When compared to mice, the canine retina serves as a better model to study RP with about 10 different canine models that are currently in use for the study of retinal

degeneration. While dogs also lack the macula, they possess a region known as *area centralis* that is rich in cones and therefore, more closely resembles the human retina. Further, since dogs are more dependent on vision as opposed to mice, visual behavior and visual acuity tests are feasible. Proof of principle studies for various gene replacement strategies have met with great success in dogs with restoration of visual function and behavior, even when the gene was delivered at late stages of disease (also discussed in introduction). Further, since the size of the canine retina is larger than the mouse retina, it is easier to perform multi-focal ERGs, which is used to assess cone function across different regions in the retina. Therefore, for applications like gene therapy where only a portion of the retina may be infected with the therapeutic gene, multi-focal ERGs allow for the assessment of visual responses specifically in the infected region. Besides dogs, there are also cat and pig models but no known primate models for RP. Therefore, testing the efficiency of mTORC1-based therapies in these larger animal models would be the next step before moving to clinical trials in humans.

Bench to bedside translation: Our findings are not directly translatable into a therapy, since cell-type specific deletion of *Tsc1* or *Pten* is not feasible in humans. Delivery of silencing vectors to inhibit *Tsc1* or *Pten* in cone PRs may also lead to undesirable effects if they target the adjacent RPE cells, where loss of *Pten* is known to induce metastasis of RPE cells and eventual loss of PRs[298]. Our results however may redirect efforts aimed at developing therapies for patients with RP. Our detailed characterization of cone survival kinetics upon loss of *Tsc1* under both disease and wild type conditions, as well as its

effect on autophagy highlight the potential undesirable effects of increasing mTORC1 signaling in cone PRs. However the absence of any reduction in cone survival or function upon loss of *Pten* in a wild type background suggests that mTORC1 can be activated to fairly high levels in cones without causing any detrimental effects (Figure 3.10). Therefore, while it may seem disappointing that loss of *Tsc1*, which promotes an initial robust rescue of cones, also has toxic side effects, this may be advantageous from a therapeutic perspective. This is because the data suggests that sustenance of cone PRs over a long duration does not require a drastic increase in mTORC1 activity. Consequently, drugs that increase mTORC1 activity can be administered at low doses through the use of slow-release eye implants, similar to the ones used for CNTF delivery[92]. It is unlikely that a compound increases mTORC1 activity to the same extent that genetic loss of *Tsc1* does and therefore, this approach may greatly benefit survival of cones in RP. Alternatively, rAAV mediated expression of mTORC1 target genes that promote glucose uptake and utilization in cones PRs may also be a feasible approach. This approach has the advantage that over-expression may induce gene expression more strongly than an increase in mTORC1 activity and that one could principally improve glycolytic metabolism in cones without altering mTORC1 activity. However, the approach may have a limitation that over-expression of any one target gene may not be sufficient to afford cone survival and therefore, it rests on the identification of a minimum combination of genes that would be sufficient to achieve cone survival. For example, a combination of *Glut1* and *G6pd* may be sufficient to confer survival, however there are limitations to the size of the gene that can be packaged into a single rAAV

vector and hence, this approach may require simultaneous infection of two or three rAAV vectors in each cone cell. Therefore, expression of transcription factors like *Hif-1α* that regulate expression of multiple glycolytic genes may be a better approach.

While our study is based on the hypothesis that cones are suffering from a shortage of glucose and improving glycolytic metabolism is required to confer cone survival, it is also possible that promoting lipid synthesis to regenerate the outer segment may be sufficient for cone survival. In this regard, expression of a transcription factor like *Srebp1*, which regulates the expression of various genes involved in lipid synthesis, may improve both cone survival and function.

Since cone death begins only after about 90% of rods have died and is tightly linked to the structural integrity of the retina, it may also be worthwhile to consider if preserving the structure of the PR layer would delay cone loss. In this regard, administration of self-assembly polymers or nanoparticles may assist the formation of a matrix thereby preventing the collapse of the PR layer, especially when administered during early stages of the disease. These polymers could also be engineered to deliver therapeutic genes or release mTORC1-activating drugs upon assembly, which may improve the efficiency of cone survival.

Finally, extending cone survival may also benefit other strategies that are currently being developed for retinal degeneration such as stem cell therapies. Since cones in RP, which

do not have any genetic defects, die following the loss of rods, the newly transplanted cells may also face the same fate if we cannot efficiently prevent their death.

Implications of mTORC1 in other retinal degenerative diseases: Besides being a mutation independent approach to prolong vision across various RP mutations, it is interesting to note that mTORC1 activation can also be employed to treat age-related macular degeneration (AMD), which is the most common cause of blindness. While RP has a clear genetic etiology, AMD is caused by a multitude of genetic and environmental factors and primarily affects the macula, which is the cone-rich region that confers high-acuity vision in humans[299]. The disease is initially characterized by the accumulation of drusen, which are lipid deposits on the basal side of the RPE, thereby impinging nutrient transfer from the choriocappilaries to the RPE cells[300]. This affects RPE cell health and function. Because RPE cells are the main source of nutrients and required for various functions of PRs, a reduction in RPE cell function also affects PRs. Our laboratory employed an advanced stage model of AMD, known as geographic atrophy, where RPE cells are lost in patches across the retina. We interrogated whether activation of mTORC1 can also improve survival of PRs when they are deprived of their primary source of nutrients, the RPE cells[301]. Indeed, activation of mTORC1 by loss of *Tsc1* promoted survival of both rod and cone PRs in a model of geographic atrophy, where RPE cell death was chemically induced[302]. Further, the mechanism of protection involved an upregulation of glycolytic genes such as *HkII* and *G6pd*, suggesting that the same

approach of improving cone metabolism in RP can also be employed to treat the most common form of retinal degeneration.

Similar to AMD, diabetic retinopathy (DR) is also a multifactorial disease that does not have a clear genetic cause, and commonly develops in people with diabetes mellitus. In fact, patients with diabetes show a reduction in visual function before developing any clinical signs of DR[303]. Diabetes involves a systemic deregulation of the insulin/mTOR pathway and therefore insulin signaling is likely affected in all retinal neurons including cone PRs[304,305]. We have shown that loss of *Tsc1* induces a progressive decline in cone function (Figure 3.1). Similarly, while loss of mTORC1 or mTORC2 does not affect cone function, concurrent loss of both mTOR complexes also causes a reduction of cone function[282]. The decline in cone function upon either activation or removal of mTOR signaling may thus explain why patients with diabetes also experience signs of visual dysfunction.

Further, while cone death in RP progresses from the periphery to center in humans, in both DR and AMD, PR death is regional and can be randomly distributed across the retina. While DR and AMD are both caused due to different factors, it is likely that once a certain number of PRs in a region die, the remaining surrounding ‘healthy’ PRs are also affected, similar to cones in RP[13,306]. Therefore improving metabolism of PRs may not only be useful to prolong survival of cones in RP, but also prolong vision in various kinds of retinal degenerations, thereby improving the quality of life.

Increasing mTORC1 activity, more than meets the eye: The mTOR pathway in frequently deregulated in diseases like cancer, where rapamycin and other catalytic mTOR inhibitors are used to suppress its activation. On the contrary, increasing mTORC1 activity may be beneficial in other diseases/conditions besides retinal degeneration. For example, conditions where muscle health and function are affected such as sarcopenia or muscle atrophy may benefit from an increase in protein synthesis and growth driven by an increase in mTORC1 activity. Amino acids like L-leucine that induce mTORC1 activity are an integral component of supplements used to build muscle mass and hence compounds or drugs that potently activate mTORC1 may find application in this area. Further, it has been demonstrated that mTORC1 is a critical regulator of red blood cell (RBC) formation and proliferation[307]. Therefore, in diseases like anemia where RBC population is compromised, increasing mTORC1 may prove beneficial. Additionally, increasing mTORC1 activity in tissues like the pancreas promotes increase in β-cell mass and insulin synthesis[308], which may help in the control of diabetes. Lastly, in neurodegenerative diseases such as amyotrophic lateral sclerosis and Parkinson's disease that are characterized by the accumulation of protein aggregates, inhibition of mTORC1 activity has been shown to confer neuroprotection by promoting autophagy, which results in the clearance of aggregated proteins[309,310]. However, some studies report that inhibition of mTORC1 activity accelerates neurodegeneration[311], since its inhibition over time may also affect neuronal metabolism in general, similar to loss of mTORC1 activity in *rd1* cones. A different approach to tackle the problem would be to consider if an overall boost in neuronal metabolism mediated by a moderate increase in

mTORC1 activity could benefit neuronal survival, as opposed to suppressing mTORC1. Therefore, there may be more to increasing mTORC1 activity than meets the ‘eye’ and research in the coming years will reveal novel applications of this approach.

CHAPTER V

Materials and Methods

Study approval. The IACUC of the University of Massachusetts Medical School approved the animal study. All procedures involving animals were performed in compliance with the Association for Research in Vision and Ophthalmology (ARVO) Statement for the Use of Animals in Ophthalmic and Vision Research.

Animals. Mice were maintained on a 12-hour light/12-hour dark cycle with unrestricted access to food and water. Lighting conditions were kept constant in all cages, with illumination ranging between 10 and 15 lux. The *Pde6b*$^{rd1/rd1}$ (*rd1*), *Casp2*$^{-/-}$, C57BL/6J, *Pten*$^{c/c}$, *Tsc1*$^{c/c}$ were purchased from The Jackson Laboratory[39,147,237,271]. The M-opsin-*Cre* (cone-specific Cre line using the human medium wavelength promoter), *Raptor*$^{c/c}$, *Rictor*$^{c/c}$, and *Rho*$^{-/-}$ mice have been described previously by Yun Z. Le, Michael N. Hall, Markus A. Rüegg, and Janis Lem, respectively[261,262,267]. Genotyping was performed as described in the original publications. None of the mice used for analysis were on an albino background, and all mice were genotyped for absence of the *rd8* mutation[312]. To dissect the role of the insulin/mTOR pathway in cone survival, the conditional allele was first crossed with the cone-specific Cre-driver line and then with the *rd1* line to generate *Cre*$^{-}$ and *Cre*$^{+}$ *rd1*–conditional allele (*cKO*) lines. In some cases, double-conditional alleles were also generated. The *Cre*$^{+}$ and *Cre*$^{-}$ lines were crossed with each other (e.g., *rd1-Pten*$^{c/c}$ X *rd1-Pten*$^{c/c}$ M-opsin-*Cre*$^{+/-}$) to generate the *Cre*$^{+}$ and *Cre*$^{-}$ littermates that

were used for analyses. Because various strains were interbred, strain background differences may account for the slight variations in cone survival in *Cre*$^{-}$ animals at 2 months of age. Nonetheless, our data clearly show that mTORC1 was required for cone survival during disease, since loss of *Raptor* always accelerated cone death, while increasing mTORC1 activity consistently improved cone survival. Because loss of *Casp2* did not allow us to compare *Cre*$^{-}$ and *Cre*$^{+}$ littermates, we generated a congenic *rd1 Casp2*$^{-/-}$ line to study the effect of loss of CASP2 on cone survival. The *Casp2*$^{-/-}$ allele was on a C57BL/6J background and was crossed with *rd1* C57BL/6J mice that were generated by backcrossing the *Pde6b*$^{rd1/rd1}$ allele of the FVB strain with C57BL/6J mice for 10 generations. *rd1* C57BL/6J mice were then compared with *rd1 Casp2*$^{-/-}$ C57BL/6J mice to quantify cone survival.

Quantification of cone survival. Retinal flat-mount images for the cone survival quantification were acquired by tiling individual images taken at ×16 magnification (Leica DM5500) over the entire retinal surface area with an automated scanning stage. For all cone survival quantifications in the *rd1* and *Rho*$^{-/-}$ models of RP, the percentage of surviving cones is based on a calculation of the percentage of the retinal surface area that is covered by cones. To determine the area that was covered by cones, we used the staining detected by the cone arrestin antibody (Figure 5.1 A and B, red signal in the first column, gray scale signal in second and white signal in last column) as a proxy for surviving cones. To determine the retinal surface area, retinae were stained with PNA-coupled FITC (Figure 5.1 A and B, green signal in the first and last columns and gray scale signal in the third column) at a dilution that was 3 times higher than that used for all

other staining procedures, with the goal to only elicit sufficient background fluorescence to highlight the entire retinal surface area rather than detect cone OSs. The ratio of red to green pixels, which was calculated using CoLocalizer Pro software[313] (CoLocalization Research Software) with its integrated background correction, thus directly representing the percentage of the retinal surface area that was covered by the cone arrestin antibody staining. Before calculating the percentage of colocalization of red and green, the upper and lower thresholds of each signal were adjusted, such that only cones were visible in the red signal (Figure 5.1 C and D) and the entire retina was visible in the green signal. To calibrate the percentage of colocalization of red and green signals on an *rd1*-mutant background to the actual percentage of surviving cones, we performed a real cone count rather than determining the percentage of cone arrestin staining that covered the retina in WT mice. The reason for this is that during degeneration, cone arrestin was also found in the cell body, resulting in a different pattern of expression; thus, the percentage of colocalization was different when compared with that in retinae of WT mice (Figure 5.1 E and F). A cone count was performed across 3 WT retinae and across 3 *rd1 Tsc1*^{cKO} retinae at P21 (Figure 5.1 H and I). The mutant strain and time point were chosen at P21, since at this point, cone death had just started, and the percentage of colocalization of red and green signals was the highest upon loss of TSC1 (52.7%). The actual cone count in WT retinae was in agreement with published data[314] and revealed that at P21, 95.2% of cones were still present in the *rd1 Tsc1*^{cKO} retinae when compared with those in WT retinae, meaning that 52.7% of colocalization (red to green signal) corresponds to 95.2%

of cones. These numbers were used to calibrate all colocalization data representing cone survival.

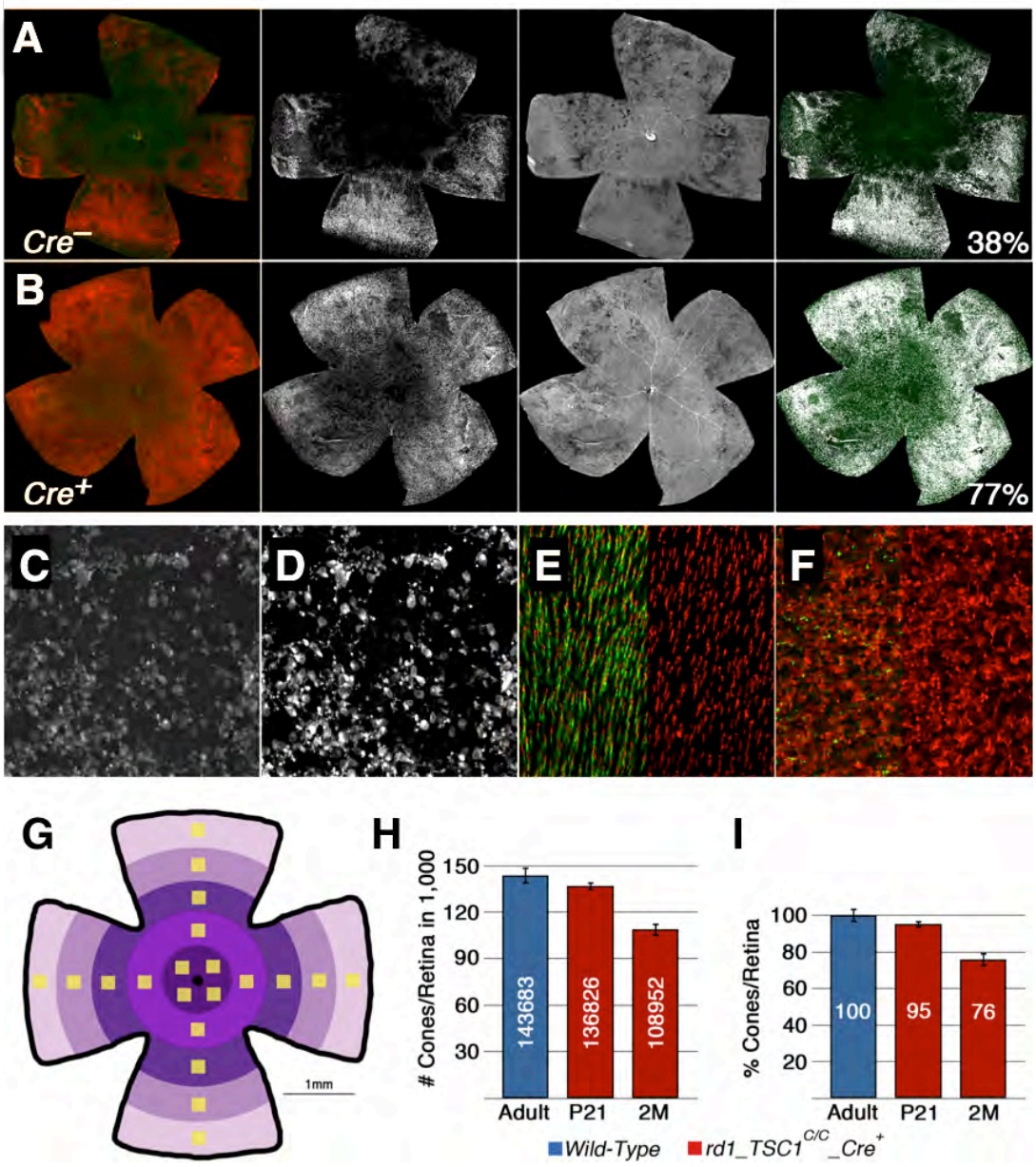

Figure 5.1: Cone Survival analysis (legend on following page)

Figure 5.1: Cone Survival analysis. (**A,B**) Examples of tiled retinal flat mounts used for cone survival quantification at 2 months of age in *rd1-Tsc1*$^{c/c}$;*Cre* ± mice (Compare to **Figure 2.6**). First column, actual scan showing cone arrestin (red signal) and the diluted FITC-PNA signal (green). Second and third columns gray scale images of cone arrestin and PNA-FITC, respectively. Last column, actual colocalization as seen after analysis (white signal) with Colocalizer Pro. Percentage of cone arrestin positive cones is indicated in panel. (**C**) Example of the actual image resolution obtained by the tile scan used for the cone survival quantification. Shown is cone arrestin staining in gray scale. (**D**) Same image as in (**C**) after adjusting the upper and lower thresholds such that only cones are visible (same as second column in **A** and **B**). After this initial adjustment images were used to calculate colocalization in Colocalizer Pro. (**E-F**) Example of retinal flat mount stained for cone arrestin (red signal) and PNA (green signal) in a wild type (**E**) and *rd1* mutant (**F**) background. In left half of each panel PNA has been removed to better visualize cone arrestin staining. In wild type less red signal is seen, as cone arrestin is in the inner an outer segments. Therefore colocalization values of red versus green in *rd1* cannot be calibrated with colocalization values obtained in wild type. (**G**) Cartoon of the 5 sectors used to count cones and location of squares in which cones were counted. (**H**) Average cone count per retina (n=3) for genotypes and ages indicated. (**I**) Percentage representation of cones per retina of values in (**H**) where wild type is set at 100%. Percentage of cone survival obtained in the *rd1-Tsc1*^{cKO} at 2 months of age is similar between the counting method (75.8% ± 3.7%) and the colocalization method (77.6% ± 3.9%; compare to **Figure 2.6**). (**H, I**) Numbers in bars: actual value of graph rounded to the next number. Error bars: SD.

To validate the method, we counted cones in retinae of *rd1-Tsc1*^{cKO} mice at 2 months of age (Figure 5.1 G and I). This time point was chosen because upon loss of TSC1, cone survival at 2 months of age is still quite homogenous, rather than demonstrating a patchy pattern of survival, thus making it more accurate to determine the number of cones across the entire retina by counting individual fields. The colocalization and actual cone count data for mice at 2 months of age were in agreement, with no statistically significant

difference between them (77.6% ± 3.9% vs. 75.8% ± 3.7%, respectively), indicating that the colocalization method can be used to determine the percentage of surviving cones. The method of quantifying cones by colocalization over the entire retinal surface, rather than counting the number of cones in a few individual fields, was chosen because cone degeneration is quite patchy, progressing from the center to the periphery. Therefore, counting a few individual fields, even if always done in the exact same location, is not likely to properly represent the number of surviving cones. Thus, this method is independent of the degeneration pattern and the orientation of the retina.

For quantification of cones by cone count, retinae were first divided into 5 different sectors with increasing radiuses of 500 mm per sector (Figure 5.1 G). Cones were then counted manually in 4 squares per sector (20 squares/retina), each square measuring 40,000 mm^2, to determine the average cone density per sector (cones/mm^2). The average cone density per sector was then multiplied with the sector surface area to obtain the number of cones per sector. The surface area of each sector was calculated as the sector surface area of a sphere. The total number of cones per retina was then obtained by adding the number of cones across the 5 sectors. The numbers shown represent an average of 3 retinae per genotype and age. The same method was used to count cones in a wild type background in Chapter III.

Electroretinography. ERG was performed using the Espion E3 console in conjunction with the ColorDome (Diagnosys LLC). Mice were anesthetized by an i.p. injection of a ketamine-xylazine (100 mg/kg and 10 mg/kg, respectively) mixture. One drop each of

phenylephrine (2.5%) and tropicamide (1%) was applied for pupil dilation 10 minutes before to recording. Animals were kept on a warming plate during the entire ERG procedure to maintain body temperature at 37°C. Photopic ERGs were recorded after light adaptation with a background illumination of 34 cd/m^2 (white 6500 K, produced by a Ganzfeld stimulator) for 8 minutes. For *rd1* mice, flashes were presented at 1-minute intervals with a pulse length of 4 ms, and each recording consisted of a single flash of 35 cd × s/m^2. For mice in a wild type background, each recording consisted of 10 single flashes of 10 cd s/m^2, with flashes presented at 1 sec intervals. In both cases, six to nine trial recordings were averaged.

Histological methods. For antibody staining on retinal whole mounts, retinae were dissected in PBS, fixed for 30 min in 4% paraformaldehyde/PBS, washed 3 × 10 min in PBS, washed for 1 hr in PBT (PBS, 0.3% Triton 100), blocked for 1 hr in PBTB (PBT, 5% BSA), incubated overnight at 4°C with primary antibody in PBTB, washed 3 × 20 min with PBTB, incubated 2 hr with secondary antibody in PBTB, washed 5 × 20 min in PBT. Triton was replaced by 0.1% Saponin for staining procedures involving autophagy and lysosomal proteins. For sections, after fixation, retinae were equilibrated in increasing sucrose concentrations (from 5% to 30% sucrose/PBS), mounted in OCT (Optimal Cutting Temperature, Fisher), frozen, sectioned, re-hydrated in PBS for 30 min, and then the same procedure was used again as for whole-mount starting with the 1 hr wash step in PBT. CASP2 activity on retinal whole mounts was detected using the Green FLICA Caspase 2 Activity Kit (catalog 918; ImmunoChemistry Technologies) according to the manufacturer's instructions. Briefly, retinae were incubated in DMEM media with

the detection reagent at 37°C for 30 minutes, followed by 2 washes of 5 minutes each in apoptosis wash buffer. Retinae were then fixed and processed for antibody staining as described. Antibody stainings were performed in TBS buffer for phospho-specific antibodies and in PBS buffer for all other antibodies. The following primary antibodies and concentrations were used: rabbit α–p-AKT (Thr308) (1:1,000; catalog 2965); rabbit α–p-AKT (Ser473) (1:1,000; catalog 4060); rabbit α–p-S6 (Ser240) (1:300; catalog 5364); rabbit α–p-S6 (Ser235/236) (1:300; catalog 4856); rabbit α-PKM2 (1:300; catalog 4053); rabbit α-HK2 (1:300; catalog 2867) rabbit α–FOXO3A (1:300; catalog 12829); rabbit α–mTOR (1:500; catalog 2983); rabbit α–p-ULK1 (Ser757) (1:300; catalog 6888); rabbit α–p-ULK1 (Ser555) (1:300; catalog 5869); rabbit α–p-AMPKβ1 (Ser182) (1:300; catalog 4186); rabbit α–ATG12 (1:300; catalog 2011) (all from Cell Signaling Technology); rabbit α–p-SGK (Ser422) (1:300; catalog ab55281); rabbit α-G6PD (1:300; catalog ab993); rabbit α-ME1 (1:300; catalog ab97445); rabbit α-Ki67 (1:300; catalog ab15580); rabbit α–ALFY (WDFY3) (1:500; catalog 84888) (all from Abcam); rat α–LAMP1 (1:500; catalog 1D4B-c) and rat α–LAMP2 (1:500; catalog GL2A7-c) from Developmental Studies Hybridoma Bank; guinea pig α–p62 (1:300; catalog GP62-C) from Progen; goat α–short wave opsin (SW OPSIN) (1:500; catalog 14363) from Santa Cruz; rabbit α–HIF-1α (1:300; catalog ab1536; R&D Systems); rabbit α-GLUT1 (1:30; catalog GT11-A; Alpha Diagnostics); mouse α-Cre (1:500; catalog MMS-106P; Covance); goat α–short wave opsin (SW OPSIN) (1:500; catalog 14363; Santa Cruz); rabbit α–cone arrestin (1:300; catalog AB15282); rabbit α–red-green opsin (1:300; catalog AB5405); mouse α–Ubiquitin (1:500; catalog 1510) (all from EMD Millipore)

and fluorescein-labeled peanut agglutinin lectin (PNA) (1:500; catalog FL-1071; Vector Laboratories). All secondary antibodies (donkey) were purchased from Jackson ImmunoResearch and were purified $F(ab)_2$ fragments that displayed minimal cross-reactivity with other species.

Quantitative real time polymerase chain reaction (qRT-PCR). RNA was isolated using TRIzol (Life Technologies) as described previously. Three biological samples of each genotype were analyzed, and each sample consisted of retinae from 2 different animals. One microgram of total RNA was used for reverse transcription cDNAs were generated using the Transcriptor First Strand cDNA Synthesis Kit (Roche Diagnostics), and SYBR green–based qRT-PCR (Kapa Biosystems) was performed using the Bio-Rad CFX96 Real-Time System. Samples were run in duplicate and normalized to β-actin using the $2^{-\Delta\Delta Ct}$ method. The primer sets used are provided in provided in the table below.

Gene	Forward Primer (5'-3')	Reverse Primer (5'-3')
Hif-1α	GATGACGGCGACATGGTTTAC	CTCACTGGGCCATTTCTGTGT
Glut1	TCAACACGGCCTTCACTG	CACGATGCTCAGATAGGACATC
HkI	GACAAAGCGGTTCAAAGCCAG	CGACTTCACACTGTTGGTCATCG
HkII	GGAACCCAGCTGTTTGACCA	CAGGGGAACGAGAAGGTGAAA
6pgd	AGACAGGCAGCCACTGAGTT	AAGTTCTGGGTTTCGCTCAA
G6pd	CCTACCATCTGGTGGCTGTT	TGGCTTTAAAGAAGGGCTCA
Pkm2	ATTGCCCGAGAGGCAGAGGC	ATCAAGGTACAGGCACTACACGCAT
Me1	AGAGGTGTTTGCCCATGAAC	GCTGGTCGGATTACTCAAAGC
β-actin	ACTGGGACGACATGGAGAAG	GGGGTGTTGAAGGTCTCAAA

Table 5.1: List of primer sequences

Western blot analysis. Retinae from 2 animals were pooled and homogenized by sonication in ristocetin-induced platelet aggregation (RIPA) buffer containing protease and phosphatase inhibitors (cOmplete Protease Inhibitor Cocktail and PhosSTOP Phosphatase Inhibitor Cocktail; both from Roche Diagnostics). Protein concentration was assessed using a Protein Assay Kit (Bio-Rad), and 10 μg protein was loaded per lane. Proteins were separated on a 4%–20% Tris-Glycine gradient gel (Bio-Rad) at 170 V and transferred onto a nitrocellulose membrane for 2 hours at 4°C with a current of 150 mA. Membrane was blocked for 1 hour at room temperature in 5% fat-free dry milk powder, incubated with primary antibody overnight at 4°C, washed 3 times for 20 minutes each wash at room temperature, incubated with an HRP-coupled secondary antibody (1:10,000; Santa Cruz Biotechnology Inc.) for 2 hours, and washed 3 times for 20 minutes each wash at room temperature. Signal was detected with SuperSignal West Dura (Pierce Biotechnology). All incubations were performed in the presence of 0.1% Tween-20 and 5% fat-free dry milk powder. Incubations were performed either in TBS buffer for phospho-specific antibodies or in PBS buffer for all other antibodies. The following primary antibodies were used: rabbit α–p-AKT(308) (1:1,000; catalog 2965); rabbit α–p-AKT(473) (1:1,000; catalog 4060); mouse α-AKT (1:1,000; catalog 2967); rabbit α–p-S6 (1:1,000; catalog 5364); and rabbit α-S6 (1:1,000; catalog 2217) (all from Cell Signaling Technology); mouse α-β–actin (1:2,000; catalog A5316; Sigma-Aldrich); mouse α-CRE (1:2,000; catalog 69050-3; Novagen); rabbit α-cone arrestin (1:1,000; catalog AB15282; EMD Millipore); rat α-CASP2 (1:1,000; catalog ALX-804-356; clone 11B4; Enzo Life Sciences); and mouse α- β-tubulin (1:2,000; catalog 8328) from Sigma-

Aldrich. For the western blots depicted in Figure 3.7, instead of fat-free milk powder, Odyssey Blocking Buffer (catalog 927-40000) from LI-COR was used for blocking and antibody incubations. No detergent was added during blocking and antibody incubations. Primary antibodies used were same as above while secondary antibodies were infrared dye-conjugated (1:10,000; LI-COR). Membrane was scanned on an Odyssey Infrared Scanner from LI-COR to detect signal.

NADPH measurement. NADPH was measured using the Fluoro NADP/NADPH kit from Cell Technology Inc. (NADPH100-2). The assay was performed in triplicate using 3 biological samples, with each biological sample consisting of 3 retinae. Retinae were dissected in DMEM media, rinsed with 1X PBS, and processed following the manufacturer's instructions. Retinae were sonicated after the addition of the lysis buffer to ensure efficient dissociation.

Cell culture. *Casp2* was amplified by PCR (forward: 5′ATGGCGGCGCCGAGCGGGAGGTCG-3′; reverse: 5′-TCACGTGGGTGGGTAGCCTGGG-3′) from a C57BL/6J retinal cDNA library. The PCR product (1359 bp) was subcloned into the pGEM-T easy vector (Promega) and sequence verified. The *Casp2* cDNA was then cloned into an rAAV2 plasmid carrying a *CMV* promoter and the SV40 polyadenylation site. HEK293 cells were transfected with PEI (23966; Polyscience Inc.) and maintained in regular DMEM media containing 10% FCS and a penicillin-streptomycin mixture. The same media were used to maintain the Y79 cell line. Protein extractions were performed as described above.

Retinal explant culture. Retina was dissected free from other ocular tissue in PBS and then incubated either in regular DMEM media or glucose-free DMEM media. Fetal calf serum was added at 10% (vol/vol) in both cases. Incubation was performed for 2 hours at 37°C and 5% CO_2. Thereafter retinae were fixed and processed for antibody staining as described.

Autophagy flux, mTOR and LAMP quantifications. The mCherry-GFP-LC3 vector[315] (Plasmid: Claudio Hetz; packaging: UMass Vector Core, rAAV9) was injected subretinally at birth (1µL of $1X10^{13}$ genome copies/mL) as described previously[316]. Retinae were harvested at 2 months of age and processed as described. Images from *Cre*$^{-}$ and *Cre*$^{+}$ retinae were acquired (100x) at the same exposure and manual counting of the GFP and mCherry spots was performed in a blind manner. The same method was used to assess mTOR and LAMP2 colocalization as well as for LAMP1/2 counting. All images were acquired on a Leica DM5500 fluorescence microscope.

Rapamycin and trehalose administration. Rapamycin was diluted in 50% Ethanol to 10 mg/ml. Prior to injection, the solution was diluted to a concentration of 2 mg/ml in 50% Ethanol. All mice were treated with 2mg/kg body weight of rapamycin by intra-peritoneal injections. Mice were either injected at 5-day intervals beginning at P28 until 2 or 4 months of age, or at P28, P35, P49, P63, P77 and P105 for the 6-injection regimen, or at P28 and P90 for the two-injection regimen. 50% Ethanol was used as the vehicle control. Trehalose (100%, Swanson Ultra) was administered at libitum in drinking water (4% w/v) between P28 and 4 months of age.

Statistics. The Student's *t* test was used for statistical analyses. *P* values of less than 0.05 were considered statistically significant. If not otherwise noted in the figure legend, all error bars represent the SEM.

Bibliography

1 Rodieck, R. *The First Steps in Seeing*. (Sinauer, 1998).

2 Jeon, C. J., Strettoi, E. & Masland, R. H. The major cell populations of the mouse retina. *The Journal of neuroscience : the official journal of the Society for Neuroscience* **18**, 8936-8946 (1998).

3 Masland, R. H. The fundamental plan of the retina. *Nature neuroscience* **4**, 877-886, doi:10.1038/nn0901-877nn0901-877 [pii] (2001).

4 Masland, R. H. Cell populations of the retina: the Proctor lecture. *Investigative ophthalmology & visual science* **52**, 4581-4591, doi:10.1167/iovs.10-708352/7/4581 [pii] (2011).

5 Lisman, J. E. & Bering, H. Electrophysiological measurement of the number of rhodopsin molecules in single Limulus photoreceptors. *J Gen Physiol* **70**, 621-633 (1977).

6 Scott, B. L., Racz, E., Lolley, R. N. & Bazan, N. G. Developing rod photoreceptors from normal and mutant Rd mouse retinas: altered fatty acid composition early in development of the mutant. *J Neurosci Res* **20**, 202-211, doi:10.1002/jnr.490200209 (1988).

7 Nathans, J. The evolution and physiology of human color vision: insights from molecular genetic studies of visual pigments. *Neuron* **24**, 299-312, doi:S0896-6273(00)80845-4 [pii] (1999).

8 Akeo, K., Tsukamoto, H., Okisaka, S., Hiramitsu, T. & Watanabe, K. The localization of glutathione peroxidase in the photoreceptor cells and the retinal pigment epithelial cells of Wistar and Royal College of Surgeons dystrophic rats. *Pigment cell research / sponsored by the European Society for Pigment Cell Research and the International Pigment Cell Society* **12**, 107-117 (1999).

9 Jonas, J. B., Schneider, U. & Naumann, G. O. Count and density of human retinal photoreceptors. *Graefe's archive for clinical and experimental ophthalmology = Albrecht von Graefes Archiv fur klinische und experimentelle Ophthalmologie* **230**, 505-510 (1992).

10 Lamb, T. D. Why rods and cones? *Eye* **30**, 179-185, doi:10.1038/eye.2015.236 (2016).

11 Mollon, J. D. Color vision: opsins and options. *Proceedings of the National Academy of Sciences of the United States of America* **96**, 4743-4745 (1999).

12 Applebury, M. L. *et al.* The murine cone photoreceptor: a single cone type expresses both S and M opsins with retinal spatial patterning. *Neuron* **27**, 513-523 (2000).

13 Punzo, C., Kornacker, K. & Cepko, C. L. Stimulation of the insulin/mTOR pathway delays cone death in a mouse model of retinitis pigmentosa. *Nature neuroscience* **12**, 44-52, doi:nn.2234 [pii]10.1038/nn.2234 (2009).

14 Fu, Y. & Yau, K. W. Phototransduction in mouse rods and cones. *Pflugers Archiv : European journal of physiology* **454**, 805-819, doi:10.1007/s00424-006-0194-y (2007).

15 Luo, D. G., Xue, T. & Yau, K. W. How vision begins: an odyssey. *Proceedings of the National Academy of Sciences of the United States of America* **105**, 9855-9862, doi:10.1073/pnas.0708405105 (2008).

16 Reichenbach, A. & Bringmann, A. New functions of Muller cells. *Glia* **61**, 651-678, doi:10.1002/glia.22477 (2013).

17 Bok, D. The retinal pigment epithelium: a versatile partner in vision. *Journal of cell science. Supplement* **17**, 189-195 (1993).

18 Marmorstein, A. D., Finnemann, S. C., Bonilha, V. L. & Rodriguez-Boulan, E. Morphogenesis of the retinal pigment epithelium: toward understanding retinal degenerative diseases. *Annals of the New York Academy of Sciences* **857**, 1-12 (1998).

19 Parker, R. O. & Crouch, R. K. Retinol dehydrogenases (RDHs) in the visual cycle. *Experimental eye research* **91**, 788-792, doi:S0014-4835(10)00257-5 [pii]10.1016/j.exer.2010.08.013 (2010).

20 Winkler, B. S. An hypothesis to account for the renewal of outer segments in rod and cone photoreceptor cells: renewal as a surrogate antioxidant. *Investigative ophthalmology & visual science* **49**, 3259-3261, doi:10.1167/iovs.08-1785 (2008).

21 Kevany, B. M. & Palczewski, K. Phagocytosis of retinal rod and cone photoreceptors. *Physiology (Bethesda)* **25**, 8-15, doi:25/1/8 [pii] 10.1152/physiol.00038.2009 (2010).

22 Borovanský, J. & Riley, P. A. *Melanins and melanosomes : biosynthesis, biogenesis, physiological, and pathological functions*. (Wiley-Blackwell, 2011).

23 den Hollander, A. I., Black, A., Bennett, J. & Cremers, F. P. Lighting a candle in the dark: advances in genetics and gene therapy of recessive retinal dystrophies. *The Journal of clinical investigation* **120**, 3042-3053, doi:10.1172/JCI42258 (2010).

24 Biel, M. *et al.* Selective loss of cone function in mice lacking the cyclic nucleotide-gated channel CNG3. *Proceedings of the National Academy of Sciences of the United States of America* **96**, 7553-7557 (1999).

25 Yang, R. B. *et al.* Disruption of a retinal guanylyl cyclase gene leads to cone-specific dystrophy and paradoxical rod behavior. *The Journal of neuroscience : the official journal of the Society for Neuroscience* **19**, 5889-5897 (1999).

26 Cho, K. I. *et al.* Distinct and atypical intrinsic and extrinsic cell death pathways between photoreceptor cell types upon specific ablation of Ranbp2 in cone photoreceptors. *PLoS genetics* **9**, e1003555, doi:10.1371/journal.pgen.1003555 (2013).

27 Xu, J. *et al.* CNGA3 deficiency affects cone synaptic terminal structure and function and leads to secondary rod dysfunction and degeneration. *Investigative ophthalmology & visual science* **53**, 1117-1129, doi:10.1167/iovs.11-8168 (2012).

28 Jones, B. W. *et al.* Retinal remodeling triggered by photoreceptor degenerations. *J Comp Neurol* **464**, 1-16, doi:10.1002/cne.10703 (2003).

29 Hartong, D. T., Berson, E. L. & Dryja, T. P. Retinitis pigmentosa. *Lancet* **368**, 1795-1809 (2006).

30 Milam, A. H., Li, Z. Y. & Fariss, R. N. Histopathology of the human retina in retinitis pigmentosa. *Prog Retin Eye Res* **17**, 175-205 (1998).

31 Li, Z. Y., Possin, D. E. & Milam, A. H. Histopathology of bone spicule pigmentation in retinitis pigmentosa. *Ophthalmology* **102**, 805-816 (1995).

32 D'Cruz, P. M. *et al.* Mutation of the receptor tyrosine kinase gene Mertk in the retinal dystrophic RCS rat. *Human molecular genetics* **9**, 645-651, doi:ddd061 [pii] (2000).

33 Umen, J. G. & Guthrie, C. Prp16p, Slu7p, and Prp8p interact with the 3' splice site in two distinct stages during the second catalytic step of pre-mRNA splicing. *Rna* **1**, 584-597 (1995).

34 Lauber, J. *et al.* The human U4/U6 snRNP contains 60 and 90kD proteins that are structurally homologous to the yeast splicing factors Prp4p and Prp3p. *Rna* **3**, 926-941 (1997).

35 Beales, P. L., Elcioglu, N., Woolf, A. S., Parker, D. & Flinter, F. A. New criteria for improved diagnosis of Bardet-Biedl syndrome: results of a population survey. *Journal of medical genetics* **36**, 437-446 (1999).

36 Berson, E. L. Retinitis pigmentosa. The Friedenwald Lecture. *Investigative ophthalmology & visual science* **34**, 1659-1676 (1993).

37 Holopigian, K., Greenstein, V., Seiple, W. & Carr, R. E. Rates of change differ among measures of visual function in patients with retinitis pigmentosa. *Ophthalmology* **103**, 398-405 (1996).

38 Berson, E. L. *et al.* A randomized trial of vitamin A and vitamin E supplementation for retinitis pigmentosa. *Archives of ophthalmology* **111**, 761-772 (1993).

39 Bowes, C. *et al.* Retinal degeneration in the rd mouse is caused by a defect in the beta subunit of rod cGMP-phosphodiesterase. *Nature* **347**, 677-680, doi:10.1038/347677a0 (1990).

40 Punzo, C. & Cepko, C. Cellular responses to photoreceptor death in the rd1 mouse model of retinal degeneration. *Investigative ophthalmology & visual science* **48**, 849-857, doi:48/2/849 [pii]10.1167/iovs.05-1555 (2007).

41 Mitamura, Y. *et al.* Diagnostic imaging in patients with retinitis pigmentosa. *The journal of medical investigation : JMI* **59**, 1-11 (2012).

42 Fahim, A. T., Daiger, S. P. & Weleber, R. G. in *GeneReviews(R)* (eds R. A. Pagon *et al.*) (1993).

43 Robson, J. G. & Frishman, L. J. Dissecting the dark-adapted electroretinogram. *Documenta ophthalmologica. Advances in ophthalmology* **95**, 187-215 (1998).

44 McCall, M. A. & Gregg, R. G. Comparisons of structural and functional abnormalities in mouse b-wave mutants. *The Journal of physiology* **586**, 4385-4392, doi:10.1113/jphysiol.2008.159327 (2008).

45 Fishman, G. A. Basic principles of clinical electroretinography. *Retina* **5**, 123-126 (1985).

46 Zhong, M., Kawaguchi, R., Kassai, M. & Sun, H. Retina, retinol, retinal and the natural history of vitamin A as a light sensor. *Nutrients* **4**, 2069-2096, doi:10.3390/nu4122069 (2012).

47 Berson, E. L. *et al.* Vitamin A supplementation for retinitis pigmentosa. *Archives of ophthalmology* **111**, 1456-1459 (1993).

48 Fliesler, S. J. & Anderson, R. E. Chemistry and metabolism of lipids in the vertebrate retina. *Progress in lipid research* **22**, 79-131 (1983).

49 Berson, E. L. *et al.* Clinical trial of docosahexaenoic acid in patients with retinitis pigmentosa receiving vitamin A treatment. *Archives of ophthalmology* **122**, 1297-1305, doi:10.1001/archopht.122.9.1297 (2004).

50 Hoffman, D. R. *et al.* A randomized, placebo-controlled clinical trial of docosahexaenoic acid supplementation for X-linked retinitis pigmentosa. *American journal of ophthalmology* **137**, 704-718, doi:10.1016/j.ajo.2003.10.045 (2004).

51 Schaefer, E. J. *et al.* Red blood cell membrane phosphatidylethanolamine fatty acid content in various forms of retinitis pigmentosa. *Journal of lipid research* **36**, 1427-1433 (1995).

52 Hoffman, D. R. *et al.* Docosahexaenoic Acid Slows Visual Field Progression in X-Linked Retinitis Pigmentosa: Ancillary Outcomes of the DHAX Trial. *Investigative ophthalmology & visual science* **56**, 6646-6653, doi:10.1167/iovs.15-17786 (2015).

53 Lammer, E. J. *et al.* Retinoic acid embryopathy. *The New England journal of medicine* **313**, 837-841, doi:10.1056/NEJM198510033131401 (1985).

54 Lim, L. S., Harnack, L. J., Lazovich, D. & Folsom, A. R. Vitamin A intake and the risk of hip fracture in postmenopausal women: the Iowa Women's Health Study. *Osteoporosis international : a journal established as result of cooperation between the European Foundation for Osteoporosis and the National Osteoporosis Foundation of the USA* **15**, 552-559, doi:10.1007/s00198-003-1577-y (2004).

55 Boucher, B. J. Serum retinol levels and fracture risk. *The New England journal of medicine* **348**, 1927-1928; author reply 1927-1928, doi:10.1056/NEJM200305083481917 (2003).

56 Moiseyev, G., Chen, Y., Takahashi, Y., Wu, B. X. & Ma, J. X. RPE65 is the isomerohydrolase in the retinoid visual cycle. *Proceedings of the National Academy of Sciences of the United States of America* **102**, 12413-12418, doi:10.1073/pnas.0503460102 (2005).

57 Narfstrom, K. *et al.* In vivo gene therapy in young and adult RPE65-/- dogs produces long-term visual improvement. *The Journal of heredity* **94**, 31-37 (2003).

58 Mowat, F. M. *et al.* RPE65 gene therapy slows cone loss in Rpe65-deficient dogs. *Gene therapy* **20**, 545-555, doi:10.1038/gt.2012.63 (2013).

59 Annear, M. J. *et al.* Gene therapy in the second eye of RPE65-deficient dogs improves retinal function. *Gene therapy* **18**, 53-61, doi:10.1038/gt.2010.111 (2011).

60 Narfstrom, K. *et al.* Assessment of structure and function over a 3-year period after gene transfer in RPE65-/- dogs. *Documenta ophthalmologica. Advances in ophthalmology* **111**, 39-48, doi:10.1007/s10633-005-3159-0 (2005).

61 Acland, G. M. *et al.* Gene therapy restores vision in a canine model of childhood blindness. *Nature genetics* **28**, 92-95, doi:10.1038/88327 (2001).

62 Cideciyan, A. V. *et al.* Human retinal gene therapy for Leber congenital amaurosis shows advancing retinal degeneration despite enduring visual improvement. *Proceedings of the National Academy of Sciences of the United States of America* **110**, E517-525, doi:10.1073/pnas.1218933110 (2013).

63 Bainbridge, J. W. *et al.* Long-term effect of gene therapy on Leber's congenital amaurosis. *The New England journal of medicine* **372**, 1887-1897, doi:10.1056/NEJMoa1414221 (2015).

64 Jacobson, S. G. *et al.* Improvement and decline in vision with gene therapy in childhood blindness. *The New England journal of medicine* **372**, 1920-1926, doi:10.1056/NEJMoa1412965 (2015).

65 Punzo, C., Xiong, W. & Cepko, C. L. Loss of daylight vision in retinal degeneration: are oxidative stress and metabolic dysregulation to blame? *The Journal of biological chemistry* **287**, 1642-1648, doi:R111.304428 [pii]10.1074/jbc.R111.304428 (2012).

66 Pang, J. J. *et al.* AAV-mediated gene therapy for retinal degeneration in the rd10 mouse containing a recessive PDEbeta mutation. *Investigative ophthalmology & visual science* **49**, 4278-4283 (2008).

67 Zou, J. *et al.* Whirlin replacement restores the formation of the USH2 protein complex in whirlin knockout photoreceptors. *Investigative ophthalmology & visual science* **52**, 2343-2351, doi:iovs.10-6141 [pii]10.1167/iovs.10-6141 (2011).

68 Palfi, A. *et al.* Adeno-associated virus-mediated rhodopsin replacement provides therapeutic benefit in mice with a targeted disruption of the rhodopsin gene. *Human gene therapy* **21**, 311-323 (2010).

69 Hauswirth, W. W., LaVail, M. M., Flannery, J. G. & Lewin, A. S. Ribozyme gene therapy for autosomal dominant retinal disease. *Clin Chem Lab Med* **38**, 147-153, doi:10.1515/CCLM.2000.022 (2000).

70 LaVail, M. M. *et al.* Ribozyme rescue of photoreceptor cells in P23H transgenic rats: long-term survival and late-stage therapy. *Proceedings of the National Academy of Sciences of the United States of America* **97**, 11488-11493, doi:10.1073/pnas.210319397210319397 [pii] (2000).

71 Gorbatyuk, M., Justilien, V., Liu, J., Hauswirth, W. W. & Lewin, A. S. Suppression of mouse rhodopsin expression in vivo by AAV mediated siRNA delivery. *Vision research* **47**, 1202-1208, doi:10.1016/j.visres.2006.11.026 (2007).

72 Pittler, S. J. & Baehr, W. Identification of a nonsense mutation in the rod photoreceptor cGMP phosphodiesterase beta-subunit gene of the rd mouse. *Proceedings of the National Academy of Sciences of the United States of America* **88**, 8322-8326 (1991).

73 Sancho-Pelluz, J. *et al.* Photoreceptor cell death mechanisms in inherited retinal degeneration. *Molecular neurobiology* **38**, 253-269, doi:10.1007/s12035-008-8045-9 (2008).

74 Bowes, C. *et al.* Localization of a retroviral element within the rd gene coding for the beta subunit of cGMP phosphodiesterase. *Proceedings of the National Academy of Sciences of the United States of America* **90**, 2955-2959 (1993).

75 Kaushal, S. & Khorana, H. G. Structure and function in rhodopsin. 7. Point mutations associated with autosomal dominant retinitis pigmentosa. *Biochemistry* **33**, 6121-6128 (1994).

76 Kurada, P., Tonini, T. D., Serikaku, M. A., Piccini, J. P. & O'Tousa, J. E. Rhodopsin maturation antagonized by dominant rhodopsin mutants. *Visual neuroscience* **15**, 693-700 (1998).

77 Illing, M. E., Rajan, R. S., Bence, N. F. & Kopito, R. R. A rhodopsin mutant linked to autosomal dominant retinitis pigmentosa is prone to aggregate and interacts with the ubiquitin proteasome system. *The Journal of biological chemistry* **277**, 34150-34160, doi:10.1074/jbc.M204955200 (2002).

78 Chang, G. Q., Hao, Y. & Wong, F. Apoptosis: final common pathway of photoreceptor death in rd, rds, and rhodopsin mutant mice. *Neuron* **11**, 595-605 (1993).

79 Boatright, K. M. *et al.* A unified model for apical caspase activation. *Molecular cell* **11**, 529-541, doi:S1097276503000510 [pii] (2003).

80 Deveraux, Q. L., Takahashi, R., Salvesen, G. S. & Reed, J. C. X-linked IAP is a direct inhibitor of cell-death proteases. *Nature* **388**, 300-304, doi:10.1038/40901 (1997).

81 Leonard, K. C. *et al.* XIAP protection of photoreceptors in animal models of retinitis pigmentosa. *PloS one* **2**, e314, doi:10.1371/journal.pone.0000314 (2007).

82 Chang, B. *et al.* Retinal degeneration mutants in the mouse. *Vision research* **42**, 517-525 (2002).

83 Yao, J. *et al.* Caspase inhibition with XIAP as an adjunct to AAV vector gene-replacement therapy: improving efficacy and prolonging the treatment window. *PloS one* **7**, e37197, doi:10.1371/journal.pone.0037197 (2012).

84 Yao, J. *et al.* XIAP therapy increases survival of transplanted rod precursors in a degenerating host retina. *Investigative ophthalmology & visual science* **52**, 1567-1572, doi:10.1167/iovs.10-5998 (2011).

85 MacLaren, R. E. *et al.* Retinal repair by transplantation of photoreceptor precursors. *Nature* **444**, 203-207, doi:10.1038/nature05161 (2006).

86 Wang, S. *et al.* Long-term vision rescue by human neural progenitors in a rat model of photoreceptor degeneration. *Investigative ophthalmology & visual science* **49**, 3201-3206, doi:10.1167/iovs.08-1831 (2008).

87 Lamba, D. A., Gust, J. & Reh, T. A. Transplantation of human embryonic stem cell-derived photoreceptors restores some visual function in Crx-deficient mice. *Cell stem cell* **4**, 73-79, doi:10.1016/j.stem.2008.10.015 (2009).

88 Okoye, G. *et al.* Increased expression of brain-derived neurotrophic factor preserves retinal function and slows cell death from rhodopsin mutation or

oxidative damage. *The Journal of neuroscience : the official journal of the Society for Neuroscience* **23**, 4164-4172 (2003).

89 McGee Sanftner, L. H., Abel, H., Hauswirth, W. W. & Flannery, J. G. Glial cell line derived neurotrophic factor delays photoreceptor degeneration in a transgenic rat model of retinitis pigmentosa. *Molecular therapy : the journal of the American Society of Gene Therapy* **4**, 622-629, doi:10.1006/mthe.2001.0498 (2001).

90 Chong, N. H. *et al.* Repeated injections of a ciliary neurotrophic factor analogue leading to long-term photoreceptor survival in hereditary retinal degeneration. *Investigative ophthalmology & visual science* **40**, 1298-1305 (1999).

91 Liang, F. Q. *et al.* AAV-mediated delivery of ciliary neurotrophic factor prolongs photoreceptor survival in the rhodopsin knockout mouse. *Molecular therapy : the journal of the American Society of Gene Therapy* **3**, 241-248, doi:10.1006/mthe.2000.0252 (2001).

92 Tao, W. *et al.* Encapsulated cell-based delivery of CNTF reduces photoreceptor degeneration in animal models of retinitis pigmentosa. *Investigative ophthalmology & visual science* **43**, 3292-3298 (2002).

93 Lipinski, D. M. *et al.* CNTF Gene Therapy Confers Lifelong Neuroprotection in a Mouse Model of Human Retinitis Pigmentosa. *Molecular therapy : the journal of the American Society of Gene Therapy* **23**, 1308-1319, doi:10.1038/mt.2015.68 (2015).

94 Chen, B. & Cepko, C. L. HDAC4 regulates neuronal survival in normal and diseased retinas. *Science* **323**, 256-259, doi:323/5911/256 [pii]10.1126/science.1166226 (2009).

95 Guo, X. *et al.* A short N-terminal domain of HDAC4 preserves photoreceptors and restores visual function in retinitis pigmentosa. *Nature communications* **6**, 8005, doi:10.1038/ncomms9005 (2015).

96 Daniele, L. L. *et al.* Cone-like morphological, molecular, and electrophysiological features of the photoreceptors of the Nrl knockout mouse. *Investigative ophthalmology & visual science* **46**, 2156-2167, doi:10.1167/iovs.04-1427 (2005).

97 Montana, C. L. *et al.* Reprogramming of adult rod photoreceptors prevents retinal degeneration. *Proceedings of the National Academy of Sciences of the United States of America* **110**, 1732-1737, doi:10.1073/pnas.1214387110 (2013).

98 Gupta, N., Brown, K. E. & Milam, A. H. Activated microglia in human retinitis pigmentosa, late-onset retinal degeneration, and age-related macular degeneration. *Experimental eye research* **76**, 463-471, doi:S0014483502003329 [pii] (2003).

99 Steinberg, R. H. Survival factors in retinal degenerations. *Curr Opin Neurobiol* **4**, 515-524 (1994).

100 Mohand-Said, S. *et al.* Normal retina releases a diffusible factor stimulating cone survival in the retinal degeneration mouse. *Proceedings of the National Academy of Sciences of the United States of America* **95**, 8357-8362 (1998).

101 Streichert, L. C., Birnbach, C. D. & Reh, T. A. A diffusible factor from normal retinal cells promotes rod photoreceptor survival in an in vitro model of retinitis pigmentosa. *Journal of neurobiology* **39**, 475-490 (1999).

102 Leveillard, T. *et al.* Identification and characterization of rod-derived cone viability factor. *Nature genetics* **36**, 755-759, doi:10.1038/ng1386ng1386 [pii] (2004).

103 Shen, J. *et al.* Oxidative damage is a potential cause of cone cell death in retinitis pigmentosa. *Journal of cellular physiology* **203**, 457-464, doi:10.1002/jcp.20346 (2005).

104 Komeima, K., Rogers, B. S., Lu, L. & Campochiaro, P. A. Antioxidants reduce cone cell death in a model of retinitis pigmentosa. *Proceedings of the National Academy of Sciences of the United States of America* **103**, 11300-11305, doi:0604056103 [pii]10.1073/pnas.0604056103 (2006).

105 Yu, D. Y. *et al.* Photoreceptor death, trophic factor expression, retinal oxygen status, and photoreceptor function in the P23H rat. *Investigative ophthalmology & visual science* **45**, 2013-2019 (2004).

106 Ames, A., 3rd. CNS energy metabolism as related to function. *Brain Res Brain Res Rev* **34**, 42-68, doi:S0165017300000382 [pii] (2000).

107 Ames, A., 3rd, Li, Y. Y., Heher, E. C. & Kimble, C. R. Energy metabolism of rabbit retina as related to function: high cost of Na+ transport. *The Journal of neuroscience : the official journal of the Society for Neuroscience* **12**, 840-853 (1992).

108 Hoang, Q. V., Linsenmeier, R. A., Chung, C. K. & Curcio, C. A. Photoreceptor inner segments in monkey and human retina: mitochondrial density, optics, and regional variation. *Visual neuroscience* **19**, 395-407 (2002).

109 Perkins, G. A., Ellisman, M. H. & Fox, D. A. Three-dimensional analysis of mouse rod and cone mitochondrial cristae architecture: bioenergetic and functional implications. *Molecular vision* **9**, 60-73 (2003).

110 Murphy, M. P. How mitochondria produce reactive oxygen species. *The Biochemical journal* **417**, 1-13, doi:10.1042/BJ20081386 (2009).

111 Kagan, V. E., Shvedova, A. A., Novikov, K. N. & Kozlov, Y. P. Light-induced free radical oxidation of membrane lipids in photoreceptors of frog retina. *Biochimica et biophysica acta* **330**, 76-79 (1973).

112 Oguni, M., Tamura, H., Kato, K. & Setogawa, T. Chronic retinal effects by ultraviolet irradiation, with special reference to superoxide dismutases. *Histology and histopathology* **11**, 695-702 (1996).

113 Sparrow, J. R. & Boulton, M. RPE lipofuscin and its role in retinal pathobiology. *Experimental eye research* **80**, 595-606, doi:S0014-4835(05)00019-9 [pii]10.1016/j.exer.2005.01.007 (2005).

114 Haruta, M. *et al.* Depleting Rac1 in mouse rod photoreceptors protects them from photo-oxidative stress without affecting their structure or function. *Proceedings of the National Academy of Sciences of the United States of America* **106**, 9397-9402, doi:0808940106 [pii]10.1073/pnas.0808940106 (2009).

115 Yu, D. Y., Cringle, S. J., Su, E. N. & Yu, P. K. Intraretinal oxygen levels before and after photoreceptor loss in the RCS rat. *Investigative ophthalmology & visual science* **41**, 3999-4006 (2000).

116 Bill, A. & Sperber, G. O. Control of retinal and choroidal blood flow. *Eye* **4 (Pt 2)**, 319-325 (1990).
117 Komeima, K., Rogers, B. S. & Campochiaro, P. A. Antioxidants slow photoreceptor cell death in mouse models of retinitis pigmentosa. *J Cell Physiol* **213**, 809-815, doi:10.1002/jcp.21152 (2007).
118 Usui, S. *et al.* Increased expression of catalase and superoxide dismutase 2 reduces cone cell death in retinitis pigmentosa. *Molecular therapy : the journal of the American Society of Gene Therapy* **17**, 778-786, doi:10.1038/mt.2009.47 (2009).
119 Xiong, W., MacColl Garfinkel, A. E., Li, Y., Benowitz, L. I. & Cepko, C. L. NRF2 promotes neuronal survival in neurodegeneration and acute nerve damage. *The Journal of clinical investigation* **125**, 1433-1445, doi:10.1172/JCI79735 (2015).
120 Finkel, T. Oxidant signals and oxidative stress. *Curr Opin Cell Biol* **15**, 247-254 (2003).
121 Fridlich, R. *et al.* The thioredoxin-like protein rod-derived cone viability factor (RdCVFL) interacts with TAU and inhibits its phosphorylation in the retina. *Mol Cell Proteomics* **8**, 1206-1218 (2009).
122 Yang, Y. *et al.* Functional cone rescue by RdCVF protein in a dominant model of retinitis pigmentosa. *Molecular therapy : the journal of the American Society of Gene Therapy* **17**, 787-795, doi:10.1038/mt.2009.28 (2009).
123 Byrne, L. C. *et al.* Viral-mediated RdCVF and RdCVFL expression protects cone and rod photoreceptors in retinal degeneration. *The Journal of clinical investigation* **125**, 105-116, doi:10.1172/JCI65654 (2015).
124 Cronin, T. *et al.* The disruption of the rod-derived cone viability gene leads to photoreceptor dysfunction and susceptibility to oxidative stress. *Cell death and differentiation* **17**, 1199-1210, doi:10.1038/cdd.2010.2 (2010).
125 Ait-Ali, N. *et al.* Rod-derived cone viability factor promotes cone survival by stimulating aerobic glycolysis. *Cell* **161**, 817-832, doi:10.1016/j.cell.2015.03.023 (2015).
126 Young, R. W. The renewal of photoreceptor cell outer segments. *The Journal of cell biology* **33**, 61-72 (1967).
127 Dudley, P. A. & Anderson, R. E. Phospholipid transfer protein from bovine retina with high activity towards retinal rod disc membranes. *FEBS letters* **95**, 57-60 (1978).
128 Tsacopoulos, M., Poitry-Yamate, C. L., MacLeish, P. R. & Poitry, S. Trafficking of molecules and metabolic signals in the retina. *Prog Retin Eye Res* **17**, 429-442, doi:S1350-9462(98)00010-X [pii] (1998).
129 Poitry-Yamate, C. L., Poitry, S. & Tsacopoulos, M. Lactate released by Muller glial cells is metabolized by photoreceptors from mammalian retina. *The Journal of neuroscience : the official journal of the Society for Neuroscience* **15**, 5179-5191 (1995).

130 Gladden, L. B. Lactate metabolism: a new paradigm for the third millennium. *The Journal of physiology* **558**, 5-30, doi:10.1113/jphysiol.2003.058701 jphysiol.2003.058701 [pii] (2004).
131 Vander Heiden, M. G., Cantley, L. C. & Thompson, C. B. Understanding the Warburg effect: the metabolic requirements of cell proliferation. *Science* **324**, 1029-1033, doi:324/5930/1029 [pii]10.1126/science.1160809 (2009).
132 Vander Heiden, M. G. *et al.* Evidence for an alternative glycolytic pathway in rapidly proliferating cells. *Science* **329**, 1492-1499, doi:329/5998/1492 [pii]10.1126/science.1188015 (2010).
133 Snodderly, D. M., Sandstrom, M. M., Leung, I. Y., Zucker, C. L. & Neuringer, M. Retinal pigment epithelial cell distribution in central retina of rhesus monkeys. *Investigative ophthalmology & visual science* **43**, 2815-2818 (2002).
134 John, S. K., Smith, J. E., Aguirre, G. D. & Milam, A. H. Loss of cone molecular markers in rhodopsin-mutant human retinas with retinitis pigmentosa. *Mol Vis* **6**, 204-215, doi:v6/a28 [pii] (2000).
135 Winkler, B. S., DeSantis, N. & Solomon, F. Multiple NADPH-producing pathways control glutathione (GSH) content in retina. *Experimental eye research* **43**, 829-847 (1986).
136 Harris, A. L. Hypoxia--a key regulatory factor in tumour growth. *Nat Rev Cancer* **2**, 38-47, doi:10.1038/nrc704 (2002).
137 Zoncu, R., Efeyan, A. & Sabatini, D. M. mTOR: from growth signal integration to cancer, diabetes and ageing. *Nature reviews. Molecular cell biology* **12**, 21-35, doi:nrm3025 [pii]10.1038/nrm3025 (2011).
138 Sahel, J. A. & Roska, B. Gene therapy for blindness. *Annual review of neuroscience* **36**, 467-488, doi:10.1146/annurev-neuro-062012-170304 (2013).
139 Deisseroth, K. Optogenetics: 10 years of microbial opsins in neuroscience. *Nature neuroscience* **18**, 1213-1225, doi:10.1038/nn.4091 (2015).
140 Boyden, E. S., Zhang, F., Bamberg, E., Nagel, G. & Deisseroth, K. Millisecond-timescale, genetically targeted optical control of neural activity. *Nature neuroscience* **8**, 1263-1268, doi:10.1038/nn1525 (2005).
141 Busskamp, V. *et al.* Genetic reactivation of cone photoreceptors restores visual responses in retinitis pigmentosa. *Science* **329**, 413-417, doi:10.1126/science.1190897 (2010).
142 Lagali, P. S. *et al.* Light-activated channels targeted to ON bipolar cells restore visual function in retinal degeneration. *Nature neuroscience* **11**, 667-675, doi:10.1038/nn.2117 (2008).
143 Bi, A. *et al.* Ectopic expression of a microbial-type rhodopsin restores visual responses in mice with photoreceptor degeneration. *Neuron* **50**, 23-33, doi:10.1016/j.neuron.2006.02.026 (2006).
144 Zhang, Y., Ivanova, E., Bi, A. & Pan, Z. H. Ectopic expression of multiple microbial rhodopsins restores ON and OFF light responses in retinas with photoreceptor degeneration. *The Journal of neuroscience : the official journal of the Society for Neuroscience* **29**, 9186-9196, doi:10.1523/JNEUROSCI.0184-09.2009 (2009).

145 Doroudchi, M. M. *et al.* Virally delivered channelrhodopsin-2 safely and effectively restores visual function in multiple mouse models of blindness. *Molecular therapy : the journal of the American Society of Gene Therapy* **19**, 1220-1229, doi:10.1038/mt.2011.69 (2011).

146 White, M. F. The IRS-signalling system: a network of docking proteins that mediate insulin action. *Molecular and cellular biochemistry* **182**, 3-11 (1998).

147 Hollander, M. C., Blumenthal, G. M. & Dennis, P. A. PTEN loss in the continuum of common cancers, rare syndromes and mouse models. *Nat Rev Cancer* **11**, 289-301, doi:nrc3037 [pii]10.1038/nrc3037 (2011).

148 Hers, I., Vincent, E. E. & Tavare, J. M. Akt signalling in health and disease. *Cellular signalling* **23**, 1515-1527, doi:10.1016/j.cellsig.2011.05.004 (2011).

149 Hung, C. M., Garcia-Haro, L., Sparks, C. A. & Guertin, D. A. mTOR-dependent cell survival mechanisms. *Cold Spring Harbor perspectives in biology* **4**, doi:10.1101/cshperspect.a008771 (2012).

150 Gan, X., Wang, J., Su, B. & Wu, D. Evidence for direct activation of mTORC2 kinase activity by phosphatidylinositol 3,4,5-trisphosphate. *The Journal of biological chemistry* **286**, 10998-11002, doi:10.1074/jbc.M110.195016 (2011).

151 Potter, C. J., Pedraza, L. G. & Xu, T. Akt regulates growth by directly phosphorylating Tsc2. *Nature cell biology* **4**, 658-665, doi:10.1038/ncb840 (2002).

152 Dibble, C. C. *et al.* TBC1D7 is a third subunit of the TSC1-TSC2 complex upstream of mTORC1. *Molecular cell* **47**, 535-546, doi:10.1016/j.molcel.2012.06.009 (2012).

153 Manning, B. D. & Cantley, L. C. Rheb fills a GAP between TSC and TOR. *Trends in biochemical sciences* **28**, 573-576, doi:10.1016/j.tibs.2003.09.003 (2003).

154 Laplante, M. & Sabatini, D. M. mTOR signaling at a glance. *J Cell Sci* **122**, 3589-3594, doi:122/20/3589 [pii]10.1242/jcs.051011 (2009).

155 Sengupta, S., Peterson, T. R. & Sabatini, D. M. Regulation of the mTOR complex 1 pathway by nutrients, growth factors, and stress. *Molecular cell* **40**, 310-322, doi:10.1016/j.molcel.2010.09.026 (2010).

156 Hsu, P. P. *et al.* The mTOR-regulated phosphoproteome reveals a mechanism of mTORC1-mediated inhibition of growth factor signaling. *Science* **332**, 1317-1322, doi:332/6035/1317 [pii]10.1126/science.1199498 (2011).

157 Yu, Y. *et al.* Phosphoproteomic analysis identifies Grb10 as an mTORC1 substrate that negatively regulates insulin signaling. *Science* **332**, 1322-1326, doi:332/6035/1322 [pii]10.1126/science.1199484 (2011).

158 Julien, L. A., Carriere, A., Moreau, J. & Roux, P. P. mTORC1-activated S6K1 phosphorylates Rictor on threonine 1135 and regulates mTORC2 signaling. *Molecular and cellular biology* **30**, 908-921, doi:MCB.00601-09 [pii]10.1128/MCB.00601-09 (2010).

159 Treins, C., Warne, P. H., Magnuson, M. A., Pende, M. & Downward, J. Rictor is a novel target of p70 S6 kinase-1. *Oncogene* **29**, 1003-1016, doi:onc2009401 [pii]10.1038/onc.2009.401 (2010).

160 Dibble, C. C., Asara, J. M. & Manning, B. D. Characterization of Rictor phosphorylation sites reveals direct regulation of mTOR complex 2 by S6K1. *Molecular and cellular biology* **29**, 5657-5670, doi:MCB.00735-09 [pii]10.1128/MCB.00735-09 (2009).

161 Guertin, D. A. *et al.* Ablation in mice of the mTORC components raptor, rictor, or mLST8 reveals that mTORC2 is required for signaling to Akt-FOXO and PKCalpha, but not S6K1. *Developmental cell* **11**, 859-871, doi:10.1016/j.devcel.2006.10.007 (2006).

162 Heitman, J., Movva, N. R. & Hall, M. N. Targets for cell cycle arrest by the immunosuppressant rapamycin in yeast. *Science* **253**, 905-909 (1991).

163 Sabatini, D. M., Erdjument-Bromage, H., Lui, M., Tempst, P. & Snyder, S. H. RAFT1: a mammalian protein that binds to FKBP12 in a rapamycin-dependent fashion and is homologous to yeast TORs. *Cell* **78**, 35-43 (1994).

164 Seto, B. Rapamycin and mTOR: a serendipitous discovery and implications for breast cancer. *Clinical and translational medicine* **1**, 29, doi:10.1186/2001-1326-1-29 (2012).

165 Kim, D. H. *et al.* mTOR interacts with raptor to form a nutrient-sensitive complex that signals to the cell growth machinery. *Cell* **110**, 163-175 (2002).

166 Sarbassov, D. D. *et al.* Rictor, a novel binding partner of mTOR, defines a rapamycin-insensitive and raptor-independent pathway that regulates the cytoskeleton. *Current biology : CB* **14**, 1296-1302, doi:10.1016/j.cub.2004.06.054 (2004).

167 Loewith, R. *et al.* Two TOR complexes, only one of which is rapamycin sensitive, have distinct roles in cell growth control. *Molecular cell* **10**, 457-468 (2002).

168 Peterson, T. R. *et al.* DEPTOR is an mTOR inhibitor frequently overexpressed in multiple myeloma cells and required for their survival. *Cell* **137**, 873-886, doi:10.1016/j.cell.2009.03.046 (2009).

169 Yip, C. K., Murata, K., Walz, T., Sabatini, D. M. & Kang, S. A. Structure of the human mTOR complex I and its implications for rapamycin inhibition. *Molecular cell* **38**, 768-774, doi:10.1016/j.molcel.2010.05.017 (2010).

170 Sarbassov, D. D. *et al.* Prolonged rapamycin treatment inhibits mTORC2 assembly and Akt/PKB. *Molecular cell* **22**, 159-168, doi:10.1016/j.molcel.2006.03.029 (2006).

171 Kim, E., Goraksha-Hicks, P., Li, L., Neufeld, T. P. & Guan, K. L. Regulation of TORC1 by Rag GTPases in nutrient response. *Nature cell biology* **10**, 935-945, doi:10.1038/ncb1753 (2008).

172 Sancak, Y. *et al.* The Rag GTPases bind raptor and mediate amino acid signaling to mTORC1. *Science* **320**, 1496-1501, doi:10.1126/science.1157535 (2008).

173 Demetriades, C., Doumpas, N. & Teleman, A. A. Regulation of TORC1 in response to amino acid starvation via lysosomal recruitment of TSC2. *Cell* **156**, 786-799, doi:10.1016/j.cell.2014.01.024 (2014).

174 Menon, S. *et al.* Spatial control of the TSC complex integrates insulin and nutrient regulation of mTORC1 at the lysosome. *Cell* **156**, 771-785, doi:10.1016/j.cell.2013.11.049 (2014).

175 Ma, L., Chen, Z., Erdjument-Bromage, H., Tempst, P. & Pandolfi, P. P. Phosphorylation and functional inactivation of TSC2 by Erk implications for tuberous sclerosis and cancer pathogenesis. *Cell* **121**, 179-193, doi:10.1016/j.cell.2005.02.031 (2005).

176 Inoki, K. *et al.* TSC2 integrates Wnt and energy signals via a coordinated phosphorylation by AMPK and GSK3 to regulate cell growth. *Cell* **126**, 955-968, doi:10.1016/j.cell.2006.06.055 (2006).

177 Hardie, D. G. AMP-activated/SNF1 protein kinases: conserved guardians of cellular energy. *Nature reviews. Molecular cell biology* **8**, 774-785, doi:10.1038/nrm2249 (2007).

178 Inoki, K., Zhu, T. & Guan, K. L. TSC2 mediates cellular energy response to control cell growth and survival. *Cell* **115**, 577-590 (2003).

179 Gwinn, D. M. *et al.* AMPK phosphorylation of raptor mediates a metabolic checkpoint. *Molecular cell* **30**, 214-226, doi:10.1016/j.molcel.2008.03.003 (2008).

180 Haghighat, A., Mader, S., Pause, A. & Sonenberg, N. Repression of cap-dependent translation by 4E-binding protein 1: competition with p220 for binding to eukaryotic initiation factor-4E. *The EMBO journal* **14**, 5701-5709 (1995).

181 Ma, X. M. & Blenis, J. Molecular mechanisms of mTOR-mediated translational control. *Nature reviews. Molecular cell biology* **10**, 307-318, doi:10.1038/nrm2672 (2009).

182 Holz, M. K., Ballif, B. A., Gygi, S. P. & Blenis, J. mTOR and S6K1 mediate assembly of the translation preinitiation complex through dynamic protein interchange and ordered phosphorylation events. *Cell* **123**, 569-580, doi:10.1016/j.cell.2005.10.024 (2005).

183 Wang, X. *et al.* Regulation of elongation factor 2 kinase by p90(RSK1) and p70 S6 kinase. *The EMBO journal* **20**, 4370-4379, doi:10.1093/emboj/20.16.4370 (2001).

184 Mayer, C., Zhao, J., Yuan, X. & Grummt, I. mTOR-dependent activation of the transcription factor TIF-IA links rRNA synthesis to nutrient availability. *Genes & development* **18**, 423-434, doi:10.1101/gad.285504 (2004).

185 Duvel, K. *et al.* Activation of a metabolic gene regulatory network downstream of mTOR complex 1. *Molecular cell* **39**, 171-183, doi:S1097-2765(10)00463-6 [pii]10.1016/j.molcel.2010.06.022 (2010).

186 Eberle, D., Hegarty, B., Bossard, P., Ferre, P. & Foufelle, F. SREBP transcription factors: master regulators of lipid homeostasis. *Biochimie* **86**, 839-848, doi:10.1016/j.biochi.2004.09.018 (2004).

187 Cunningham, J. T. *et al.* mTOR controls mitochondrial oxidative function through a YY1-PGC-1alpha transcriptional complex. *Nature* **450**, 736-740, doi:10.1038/nature06322 (2007).

188 Lum, J. J., DeBerardinis, R. J. & Thompson, C. B. Autophagy in metazoans: cell survival in the land of plenty. *Nature reviews. Molecular cell biology* **6**, 439-448, doi:10.1038/nrm1660 (2005).

189 Klionsky, D. J. *et al.* Guidelines for the use and interpretation of assays for monitoring autophagy. *Autophagy* **8**, 445-544 (2012).
190 Kim, J., Kundu, M., Viollet, B. & Guan, K. L. AMPK and mTOR regulate autophagy through direct phosphorylation of Ulk1. *Nature cell biology* **13**, 132-141, doi:10.1038/ncb2152 (2011).
191 Castets, P. *et al.* Sustained activation of mTORC1 in skeletal muscle inhibits constitutive and starvation-induced autophagy and causes a severe, late-onset myopathy. *Cell metabolism* **17**, 731-744, doi:10.1016/j.cmet.2013.03.015 (2013).
192 Menon, S. *et al.* Chronic activation of mTOR complex 1 is sufficient to cause hepatocellular carcinoma in mice. *Science signaling* **5**, ra24, doi:10.1126/scisignal.2002739 (2012).
193 Parkhitko, A. *et al.* Tumorigenesis in tuberous sclerosis complex is autophagy and p62/sequestosome 1 (SQSTM1)-dependent. *Proceedings of the National Academy of Sciences of the United States of America* **108**, 12455-12460, doi:10.1073/pnas.1104361108 (2011).
194 Di Nardo, A. *et al.* Neuronal Tsc1/2 complex controls autophagy through AMPK-dependent regulation of ULK1. *Human molecular genetics* **23**, 3865-3874, doi:10.1093/hmg/ddu101 (2014).
195 Di Nardo, A. *et al.* Tuberous sclerosis complex activity is required to control neuronal stress responses in an mTOR-dependent manner. *The Journal of neuroscience : the official journal of the Society for Neuroscience* **29**, 5926-5937, doi:10.1523/JNEUROSCI.0778-09.2009 (2009).
196 Efeyan, A., Zoncu, R. & Sabatini, D. M. Amino acids and mTORC1: from lysosomes to disease. *Trends in molecular medicine* **18**, 524-533, doi:10.1016/j.molmed.2012.05.007 (2012).
197 Hosokawa, N. *et al.* Nutrient-dependent mTORC1 association with the ULK1-Atg13-FIP200 complex required for autophagy. *Molecular biology of the cell* **20**, 1981-1991, doi:10.1091/mbc.E08-12-1248 (2009).
198 Mizushima, N. Autophagy: process and function. *Genes & development* **21**, 2861-2873, doi:10.1101/gad.1599207 (2007).
199 Isakson, P., Holland, P. & Simonsen, A. The role of ALFY in selective autophagy. *Cell death and differentiation* **20**, 12-20, doi:10.1038/cdd.2012.66 (2013).
200 Johansen, T. & Lamark, T. Selective autophagy mediated by autophagic adapter proteins. *Autophagy* **7**, 279-296 (2011).
201 Wang, J. & Maldonado, M. A. The ubiquitin-proteasome system and its role in inflammatory and autoimmune diseases. *Cellular & molecular immunology* **3**, 255-261 (2006).
202 Zhang, Y. *et al.* Coordinated regulation of protein synthesis and degradation by mTORC1. *Nature* **513**, 440-443, doi:10.1038/nature13492 (2014).
203 Garcia-Martinez, J. M. & Alessi, D. R. mTOR complex 2 (mTORC2) controls hydrophobic motif phosphorylation and activation of serum- and glucocorticoid-induced protein kinase 1 (SGK1). *The Biochemical journal* **416**, 375-385, doi:10.1042/BJ20081668 (2008).

204 Ikenoue, T., Inoki, K., Yang, Q., Zhou, X. & Guan, K. L. Essential function of TORC2 in PKC and Akt turn motif phosphorylation, maturation and signalling. *The EMBO journal* **27**, 1919-1931, doi:10.1038/emboj.2008.119 (2008).

205 Sarbassov, D. D., Guertin, D. A., Ali, S. M. & Sabatini, D. M. Phosphorylation and regulation of Akt/PKB by the rictor-mTOR complex. *Science* **307**, 1098-1101, doi:10.1126/science.1106148 (2005).

206 Kamada, Y. *et al.* Tor2 directly phosphorylates the AGC kinase Ypk2 to regulate actin polarization. *Molecular and cellular biology* **25**, 7239-7248, doi:10.1128/MCB.25.16.7239-7248.2005 (2005).

207 Schmidt, A., Bickle, M., Beck, T. & Hall, M. N. The yeast phosphatidylinositol kinase homolog TOR2 activates RHO1 and RHO2 via the exchange factor ROM2. *Cell* **88**, 531-542 (1997).

208 Berchtold, D. & Walther, T. C. TORC2 plasma membrane localization is essential for cell viability and restricted to a distinct domain. *Molecular biology of the cell* **20**, 1565-1575, doi:10.1091/mbc.E08-10-1001 (2009).

209 Zhang, X., Tang, N., Hadden, T. J. & Rishi, A. K. Akt, FoxO and regulation of apoptosis. *Biochimica et biophysica acta* **1813**, 1978-1986, doi:10.1016/j.bbamcr.2011.03.010 (2011).

210 Brown, J., Wang, H., Suttles, J., Graves, D. T. & Martin, M. Mammalian target of rapamycin complex 2 (mTORC2) negatively regulates Toll-like receptor 4-mediated inflammatory response via FoxO1. *The Journal of biological chemistry* **286**, 44295-44305, doi:10.1074/jbc.M111.258053 (2011).

211 Gu, Y., Lindner, J., Kumar, A., Yuan, W. & Magnuson, M. A. Rictor/mTORC2 is essential for maintaining a balance between beta-cell proliferation and cell size. *Diabetes* **60**, 827-837, doi:10.2337/db10-1194 (2011).

212 Mammucari, C. *et al.* FoxO3 controls autophagy in skeletal muscle in vivo. *Cell metabolism* **6**, 458-471, doi:10.1016/j.cmet.2007.11.001 (2007).

213 Zhao, J. *et al.* FoxO3 coordinately activates protein degradation by the autophagic/lysosomal and proteasomal pathways in atrophying muscle cells. *Cell metabolism* **6**, 472-483, doi:10.1016/j.cmet.2007.11.004 (2007).

214 Brunet, A. *et al.* Protein kinase SGK mediates survival signals by phosphorylating the forkhead transcription factor FKHRL1 (FOXO3a). *Molecular and cellular biology* **21**, 952-965, doi:10.1128/MCB.21.3.952-965.2001 (2001).

215 Lang, F. & Shumilina, E. Regulation of ion channels by the serum- and glucocorticoid-inducible kinase SGK1. *FASEB journal : official publication of the Federation of American Societies for Experimental Biology* **27**, 3-12, doi:10.1096/fj.12-218230 (2013).

216 Li, G. *et al.* Nonredundant role of Akt2 for neuroprotection of rod photoreceptor cells from light-induced cell death. *The Journal of neuroscience : the official journal of the Society for Neuroscience* **27**, 203-211, doi:27/1/203 [pii]10.1523/JNEUROSCI.0445-06.2007 (2007).

217 Rajala, A., Tanito, M., Le, Y. Z., Kahn, C. R. & Rajala, R. V. Loss of neuroprotective survival signal in mice lacking insulin receptor gene in rod

photoreceptor cells. *The Journal of biological chemistry* **283**, 19781-19792, doi:M802374200 [pii]10.1074/jbc.M802374200 (2008).

218 Ivanovic, I. *et al.* Phosphoinositide 3-Kinase Signaling in Retinal Rod Photoreceptors. *Investigative ophthalmology & visual science*, doi:iovs.10-7138 [pii]10.1167/iovs.10-7138 (2011).

219 Ivanovic, I. *et al.* Deletion of the p85alpha regulatory subunit of phosphoinositide 3-kinase in cone photoreceptor cells results in cone photoreceptor degeneration. *Investigative ophthalmology & visual science* **52**, 3775-3783, doi:iovs.10-7139 [pii]10.1167/iovs.10-7139 (2011).

220 Ouyang, L. *et al.* Programmed cell death pathways in cancer: a review of apoptosis, autophagy and programmed necrosis. *Cell proliferation* **45**, 487-498, doi:10.1111/j.1365-2184.2012.00845.x (2012).

221 McIlwain, D. R., Berger, T. & Mak, T. W. Caspase functions in cell death and disease. *Cold Spring Harbor perspectives in biology* **7**, doi:10.1101/cshperspect.a026716 (2015).

222 Li, J. & Yuan, J. Caspases in apoptosis and beyond. *Oncogene* **27**, 6194-6206, doi:10.1038/onc.2008.297 (2008).

223 Salvesen, G. S. & Dixit, V. M. Caspase activation: the induced-proximity model. *Proceedings of the National Academy of Sciences of the United States of America* **96**, 10964-10967 (1999).

224 Baliga, B. C., Read, S. H. & Kumar, S. The biochemical mechanism of caspase-2 activation. *Cell death and differentiation* **11**, 1234-1241, doi:10.1038/sj.cdd.4401492 (2004).

225 Bouchier-Hayes, L. *et al.* Characterization of cytoplasmic caspase-2 activation by induced proximity. *Molecular cell* **35**, 830-840, doi:10.1016/j.molcel.2009.07.023 (2009).

226 Poreba, M., Strozyk, A., Salvesen, G. S. & Drag, M. Caspase substrates and inhibitors. *Cold Spring Harbor perspectives in biology* **5**, a008680, doi:10.1101/cshperspect.a008680 (2013).

227 Yuan, J., Shaham, S., Ledoux, S., Ellis, H. M. & Horvitz, H. R. The C. elegans cell death gene ced-3 encodes a protein similar to mammalian interleukin-1 beta-converting enzyme. *Cell* **75**, 641-652 (1993).

228 Tinel, A. & Tschopp, J. The PIDDosome, a protein complex implicated in activation of caspase-2 in response to genotoxic stress. *Science* **304**, 843-846, doi:10.1126/science.1095432 (2004).

229 Fava, L. L., Bock, F. J., Geley, S. & Villunger, A. Caspase-2 at a glance. *Journal of cell science* **125**, 5911-5915, doi:10.1242/jcs.115105 (2012).

230 Guo, Y., Srinivasula, S. M., Druilhe, A., Fernandes-Alnemri, T. & Alnemri, E. S. Caspase-2 induces apoptosis by releasing proapoptotic proteins from mitochondria. *The Journal of biological chemistry* **277**, 13430-13437, doi:10.1074/jbc.M108029200 (2002).

231 Robertson, J. D., Enoksson, M., Suomela, M., Zhivotovsky, B. & Orrenius, S. Caspase-2 acts upstream of mitochondria to promote cytochrome c release during

etoposide-induced apoptosis. *The Journal of biological chemistry* **277**, 29803-29809, doi:10.1074/jbc.M204185200 (2002).

232 Jones, R. G. *et al.* AMP-activated protein kinase induces a p53-dependent metabolic checkpoint. *Molecular cell* **18**, 283-293, doi:10.1016/j.molcel.2005.03.027 (2005).

233 Majewski, N. *et al.* Hexokinase-mitochondria interaction mediated by Akt is required to inhibit apoptosis in the presence or absence of Bax and Bak. *Molecular cell* **16**, 819-830, doi:10.1016/j.molcel.2004.11.014 (2004).

234 Rathmell, J. C. *et al.* Akt-directed glucose metabolism can prevent Bax conformation change and promote growth factor-independent survival. *Molecular and cellular biology* **23**, 7315-7328 (2003).

235 Danial, N. N. *et al.* BAD and glucokinase reside in a mitochondrial complex that integrates glycolysis and apoptosis. *Nature* **424**, 952-956, doi:10.1038/nature01825 (2003).

236 Nutt, L. K. *et al.* Metabolic regulation of oocyte cell death through the CaMKII-mediated phosphorylation of caspase-2. *Cell* **123**, 89-103, doi:S0092-8674(05)00802-0 [pii]10.1016/j.cell.2005.07.032 (2005).

237 Bergeron, L. *et al.* Defects in regulation of apoptosis in caspase-2-deficient mice. *Genes & development* **12**, 1304-1314 (1998).

238 Nutt, L. K. *et al.* Metabolic control of oocyte apoptosis mediated by 14-3-3zeta-regulated dephosphorylation of caspase-2. *Developmental cell* **16**, 856-866, doi:S1534-5807(09)00167-1 [pii]10.1016/j.devcel.2009.04.005 (2009).

239 Zeiss, C. J., Neal, J. & Johnson, E. A. Caspase-3 in postnatal retinal development and degeneration. *Investigative ophthalmology & visual science* **45**, 964-970 (2004).

240 Choudhury, S., Bhootada, Y., Gorbatyuk, O. & Gorbatyuk, M. Caspase-7 ablation modulates UPR, reprograms TRAF2-JNK apoptosis and protects T17M rhodopsin mice from severe retinal degeneration. *Cell death & disease* **4**, e528, doi:10.1038/cddis.2013.34 (2013).

241 Walsh, J. G. *et al.* Executioner caspase-3 and caspase-7 are functionally distinct proteases. *Proceedings of the National Academy of Sciences of the United States of America* **105**, 12815-12819, doi:10.1073/pnas.0707715105 (2008).

242 Murakami, Y. *et al.* Receptor interacting protein kinase mediates necrotic cone but not rod cell death in a mouse model of inherited degeneration. *Proceedings of the National Academy of Sciences of the United States of America* **109**, 14598-14603, doi:10.1073/pnas.1206937109 (2012).

243 Feoktistova, M. & Leverkus, M. Programmed necrosis and necroptosis signalling. *The FEBS journal* **282**, 19-31, doi:10.1111/febs.13120 (2015).

244 Suzuki, K., Akioka, M., Kondo-Kakuta, C., Yamamoto, H. & Ohsumi, Y. Fine mapping of autophagy-related proteins during autophagosome formation in Saccharomyces cerevisiae. *Journal of cell science* **126**, 2534-2544, doi:10.1242/jcs.122960 (2013).

245 Ichimura, Y. *et al.* Structural basis for sorting mechanism of p62 in selective autophagy. *The Journal of biological chemistry* **283**, 22847-22857, doi:10.1074/jbc.M802182200 (2008).

246 Noda, N. N. *et al.* Structural basis of target recognition by Atg8/LC3 during selective autophagy. *Genes to cells : devoted to molecular & cellular mechanisms* **13**, 1211-1218, doi:10.1111/j.1365-2443.2008.01238.x (2008).

247 Pankiv, S. *et al.* p62/SQSTM1 binds directly to Atg8/LC3 to facilitate degradation of ubiquitinated protein aggregates by autophagy. *The Journal of biological chemistry* **282**, 24131-24145, doi:10.1074/jbc.M702824200 (2007).

248 Randow, F. How cells deploy ubiquitin and autophagy to defend their cytosol from bacterial invasion. *Autophagy* **7**, 304-309 (2011).

249 Komatsu, M. *et al.* Homeostatic levels of p62 control cytoplasmic inclusion body formation in autophagy-deficient mice. *Cell* **131**, 1149-1163, doi:10.1016/j.cell.2007.10.035 (2007).

250 Nezis, I. P. *et al.* Ref(2)P, the Drosophila melanogaster homologue of mammalian p62, is required for the formation of protein aggregates in adult brain. *The Journal of cell biology* **180**, 1065-1071, doi:10.1083/jcb.200711108 (2008).

251 Komatsu, M. & Ichimura, Y. Physiological significance of selective degradation of p62 by autophagy. *FEBS letters* **584**, 1374-1378, doi:10.1016/j.febslet.2010.02.017 (2010).

252 Simonsen, A. *et al.* Alfy, a novel FYVE-domain-containing protein associated with protein granules and autophagic membranes. *Journal of cell science* **117**, 4239-4251, doi:10.1242/jcs.01287 (2004).

253 Stenmark, H., Aasland, R. & Driscoll, P. C. The phosphatidylinositol 3-phosphate-binding FYVE finger. *FEBS letters* **513**, 77-84 (2002).

254 Filimonenko, M. *et al.* The selective macroautophagic degradation of aggregated proteins requires the PI3P-binding protein Alfy. *Molecular cell* **38**, 265-279, doi:10.1016/j.molcel.2010.04.007 (2010).

255 Clausen, T. H. *et al.* p62/SQSTM1 and ALFY interact to facilitate the formation of p62 bodies/ALIS and their degradation by autophagy. *Autophagy* **6**, 330-344 (2010).

256 Egan, D. F. *et al.* Phosphorylation of ULK1 (hATG1) by AMP-activated protein kinase connects energy sensing to mitophagy. *Science* **331**, 456-461, doi:10.1126/science.1196371 (2011).

257 Mordier, S., Deval, C., Bechet, D., Tassa, A. & Ferrara, M. Leucine limitation induces autophagy and activation of lysosome-dependent proteolysis in C2C12 myotubes through a mammalian target of rapamycin-independent signaling pathway. *The Journal of biological chemistry* **275**, 29900-29906, doi:10.1074/jbc.M003633200 (2000).

258 Martina, J. A., Chen, Y., Gucek, M. & Puertollano, R. MTORC1 functions as a transcriptional regulator of autophagy by preventing nuclear transport of TFEB. *Autophagy* **8**, 903-914, doi:10.4161/auto.19653 (2012).

259 Settembre, C. *et al.* A lysosome-to-nucleus signalling mechanism senses and regulates the lysosome via mTOR and TFEB. *The EMBO journal* **31**, 1095-1108, doi:10.1038/emboj.2012.32 (2012).

260 Yu, L. *et al.* Termination of autophagy and reformation of lysosomes regulated by mTOR. *Nature* **465**, 942-946, doi:10.1038/nature09076 (2010).

261 Lem, J. *et al.* Morphological, physiological, and biochemical changes in rhodopsin knockout mice. *Proceedings of the National Academy of Sciences of the United States of America* **96**, 736-741 (1999).

262 Le, Y. Z. *et al.* Targeted expression of Cre recombinase to cone photoreceptors in transgenic mice. *Mol Vis* **10**, 1011-1018, doi:v10/a120 [pii] (2004).

263 Lesche, R. *et al.* Cre/loxP-mediated inactivation of the murine Pten tumor suppressor gene. *Genesis* **32**, 148-149, doi:10.1002/gene.10036 [pii] (2002).

264 Barabas, P. *et al.* Role of ELOVL4 and very long-chain polyunsaturated fatty acids in mouse models of Stargardt type 3 retinal degeneration. *Proceedings of the National Academy of Sciences of the United States of America* **110**, 5181-5186, doi:10.1073/pnas.1214707110 (2013).

265 Busskamp, V. *et al.* miRNAs 182 and 183 are necessary to maintain adult cone photoreceptor outer segments and visual function. *Neuron* **83**, 586-600, doi:10.1016/j.neuron.2014.06.020 (2014).

266 Keady, B. T., Le, Y. Z. & Pazour, G. J. IFT20 is required for opsin trafficking and photoreceptor outer segment development. *Molecular biology of the cell* **22**, 921-930, doi:10.1091/mbc.E10-09-0792 (2011).

267 Bentzinger, C. F. *et al.* Skeletal muscle-specific ablation of raptor, but not of rictor, causes metabolic changes and results in muscle dystrophy. *Cell metabolism* **8**, 411-424, doi:10.1016/j.cmet.2008.10.002 (2008).

268 Kwiatkowski, D. J. *et al.* A mouse model of TSC1 reveals sex-dependent lethality from liver hemangiomas, and up-regulation of p70S6 kinase activity in Tsc1 null cells. *Human molecular genetics* **11**, 525-534 (2002).

269 Andrieu-Soler, C. *et al.* Intravitreous injection of PLGA microspheres encapsulating GDNF promotes the survival of photoreceptors in the rd1/rd1 mouse. *Mol Vis* **11**, 1002-1011 (2005).

270 Morrow, E. M., Furukawa, T. & Cepko, C. L. Vertebrate photoreceptor cell development and disease. *Trends Cell Biol* **8**, 353-358 (1998).

271 Curatolo, P. & Maria, B. L. Tuberous sclerosis. *Handbook of clinical neurology* **111**, 323-331, doi:10.1016/B978-0-444-52891-9.00038-5 (2013).

272 Young, R. W. The renewal of rod and cone outer segments in the rhesus monkey. *The Journal of cell biology* **49**, 303-318 (1971).

273 Mathupala, S. P., Ko, Y. H. & Pedersen, P. L. Hexokinase II: cancer's double-edged sword acting as both facilitator and gatekeeper of malignancy when bound to mitochondria. *Oncogene* **25**, 4777-4786, doi:1209603 [pii] 10.1038/sj.onc.1209603 (2006).

274 Sun, Q. *et al.* Mammalian target of rapamycin up-regulation of pyruvate kinase isoenzyme type M2 is critical for aerobic glycolysis and tumor growth.

Proceedings of the National Academy of Sciences of the United States of America **108**, 4129-4134, doi:1014769108 [pii]10.1073/pnas.1014769108 (2011).

275 Earnshaw, W. C., Martins, L. M. & Kaufmann, S. H. Mammalian caspases: structure, activation, substrates, and functions during apoptosis. *Annu Rev Biochem* **68**, 383-424, doi:10.1146/annurev.biochem.68.1.383 (1999).

276 Katsuragi, Y., Ichimura, Y. & Komatsu, M. p62/SQSTM1 functions as a signaling hub and an autophagy adaptor. *The FEBS journal* **282**, 4672-4678, doi:10.1111/febs.13540 (2015).

277 Suzuki, N. N., Yoshimoto, K., Fujioka, Y., Ohsumi, Y. & Inagaki, F. The crystal structure of plant ATG12 and its biological implication in autophagy. *Autophagy* **1**, 119-126 (2005).

278 Harvey, K. F. *et al.* FOXO-regulated transcription restricts overgrowth of Tsc mutant organs. *The Journal of cell biology* **180**, 691-696, doi:10.1083/jcb.200710100 (2008).

279 Brunet, A. *et al.* Akt promotes cell survival by phosphorylating and inhibiting a Forkhead transcription factor. *Cell* **96**, 857-868, doi:S0092-8674(00)80595-4 [pii] (1999).

280 Sancak, Y. *et al.* Ragulator-Rag complex targets mTORC1 to the lysosomal surface and is necessary for its activation by amino acids. *Cell* **141**, 290-303, doi:10.1016/j.cell.2010.02.024 (2010).

281 Jiang, B. H. & Liu, L. Z. PI3K/PTEN signaling in angiogenesis and tumorigenesis. *Advances in cancer research* **102**, 19-65, doi:10.1016/S0065-230X(09)02002-8 (2009).

282 Ma, S. *et al.* Loss of mTOR signaling affects cone function, cone structure and expression of cone specific proteins without affecting cone survival. *Experimental eye research* **135**, 1-13, doi:10.1016/j.exer.2015.04.006 (2015).

283 Cloetta, D. *et al.* Inactivation of mTORC1 in the developing brain causes microcephaly and affects gliogenesis. *The Journal of neuroscience : the official journal of the Society for Neuroscience* **33**, 7799-7810, doi:10.1523/JNEUROSCI.3294-12.2013 (2013).

284 Polak, P. *et al.* Adipose-specific knockout of raptor results in lean mice with enhanced mitochondrial respiration. *Cell metabolism* **8**, 399-410, doi:10.1016/j.cmet.2008.09.003 (2008).

285 Shende, P. *et al.* Cardiac raptor ablation impairs adaptive hypertrophy, alters metabolic gene expression, and causes heart failure in mice. *Circulation* **123**, 1073-1082, doi:10.1161/CIRCULATIONAHA.110.977066 (2011).

286 Suzuki, A. *et al.* Astrocyte-neuron lactate transport is required for long-term memory formation. *Cell* **144**, 810-823 (2011).

287 Wyss, M. T., Jolivet, R., Buck, A., Magistretti, P. J. & Weber, B. In vivo evidence for lactate as a neuronal energy source. *The Journal of neuroscience : the official journal of the Society for Neuroscience* **31**, 7477-7485, doi:31/20/7477 [pii]10.1523/JNEUROSCI.0415-11.2011 (2011).

288 Lin, B., Masland, R. H. & Strettoi, E. Remodeling of cone photoreceptor cells after rod degeneration in rd mice. *Experimental eye research* **88**, 589-599, doi:10.1016/j.exer.2008.11.022 (2009).

289 Kellersch, B. & Brocker, T. Langerhans cell homeostasis in mice is dependent on mTORC1 but not mTORC2 function. *Blood* **121**, 298-307, doi:10.1182/blood-2012-06-439786 (2013).

290 Choo, A. Y. *et al.* Glucose addiction of TSC null cells is caused by failed mTORC1-dependent balancing of metabolic demand with supply. *Molecular cell* **38**, 487-499, doi:10.1016/j.molcel.2010.05.007 (2010).

291 Guenther, G. G. *et al.* Loss of TSC2 confers resistance to ceramide and nutrient deprivation. *Oncogene* **33**, 1776-1787, doi:10.1038/onc.2013.139 (2014).

292 Guertin, D. A. *et al.* mTOR complex 2 is required for the development of prostate cancer induced by Pten loss in mice. *Cancer cell* **15**, 148-159, doi:10.1016/j.ccr.2008.12.017 (2009).

293 Goto, J. *et al.* Regulable neural progenitor-specific Tsc1 loss yields giant cells with organellar dysfunction in a model of tuberous sclerosis complex. *Proceedings of the National Academy of Sciences of the United States of America* **108**, E1070-1079, doi:10.1073/pnas.1106454108 (2011).

294 Tsai, P. T. *et al.* Autistic-like behaviour and cerebellar dysfunction in Purkinje cell Tsc1 mutant mice. *Nature* **488**, 647-651, doi:10.1038/nature11310 (2012).

295 Castillo, K. *et al.* Trehalose delays the progression of amyotrophic lateral sclerosis by enhancing autophagy in motoneurons. *Autophagy* **9**, 1308-1320, doi:10.4161/auto.25188 (2013).

296 Zhang, X. *et al.* MTOR-independent, autophagic enhancer trehalose prolongs motor neuron survival and ameliorates the autophagic flux defect in a mouse model of amyotrophic lateral sclerosis. *Autophagy* **10**, 588-602, doi:10.4161/auto.27710 (2014).

297 Kang, Y. J., Lu, M. K. & Guan, K. L. The TSC1 and TSC2 tumor suppressors are required for proper ER stress response and protect cells from ER stress-induced apoptosis. *Cell death and differentiation* **18**, 133-144, doi:10.1038/cdd.2010.82 (2011).

298 Kim, J. W., Kang, K. H., Burrola, P., Mak, T. W. & Lemke, G. Retinal degeneration triggered by inactivation of PTEN in the retinal pigment epithelium. *Genes & development* **22**, 3147-3157, doi:10.1101/gad.1700108 (2008).

299 Ambati, J. & Fowler, B. J. Mechanisms of age-related macular degeneration. *Neuron* **75**, 26-39, doi:10.1016/j.neuron.2012.06.018 (2012).

300 Sarks, J. P., Sarks, S. H. & Killingsworth, M. C. Evolution of geographic atrophy of the retinal pigment epithelium. *Eye* **2 (Pt 5)**, 552-577, doi:10.1038/eye.1988.106 (1988).

301 Holz, F. G., Strauss, E. C., Schmitz-Valckenberg, S. & van Lookeren Campagne, M. Geographic atrophy: clinical features and potential therapeutic approaches. *Ophthalmology* **121**, 1079-1091, doi:10.1016/j.ophtha.2013.11.023 (2014).

302 Zieger, M. & Punzo, C. Improved cell metabolism prolongs photoreceptor survival upon retinal-pigmented epithelium loss in the sodium iodate induced model of geographic atrophy. *Oncotarget*, doi:10.18632/oncotarget.7330 (2016).

303 Jackson, G. R. & Barber, A. J. Visual dysfunction associated with diabetic retinopathy. *Curr Diab Rep* **10**, 380-384, doi:10.1007/s11892-010-0132-4 (2010).

304 Rajala, R. V., Wiskur, B., Tanito, M., Callegan, M. & Rajala, A. Diabetes reduces autophosphorylation of retinal insulin receptor and increases protein-tyrosine phosphatase-1B activity. *Investigative ophthalmology & visual science* **50**, 1033-1040, doi:iovs.08-2851 [pii]10.1167/iovs.08-2851 (2009).

305 Reiter, C. E. *et al.* Diabetes reduces basal retinal insulin receptor signaling: reversal with systemic and local insulin. *Diabetes* **55**, 1148-1156, doi:55/4/1148 [pii] (2006).

306 Stearns, G., Evangelista, M., Fadool, J. M. & Brockerhoff, S. E. A mutation in the cone-specific pde6 gene causes rapid cone photoreceptor degeneration in zebrafish. *The Journal of neuroscience : the official journal of the Society for Neuroscience* **27**, 13866-13874, doi:10.1523/JNEUROSCI.3136-07.2007 (2007).

307 Knight, Z. A., Schmidt, S. F., Birsoy, K., Tan, K. & Friedman, J. M. A critical role for mTORC1 in erythropoiesis and anemia. *eLife* **3**, e01913, doi:10.7554/eLife.01913 (2014).

308 Rachdi, L. *et al.* Disruption of Tsc2 in pancreatic beta cells induces beta cell mass expansion and improved glucose tolerance in a TORC1-dependent manner. *Proceedings of the National Academy of Sciences of the United States of America* **105**, 9250-9255, doi:10.1073/pnas.0803047105 (2008).

309 Staats, K. A. *et al.* Rapamycin increases survival in ALS mice lacking mature lymphocytes. *Molecular neurodegeneration* **8**, 31, doi:10.1186/1750-1326-8-31 (2013).

310 Santini, E., Heiman, M., Greengard, P., Valjent, E. & Fisone, G. Inhibition of mTOR signaling in Parkinson's disease prevents L-DOPA-induced dyskinesia. *Science signaling* **2**, ra36, doi:10.1126/scisignal.2000308 (2009).

311 Zhang, X. *et al.* Rapamycin treatment augments motor neuron degeneration in SOD1(G93A) mouse model of amyotrophic lateral sclerosis. *Autophagy* **7**, 412-425 (2011).

312 Mattapallil, M. J. *et al.* The Rd8 mutation of the Crb1 gene is present in vendor lines of C57BL/6N mice and embryonic stem cells, and confounds ocular induced mutant phenotypes. *Investigative ophthalmology & visual science* **53**, 2921-2927, doi:10.1167/iovs.12-9662 (2012).

313 Zinchuk, V., Wu, Y., Grossenbacher-Zinchuk, O. & Stefani, E. Quantifying spatial correlations of fluorescent markers using enhanced background reduction with protein proximity index and correlation coefficient estimations. *Nat Protoc* **6**, 1554-1567, doi:10.1038/nprot.2011.384 (2011).

314 Ortin-Martinez, A. *et al.* Number and distribution of mouse retinal cone photoreceptors: differences between an albino (Swiss) and a pigmented (C57/BL6) strain. *PloS one* **9**, e102392, doi:10.1371/journal.pone.0102392 (2014).

315 Castillo, K. *et al.* Measurement of autophagy flux in the nervous system in vivo. *Cell death & disease* **4**, e917, doi:10.1038/cddis.2013.421 (2013).
316 Venkatesh, A., Ma, S., Langellotto, F., Gao, G. & Punzo, C. Retinal gene delivery by rAAV and DNA electroporation. *Curr Protoc Microbiol* **Chapter 14**, Unit 14D 14, doi:10.1002/9780471729259.mc14d04s28 (2013).